STUDIES ON Mn, Co AND Cu COMPLEXES OF CHIRAL AMINO LCOHOL BASED SCHIFF BASES: SYNTHESIS, STRUCTURE ANDPROPERTIES

A THESIS
SUBMITTED FOR THE DEGREE OF
DOCTOR OF PHILOSOPHY

By

PRADEEP C. P.

SCHOOL OF CHEMISTRY

UNIVERSITY OF HYDERABAD

HYDERABAD 500 046

INDIA

MARCH 2006

Dedicated
To
My Parents

STATEMENT

I hereby declare that the matter embodied in the thesis entitled ***"Studies on Mn, Co and Cu Complexes of Chiral Amino Alcohol Based Schiff Bases: Synthesis, Structure and Properties"*** is the result of investigations carried out by me in the School of Chemistry, University of Hyderabad, Hyderabad, India, under the supervisions of **Prof. P. S. Zacharias** and **Dr. Samar K. Das**.

In keeping with the general practice of reporting scientific observations, due acknowledgements have been made wherever the work described is based on the findings of other investigators. Any omission, which might have occurred by oversight or error is regretted.

Pradeep C. P.

CERTIFICATE

Certified that the work contained in the thesis entitled "**Studies on Mn, Co and Cu Complexes of Chiral Amino Alcohol based Schiff bases: Synthesis, Structure and Properties"** has been carried out by Mr. C. P. Pradeep under our supervisions and the same has not been submitted elsewhere for a degree.

Hyderabad **Prof. P. S. Zacharias**

March 2006 **(Supervisor)**

Dean **Dr. Samar K. Das**

School of Chemistry **(Co-supervisor)**

ACKNOWLEDGEMENTS

I express my sincere gratitude to my research supervisors **Prof. P. S. Zacharias** and **Dr. Samar K. Das** for their guidance and encouragements. They have been always approachable, helpful and extremely patient throughout my research career.

I would like to thank The Dean, School of Chemistry for allowing me to avail school facilities. I am extremely thankful to all the faculty members of this school for their kind help and encouragements at various stages of my research work.

I am highly grateful to Prof. Samudranil Pal for his helps and suggestions during my research career.

I express my sincere thanks to Prof. A. R. Chakravarty (IISc. Bangalore) for variable temperature magnetic data and Dr. N. Arulsamy, University of Wyoming for a crystallographic data measurement.

Financial assistance from UGC, Govt. of India is gratefully acknowledged. The infrastructure support from UGC (UPE Program) and DST (National Single Crystal X-ray diffractometer facility) is also acknowledged.

I wish to thank my senior lab mates Dr. K. Srinivas Rao, Dr. Sunil Kumar, Dr. N. Mangayarkarasi, Dr. Tin Htwe, Dr. Vamsee Krishna and M. Prabhakar. They were very friendly, affectionate and always helped me profoundly.

A special word of thanks to Mr. P. Raghavaiah for various helps throughout my research career and for his pleasant company.

I would like to thank my junior labmates Shiviah, Supriya, Madhu, Arumugham and Tanmay for creating a pleasant working atmosphere. I gratefully acknowledge Dr. Satyanarayan Pal, Dr. Satyen Saha, Dr. G. Srinivas, Dr. Venugopal Rao, Dr. Jaganmohan Rao and Dr. Prashanth Kumar for their friendship and suggestions.

Friendship of Param, Biju and Prasad is deeply acknowledged. They were always there for me whenever I was in need. Special thanks are due to Raji and Sreekanth for their friendship and helps on various occasions.

My association with Anoop, Shaji, Sankarettan, Ebichan, Gireesh and Varghese are memorable. I cherish my friendship with all of them.

My stay in the campus is made pleasant by my friends Mohanan, Yasar, Ajith, Rohith, Sudheendran, Muneer, Subramanyan, Ummer, Santhosh, Joji, Jojo, Abhilash, Shinto, Rajesh, Rajesh, George, Sreenath, Vishnu and Juby. I acknowledge whole-heartedly the contributions of each and every one of them. My hostel wing- mates Satya and Ratnam are deeply acknowledged for their company.

My friends in School of Chemistry needs special acknowledgement for creating a cheerful atmosphere. Malla Reddy, Srinivas Reddy, Balu, Vasulu, Basavoju, Pavan, Narsi, Gupta, Suresh, Shyamraj, Jagdeesh, Rajesh, Rahul, Dinabandu, Prasun, Moloy, Sunirban, Abhik, Manab, Padmanabhan and Venkatesh are few to mention.

Friendship of Rajan master, Sureshji and his family is deeply acknowledged.

All the non-teaching staff of the School of Chemistry and CIL have been extremely helpful, I thank them all especially Suresh, Shetty, Asia Parwez, Vijayalakshmi, Vijaya Bhaskar and Bhaskar Rao.

I gratefully acknowledge all my teachers who taught me at various levels of my academic career. Prof. M. A. Anto and all other faculty members of Department of Chemistry, St. Thomas College, Thrissur as well as Dr. K. S. Vijayalekshmi and other faculty members of S.V.N.S.S College, Vyasagiri deserve special mention.

Without the understanding, support and blessings of my parents, I would not have reached here. The credit of all my achievements goes to them. Also the affection and support of my sisters and their families are deeply acknowledged.

Pradeep

CONTENTS

STATEMENT i

CERTIFICATE ii

ACKNOWLEDGEMENTS iii

CHAPTER 1 Introduction 1

CHAPTER 2 Materials and experimental methods 31

CHAPTER 3 Synthesis, structure, catalytic properties and supramolecular chemistry of a series of chiral mononuclear Mn(IV) complexes derived from chiral amino alcohol based Schiff bases

3.1. Abstract 59

3.2. Introduction 60

3.3. Experimental 61

3.4. Results and Discussion 65

3.5. Conclusion 84

3.6. References 86

CHAPTER 4 Synthesis and characterization of mono-, tri- and tetranuclear cobalt complexes derived from chiral amino alcohol based Schiff bases

4.1. Abstract 89

4.2. Introduction 90

4.3. Experimental 91

4.4. Results and Discussion 95

4.5. Conclusion 115

4.6. References 117

CHAPTER 5 Mono and dichlorobridged dinuclear copper(II) complexes with chiral amino alcohol based Schiff bases

5.1. Abstract 121

5.2. Introduction 122

5.3. Experimental 123

5.4. Results and Discussion 127

5.5. Conclusion 150

5.6. References 151

CHAPTER 6 Summary and scope of further work 155

APPENDIX 1 Synthesis and structural characterization of two tetranuclear copper complexes derived from symmetric and asymmetric compartmental ligands containing amino acid side arms 161

LIST OF PUBLICATIONS 183

Chapter 1

Introduction

1.1. Abstract

In this chapter, the importance of chiral amino alcohol chemistry has been briefly discussed with special emphasis to chiral amino alcohol based Schiff base metal complexes and their catalytic applications. Biological and supramolecular relevance of amino alcohol based metal complexes is mentioned. The aim of the present investigation is described in the context of known chiral amino alcohol chemistry.

1.2. Schiff base complexes

Schiff bases have the general formula Ar−CH=N−R and they are condensation products of aromatic aldehydes or ketones with primary amines.[1] Following the works of Jørgensen, Werner, Ettling *et al*, Schiff discovered in 1869 the synthetic technique of preparing salicylaldimine complexes by the reaction of preformed metal salicylaldehyde compound with primary amines.[2]

Because of the great synthetic flexibility of Schiff base formation, many ligands of diverse structural, electronic and steric properties can be synthesized. Metal complexes of Schiff bases have contributed substantially to the overall development of coordination chemistry in various aspects. Of all Schiff bases, those derived from salicylaldimines have been by far the most thoroughly studied. The particular advantage of the salicylaldimine ligand system is the flexibility of its synthetic procedure which allows one to fine tune the steric and electronic properties by choosing appropriate amine precursors and substituents on the salicylaldehyde ring.[3]

Schiff base ligands are important because of the physiological and pharmacological activities associated with them. They constitute an interesting class of chelating agents capable of coordinating metal ions to give complexes which serve as models for biological systems. Transition metal Schiff base complexes derived from salicylaldehyde/substituted salicylaldehydes have been extensively studied as models for biologically important species and play an important role in living beings. Also these types of complexes are well known for their structural diversity and reactivity patterns. Further interest in these complexes has focused on their usefulness in studying magnetic exchange interactions between bridged paramagnetic metal ions and their applications in catalytic processes.[4]

1.3. Chiral Schiff base complexes

Chirality is a fundamental symmetry property of three dimensional objects. An object is said to be chiral if it cannot be superimposed upon its mirror image. A carbon atom attached to four different groups will be chiral.[5] Chirality of a molecule was first reported in 1815 by the French physicist Jean-Baptiste Biot who found that the α-quartz rotated the plane of polarized light.[6] The first chiral separation, which laid the foundation for stereochemistry, was reported in 1848 by Louis Pasteur. He was able to separate the mirror image crystals of the isomers of sodium ammonium tartrate.[7]

Chirality is an important aspect in modern coordination chemistry which unites fields as diverse as transition metal catalysis, metallo-supramolecular chemistry and bioinorganic chemistry. Chiral coordination compounds are promising new materials in areas like enantioselective catalysis, materials chemistry, non-linear optics and supramolecular chemistry. One of the important themes in modern coordination chemistry is the exploration of methods for the stereoselective synthesis of coordination compounds. One successful approach has been the use of chiral ligands, especially chiral Schiff base ligands derived from amino acids, amino alcohols, terpenes etc.[3,8]

1.4 Chiral sources

To be useful in asymmetric synthesis and materials chemistry, the chiral source should be cheap and readily available in high enantiomeric purity. For many applications the availability of both enantiomers is advantageous. Most importantly, they must be capable of exerting a high degree of stereocontrol in the required reactions by means of steric hindrance, chelation or other specific effects.[3] The most widely used chiral sources in chemistry are of natural origin especially chiral amino acids, amino alcohols and terpenes. These compounds which occur in nature provide an enormous range and diversity of possible starting materials. Chiral amino acids are

the cheapest chiral source available. There are lots of studies employing chiral amino acids as chiral source for varied applications ranging from biological modeling, asymmetric catalysis, supramolecular chemistry etc.[9]

Chiral amino alcohols are ideal building blocks for chiral Schiff base ligands. They can be synthesized without much difficulty from easily available chiral amino acids (Scheme 1.1).[10]

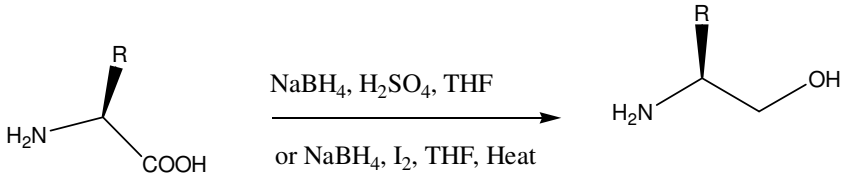

Scheme 1.1. Synthetic scheme of amino alcohols from amino acids.

Chiral amino alcohols have found applications as building blocks for biologically active compounds, as chiral auxiliaries and as ligands for asymmetric catalysis.[11] But compared to amino acids, the potential of chiral amino alcohols as chiral source has not been exploited fully in coordination chemistry. Although there is considerable literature on coordination chemistry of Schiff bases derived from achiral amino alcohols,[12] the coordination chemistry of Schiff bases derived from chiral amino alcohols with various metal ions is not explored much.

1.5. Chiral amino alcohol based Schiff base complexes

Over the past two decades, the interest in chiral amino alcohol based metal complexes has increased. They have been successfully utilized for a variety of application such as asymmetric catalysis, bio-inorganic modeling, chromatographic separations etc. Various metal ions have been employed to achieve these specific goals.

The most effective ligands for asymmetric catalysis are based on small number of successful templates as shown in Figure 1.1. The chiral influence of these

'privileged' ligands - chiral ligands that are extraordinarily effective for a wide range of mechanistically unrelated reactions - is mostly derived from naturally occurring chiral sources.[13]

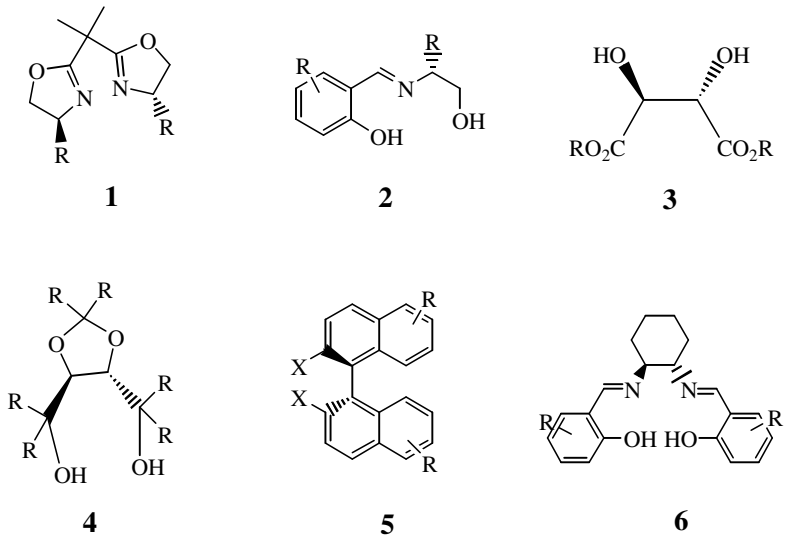

Figure 1.1. Privileged ligand templates commonly used for asymmetric catalysis.

The superiority of this class of optically active ligands can be recognized due to their low molecular weights and to the fact that they possess at least one stereogenic center, the starting precursors of which is readily available with any desirable absolute stereochemistry. In addition, it has been shown that the reaction conditions are extremely simple.

Motif 2 in the above class represents chiral Schiff base ligands derived from chiral amino alcohols and salicylaldehyde derivatives. In the following subsections, recent literature on chiral amino alcohol Schiff base complexes has been discussed.

1.5.1. Titanium complexes

Complexes derived from titanium alkoxides and chiral amino alcohol Schiff bases are well studied with respect to their catalytic efficiency in a number of asymmetric transformations. The tridentate N-salicyl-β-amino alcohols and their

parent Schiff bases (Figure 1.2) form chelating complexes with titanium. These complexes behave as Lewis acids providing a rigid asymmetric environment and therefore are useful in asymmetric reactions. They are successfully employed as catalysts in trimethylsilylcyanation, pinacol coupling, Strecker reactions etc.

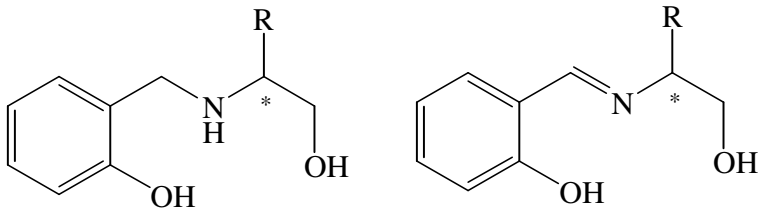

Figure 1.2. N-salicyl-β-amino alcohols and their parent Schiff bases.

Pioneering work in the catalytic properties of chiral amino alcohol Schiff base-titanium complexes has been done by Oguni and co-workers.[14(a,b)] They employed such complexes (Scheme 1.2) for the asymmetric cyanosilylation of a variety of aldehydes (aromatic, heteroaromatic, α,β-unsaturated and nonconjugate aliphatic aldehydes).

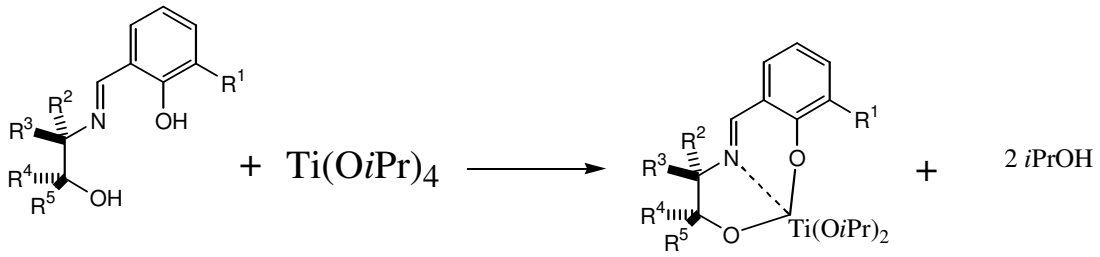

Scheme 1.2. Synthetic scheme for chiral titanium catalysts used for asymmetric cyanosilylation of aldehydes.

Chiral Schiff base ligands of *tert*-butylsalicylaldehydes bearing electron withdrawing and donating groups were synthesized by reaction with various substituted chiral amino alcohols. These ligands were used with titanium

tetraisopropoxide to study their steric and electronic effects on the enantioselectivity of the trimethylsilylcyanation of benzaldehyde (Scheme 1.3).[14(c,d)]

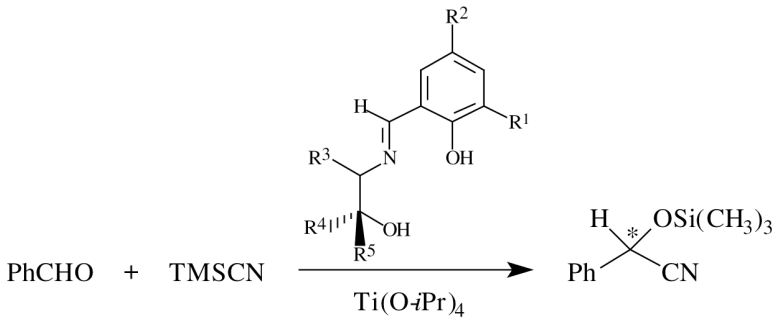

Scheme 1.3. Reaction scheme for the trimethylsilylcyanation of benzaldehyde using chiral titanium catalysts synthesized from chiral amino alcohol based Schiff bases.* indicates chiral center.

Pinacol coupling reaction of benzaldehyde catalyzed by a series of Schiff base-Ti complexes afforded pinacol with high yield and different diastereoselectivity. The relationship between the steric structure of these Schiff bases prepared from easily available amino alcohols, and the diastereoselectivity of the resulting pinacol is systemically studied.[14(e)]

N-salicyl-β-amino alcohols were synthesized and evaluated as ligands for catalytic asymmetric Strecker reactions with titanium tetra isopropoxide. It has been shown that the configuration as well as the bulkiness of the β-substituent exerts a direct influence on both the absolute stereochemical outcome and enantioselectivity of the Strecker product. Also it was shown that excellent yields and high enantioselectivities can be achieved when a substrate with a more sterically demanding N-substituent is employed.[14(f)]

Despite the success of imine-alkoxytitanium complexes in asymmetric catalysis, only few details are known about the structure of these catalysts. Crystal structure of one of the imine-alkoxytitanium complex prepared from (*R*)-2-amino-1,1,2-triphenylethanol and 3,5-disubstituted salicylaldehyde with titanium

tetraisopropoxide is reported (Figure 1.3). The structure consists of a distorted octahedron in which the central Ti is covalently bonded to phenolic and alcoholic oxygens as well as to imine nitrogen. The ligands bind in a meridional manner.[14(g)]

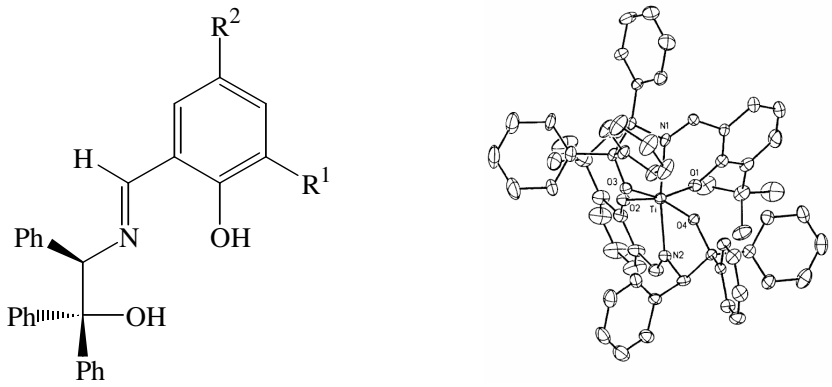

Figure 1.3. (Left): Chiral Schiff base prepared from (*R*)-2-amino-1,1,2-triphenylethanol and 3,5-disubstituted salicylaldehyde and (right): crystal structure of an imine-alkoxytitanium complex prepared from this ligand.

In addition to the above Schiff base titanium complexes, other chiral amino alcohol titanium systems are also explored with respect to catalysis. They include bidentate amino alcohol ligands derived from L-phenylalanine. Structural details of the resulting two titanium complexes and their initial reaction chemistry are reported.[14(h)] Both complexes (Figure 1.4) are dimeric in nature; amino alcohol oxygen bridges two Ti centers, each titanium has a highly distorted trigonal bipyramidal coordination arrangement.

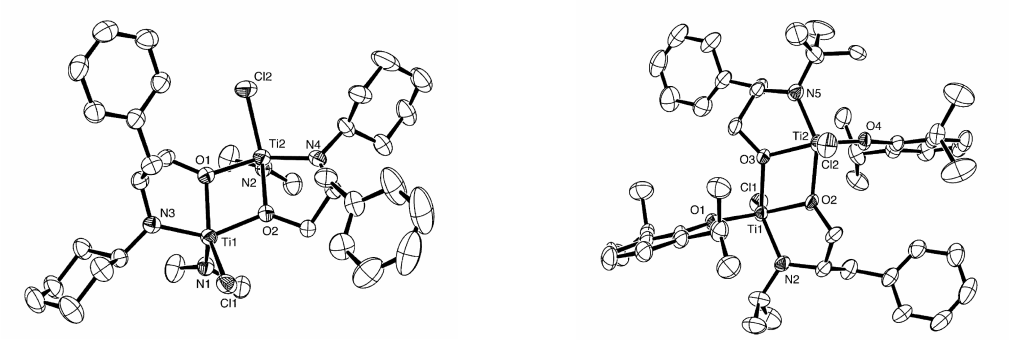

Figure 1.4. Crystal structures of two titanium complexes derived from L-phenylalanine.

Intramolecular hydroamination of di- and trisubstituted hexa-4,5-dienylamines catalyzed by a series of titanium complexes derived from sterically varied chiral amino alcohol ligands has been reported. These complexes show improved selectivity for the formation of pyrrolidines over other titanium and zirconium based catalysts (Figure 1.5).[14(i)]

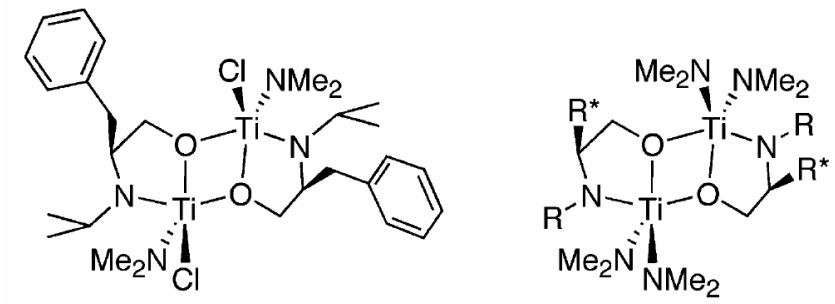

Figure 1.5. Titanium catalysts for hydroamination of dienylamines derived from chiral amino alcohol ligands.

Titanium complexes of chiral amino alcohol ligands as shown in Figure 1.6 were synthesized in connection with the intramolecular hydroamination of substituted aminoallenes.[14(j)]

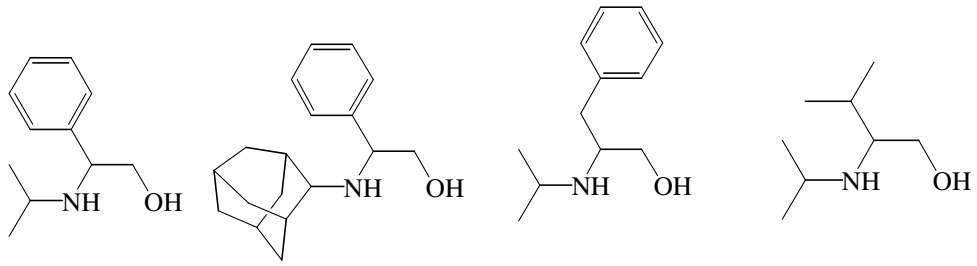

Figure 1.6. Chiral amino alcohol based ligands used for the preparation of titanium hydroamination catalysts.

1.5.2. Vanadium complexes

A catalytic system made of chiral Schiff base-vanadium complexes has been reported for the oxidation of thioethers as shown in Scheme 1.4. This system made up of chiral amino alcohol based ligands was found to be highly efficient and cost effective.[15(a)]

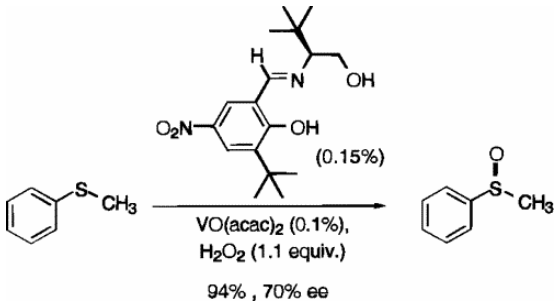

Scheme 1.4. Catalytic scheme for the oxidation of thioethers using vanadium catalysts of chiral Schiff bases.

Vanadium complexes of chiral Schiff base ligands derived from substituted salicylaldehydes and various β-amino alcohols have been successfully employed for the asymmetric oxidation of prochiral sulfides to chiral sulfoxides. Ellman *et al* first reported the asymmetric oxidation of *tert*-butyl disulfide employing H_2O_2 as stoichiometric oxidant in presence of chiral vanadium Schiff base complexes derived from chiral amino alcohols.[15(b,c,d)] They varied the substituents on both the amino

alcohol and salicylaldehyde portions of the chiral ligand to get the product *tert*-butyl-*tert*-butanethiosulfinate in good yields and enantiomeric purity.

Inspired from these results, Somanathan *et al* created a library of Schiff base ligands with subtle variations in the size of the substituents on the ligands as shown in Scheme 1.5. By varying the substituents at positions R_1, R_2, R_3 and R_4 they proved that appropriate substituents on the ligand with proper steric and electronic factors enhances the enantioselectivity of the sulfide to sulfoxide oxidation.[15(e)]

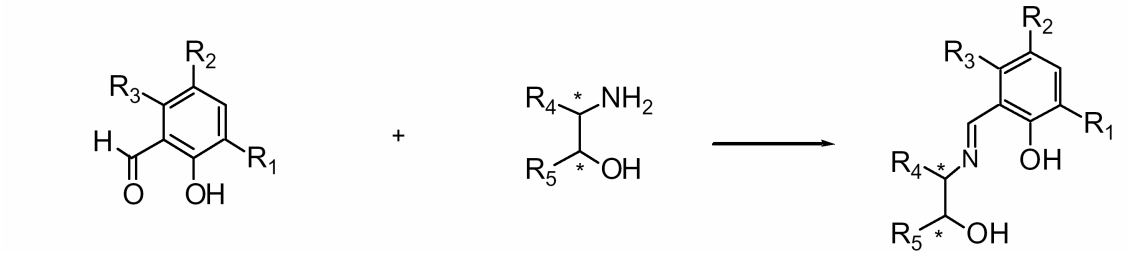

Scheme 1.5. Schiff base ligands employed to study the effect of various substituents on the vanadium catalyzed sulfide to sulfoxide oxidation.

Sartori *et al* reported a series of polymer supported chiral Schiff base ligands derived from salicylic aldehydes and chiral amino alcohols. These heterogeneous ligands have been complexed with $VO(acac)_2$ and employed to catalyze the enantioselective oxidation of sulfides to sulfoxides using H_2O_2 as the oxidant.[15(f)]

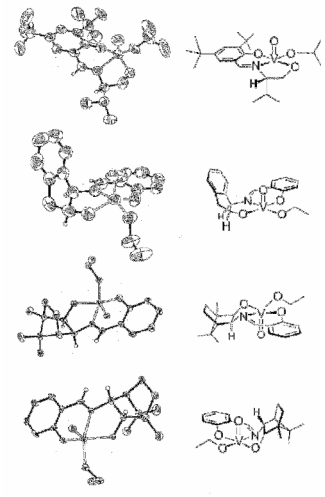

Recently Hartung *et al* reported Vanadium(V) complexes of tridentate Schiff base ligands derived from salicylaldehyde and various chiral amino alcohols as oxidation catalysts for the stereoselective synthesis of functionalized tetrahydrofurans from substituted bis(homoallylic) alcohols. Some of the chiral vanadium Schiff base complexes are characterized by X-ray crystallography and are shown in Figure 1.7.[15(g)]

Figure 1.7. Crystal structures of some chiral amino alcohol-vanadium Schiff base complexes.

1.5.3. Copper complexes

Copper Schiff base complexes derived from chiral amino alcohols and substituted salicylaldehydes are widely employed as catalysts for asymmetric cyclopropanation of olefins. Aratani first used such a catalyst for the cyclopropanation of 2,5-dimethyl-2,4-hexadiene (Scheme 1.6).[16(a,b,c)]

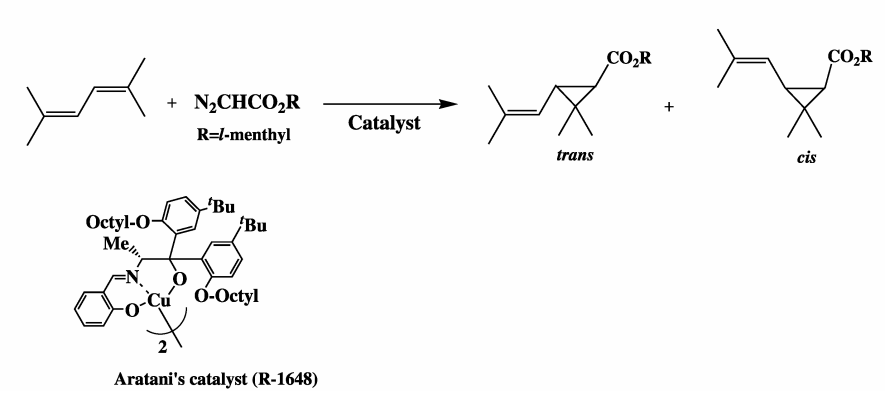

Scheme 1.6. Chiral amino alcohol based copper catalyst designed by Aratani *et al* for the cyclopropanation of dienes.

Modifying Aratani's catalyst, Li *et al* reported some new cyclopropanation catalysts derived from copper acetate monohydrate, substituted salicylaldehydes and chiral amino alcohols (Figure 1.8). Substituents on salicylaldehyde framework demonstrate a significant effect on the stereoselectivity. Those with electron-withdrawing properties enhance the selectivities whereas bulky substituents in ortho position to the phenol hydroxy group decrease the selectivities.[16(d,e)]

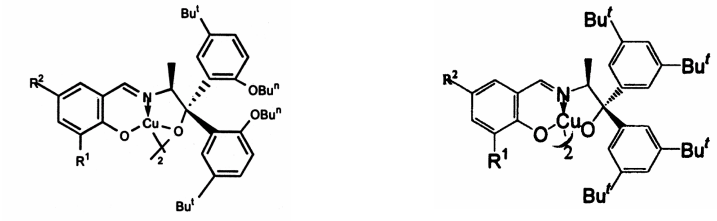

Figure 1.8. Copper catalysts derived from chiral amino alcohols and substituted salicylaldehydes for cyclopropanation reaction.

Cai *et al* reported binuclear copper-Schiff base complexes derived from substituted 2-hydroxy-1,3-benzenedialdehyde and chiral amino alcohols as catalysts for asymmetric cyclopropanation of styrene. Various bulky groups have been substituted for Ar group (Scheme 1.7). One of the catalyst, where Ar = Ph has been structurally characterized.[16(f)]

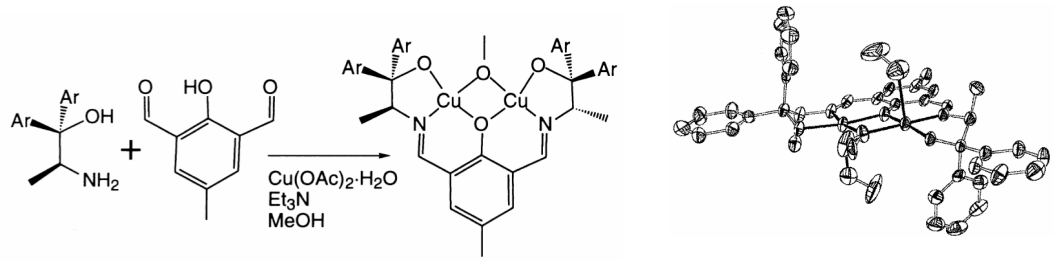

Scheme 1.7. (left) Synthetic scheme for the binuclear copper complexes used as cyclopropanation catalysts; (right) crystal structure of one of the catalysts.

You *et al* reported a series of copper-Schiff-base complexes with two chiral centers derived from 1,2-diphenyl-2-amino-ethanol as catalysts for the asymmetric cyclopropanation of ethenes with diazoacetates (Figure 1.9).[16(g)]

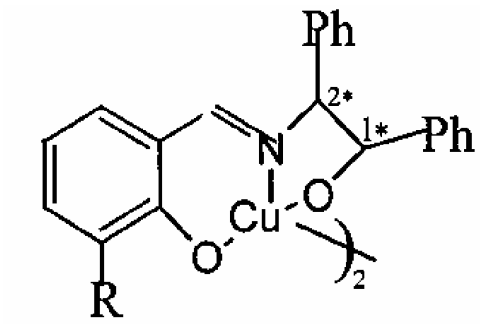

Figure 1.9. Copper Schiff base catalysts with two chiral centers for the asymmetric cyclopropanation reaction. * indicates chiral center.

In 2004, Itagaki *et al* reported the following chiral copper Schiff base complexes (Figure 1.10) which are derived from substituted salicylaldehydes, chiral amino alcohols and copper acetate monohydrate for the asymmetric cyclopropanation of 2,5-dimethyl-2,4-hexadiene with diazoacetate.[16(h)]

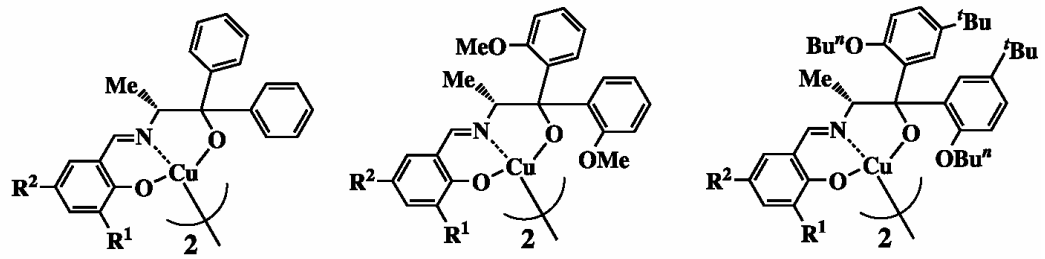

Figure 1.10. Cyclopropanation catalysts designed by Itagaki *et al.*

Structure of two chiral amino alcohol Schiff base-Copper(II) complexes have been reported by Minobe *et al* (Figure 1.11).[16(i,j)]

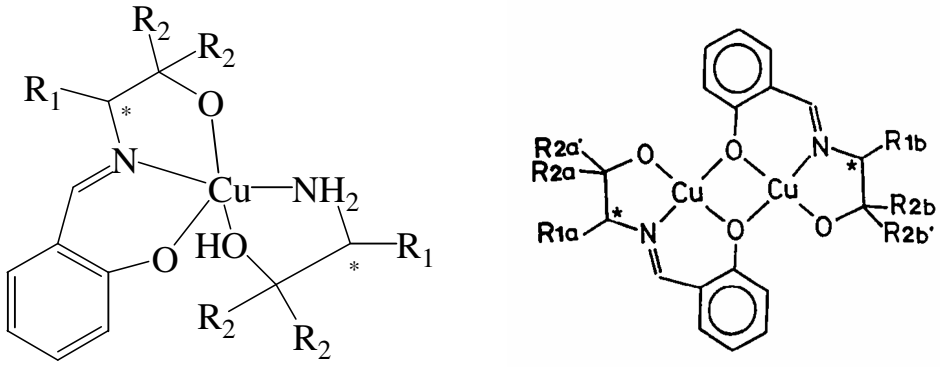

(a) **(b)**

Figure 1.11. Molecular diagram of two structurally characterized chiral amino alcohol based Schiff base copper complexes.

The complex (a) crystallizes in the chiral space group monoclinic $P2_1$. The coordination geometry of the Cu is a distorted square pyramid. The tridentate Schiff-base group occupies three of the basal square-planar sites and the N of the amino

alcohol group completes the plane. A protonated O of the amino alcohol group occupies the axial position. Complex (b) also crystallizes in monoclinic $P2_1$. The complex consists of a phenolic oxygen bridged binuclear copper(II) unit and the chiral Schiff base is incorporated as a tridentate ligand. The two 2-butoxy-5-tert-butylphenyl groups are perpendicular to the oxygen bridged binuclear copper unit plane and make a groove in the axial position of the two copper atoms. There are also some other chiral amino alcohol based copper complexes which are structurally characterized.[16(k)]

Chiral amino alcohol Schiff base-Cu(II) complexes were examined as ligand exchange phases for HPLC. Separation of enantiomers on the reverse phase silica gel, coated with a chiral binuclear Schiff base copper complex (synthesized from N-salicyliden-(R)-2-amino-1,1-bis(2-butoxy-5-tert-butylphenyl)-3-phenylpropanol-1) was examined. Various enantiomers of amino alcohols, amino acids, and amines were well resolved with Cu(II) ion solution as eluent at room temp.[16(l)]

1.5.4. Other metal complexes

A chiral P, N, O donor ligand prepared by treating (S)-phenylglycinol with 2-diphenylphosphinobenzaldehyde was complexed *in situ* with $Ru(DMSO)_4Cl_2$ in propanol and is found to be active for asymmetric transfer hydrogenation reaction. Preformed complex which is octahedral as evidenced by X-ray crystallography, was found to be less active compared to *in situ* generated complex catalyst.[17(a)] Palladium complexes prepared *in situ* from $[Pd(\eta^3\text{-}C_3H_5)Cl]_2$ and a number of chiral P, N, O donor Schiff base ligands were evaluated as catalysts for allylic substitution reactions.[17(b)]

A catalytic method for the enantioselective ring opening of meso-aziridines by $TMSN_3$ with tridentate Schiff base chromium complexes derived from 1- amino-2-indanol was reported (Scheme 1.8).[17(c)]

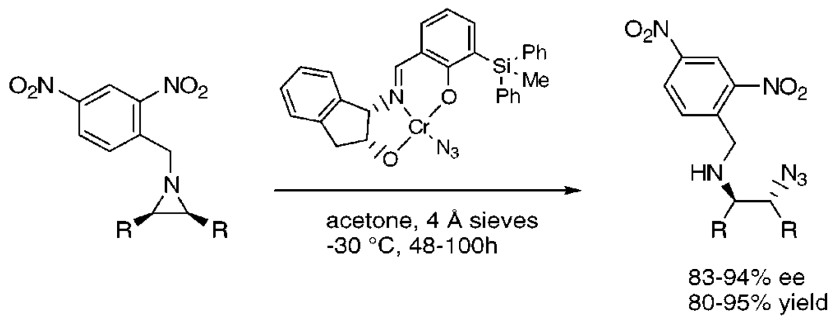

Scheme 1.8. Chiral chromium complex derived from 1- amino-2-indanol as catalyst for enantioselective ring opening of meso-aziridines.

Enantioselective reduction of acetophenone is achieved in high yields with moderate enantioselectivity by using $LiAlH_4$ in combination with chiral Schiff bases prepared from various carbonyl groups and β-amino alcohols.[17(d)]

Highly efficient and selective catalysts for the asymmetric reduction of aryl alkyl ketones were obtained by combining a class of pseudo-dipeptides derived from chiral amino alcohols with Ru precursor.[17(e)] Recently, the same group reported direct *in situ* formation of both chiral amino alcohol based pseudo-dipeptide ligand and its Ru complex catalyst in the same reaction media used for catalytic reactions.[17(f)]

The use of perfluoro substituted amino alcohols in the catalytic asymmetric additions of organo-zinc reagents to aldehydes afforded products with high enantioselectivity. In this study, features such as temperature effect on the enantioselectivity, minimal amino alcohol loading and an efficient recycling of the amino alcohols were highlighted.[17(g)]

Telfer *et al* developed a new ligand system based on chiral amino alcohols, in which the ligands are centered on a benzene core with chiral arms radiating out. These arms can be arranged in *ortho*, *meta*, *para*, or 1,3,5 fashion around the benzene core (Figure 1.12).

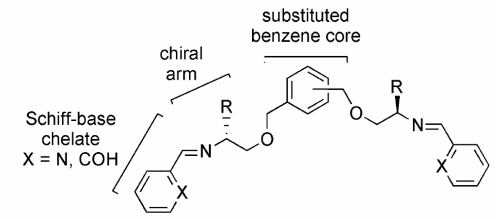

Figure 1.12. Chiral amino alcohol based ligand system anchored on a benzene ring.

The aim was to investigate the influence of their relative orientation on the structure of the resulting metallo supramolecular assembly. Since the chiral arms are derived from amino alcohols, a large number of enantiopure candidates can be prepared. The coordination chemistry of this ligand system with Co and Ni metal ions has been reported. These ligands (Scheme 1.9) react with $CoCl_2$ to give dinuclear complexes $[Co_2L_2Cl_2]_2^+$ (Figure 1.13) which form with high (>95%) diastereoselectivity; i.e., the chirality of these ligands efficiently predetermines the stereochemistry of the resulting cobalt(II) centers.[17(h,i)]

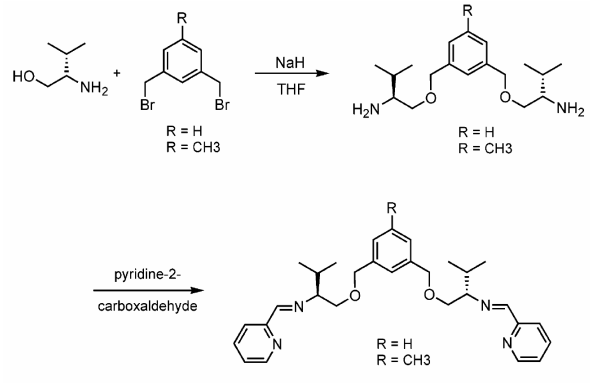

Scheme 1.9

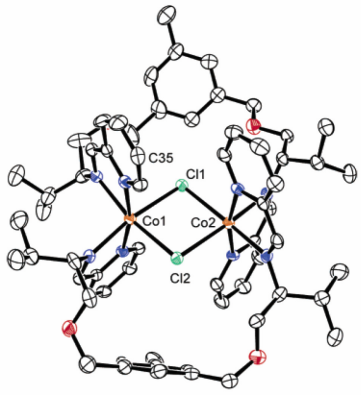

Figure 1.13

Scheme 1.9: Chiral amino alcohol based ligand system centered on a benzene and **Figure 1.13:** the crystal structure of a cobalt complex derived from this ligand.

Optically active amino alcohol chromium complexes were synthesized from enantiomerically pure indanone and have been used as chiral catalysts in the asymmetric addition of diethylzinc to benzaldehyde.[17(j)]

1.5.5. Polymer supported systems

In addition to the use of chiral amino alcohols as ancillary ligands as well as asymmetric catalyst precursors in homogeneous catalysis, they have also found application as catalysts attached to a polymer support.[18(a)] The following polymer-supported amino alcohols **a-c** (Scheme 1.10) have been prepared and subsequently used as chiral ligands in the catalytic addition of diethylzinc to aromatic and aliphatic aldehydes, to afford the corresponding (*S*)-1-substituted 1-propanols in good yields and enantiomeric excess.[18(b)]

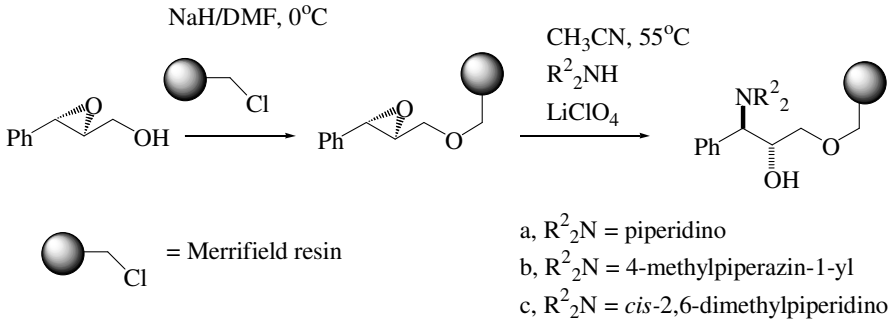

Scheme 1.10. Polymer supported chiral amino alcohols used as ligands in the catalytic addition of diethylzinc to aldehydes to give the corresponding alcohols.

A readily available chiral amino alcohol ((R)-1,1,2-triphenyl-2-(piperazin-1-yl)ethanol) has been immobilized on silica by solgel synthesis and grafting. The solid prepared according to the latter method led to the best enantioselectivity described for the asymmetric addition of diethylzinc to benzaldehyde using inorganic solids (Scheme 1.11).[18(c)]

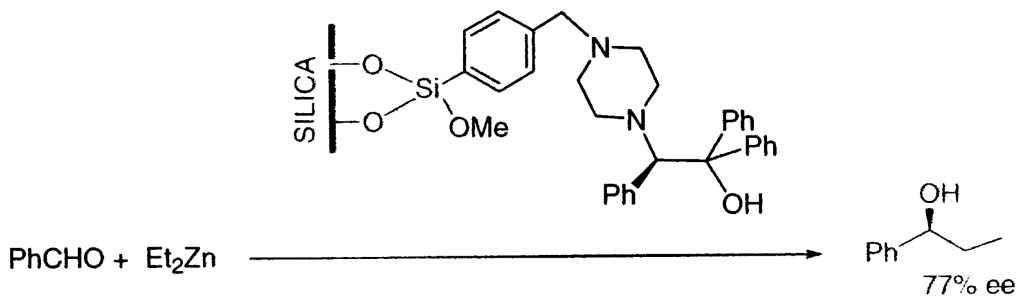

Scheme 1.11. Silica immobilized chiral amino alcohol based ligand system used as ligands in the asymmetric addition of diethylzinc to benzaldehyde.

A cross linked polystyrene resin containing chiral primary amino alcohol moieties is found to be a useful regenerable chiral auxiliary in the enantioselective catalytic alkylation of aldehydes. The primary amino groups of the chiral amino alcohols react with the aldehydes to form Schiff bases, which catalyze the addition of dialkylzinc to aldehydes leading to optically active secondary alcohols in good enantiomeric purity.[18(d)]

1.6. Biological relevance of amino alcohol based Schiff base ligands

Chiral and achiral amino alcohol based Schiff bases are generally employed as ligands for bioinorganic modeling studies. Structure and reactivity studies of the transition metal complexes of such ligands containing $-H_2C-$, NH– and –HC=N– moieties have been considered to be important in the bioinorganic chemistry owing to the biomimetic nature of such complexes in the context of metalloenzymes.

Wardeska *et al* have studied dinuclear copper complexes of chiral amino alcohols based Schiff base ligands as biomimetic models. Their argument was that chiral amino alcohol based Schiff bases can induce sufficient dissymmetry in the resulting complexes making them better models since the copper containing proteins are believed to contain copper in a dissymmetric ligand environment.[19(a)]

Pecoraro *et al* synthesized mononuclear Mn(IV) complexes in an effort to model the active site of oxygen evolving complex (OEC) of Photosystem II using hydroxyl rich Schiff base ligands derived from achiral amino alcohol derivatives.[19(b)]

In an attempt to mimic bioinorganic systems, mono- di- and trinuclear Ni(II) complexes have been synthesized from Schiff base ligands made of salicylaldehyde and β-substituted achiral amino alcohols.[12(i)] The same type of ligands has been used to prepare Cu(II) complexes which are expected to act as models for the type III copper enzymes.[19(c)] Biomimetic alkoxo bound monooxo and dioxovanadium(V) complexes are prepared and structurally characterized from achiral amino alcohol based Schiff bases containing alkoxo, phenolate and imine donor groups by the same group.[19(d)]

1.7. Supramolecular chemistry of amino alcohol based Schiff bases

Synthesis and characterization of transition metal supramolecular compounds are of current interest due to their potential applications related to inclusion phenomena, guest exchange, catalytic properties and molecular based magnetism. However, the supramolecular chemistry of chiral amino alcohol based systems is not explored much. The element of chirality in the building blocks can have considerable influence on the final outcome of the self assembly process resulting in entirely new supramolecular products. For example, the helices which are inherently chiral can possess either plus (P) or minus (M) handedness. Metal directed assembly of achiral ligands to form helicates must give a racemic mixture of enantiomeric P and M helices if parity is conserved. In order to obtain excesses of the P or M helicates, it is necessary to have an additional source of chirality in the system. This is most readily achieved through the use of chiral ligands. A number of self assembly process involving chiral ligands are reported.[20(a)]

There are some recent reports on achiral ligands derived from amino alcohols giving supramolecular arrangements in their crystal lattice. For example, Q. –L. Liu *et al* have demonstrated that various supramolecular structures can be obtained starting

from tridentate and tetradentate ligands containing amino, alcoholic and phenolic groups. In these complexes the phenol and the alkoxy groups act as bridging and hydrogen bonding functionalities. As a result of this, various coordination assemblies ranging from hexanuclear clusters, 1D heterometallic coordination polymers to undulated 2D network are obtained (Figure 1.14).[12(e)]

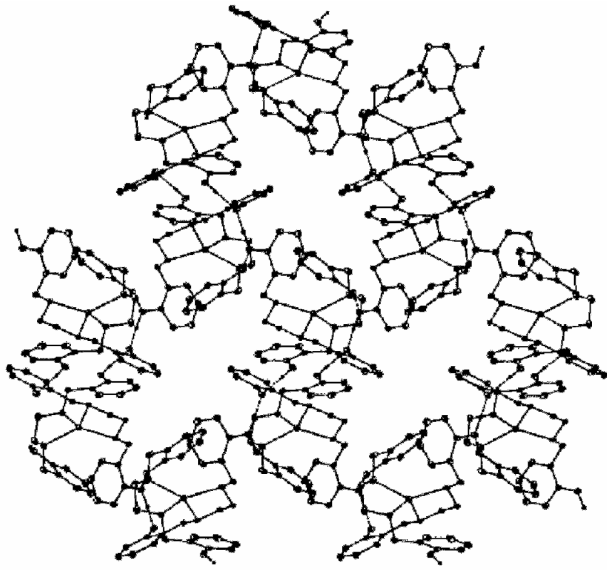

Figure 1.14. Supramolecular 2D sheet like coordination assembly obtained from achiral amino alcohol based ligands.

Supramolecular structures of Co(III) and Cu(II) complexes of a Schiff base derived polydentate ligand containing alcohol and phenol groups have been reported recently.[12(f)] In copper complex, each molecule is connected to adjacent ones through multiple hydrogen bonds involving the alcoholic, phenolic and amino groups affording a 2D structure (Figure 1.15).

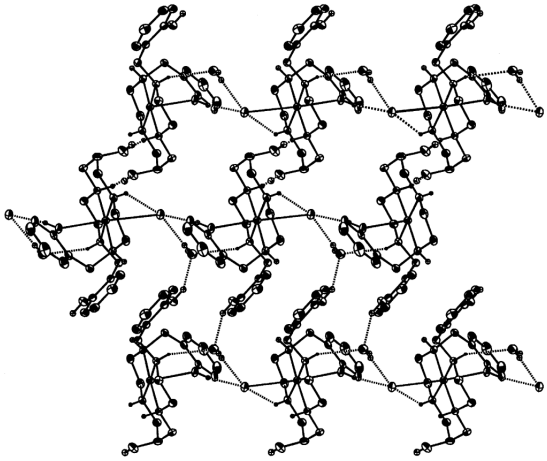

Figure 1.15. A two dimensional supramolecular coordination assembly of copper complexes prepared from phenol and alcohol containing ligands.

In the crystal structure of the Co complex, alcoholic hydrogen bonding forms a 1D supramolecular structure along *c*-axis (Figure 1.16).

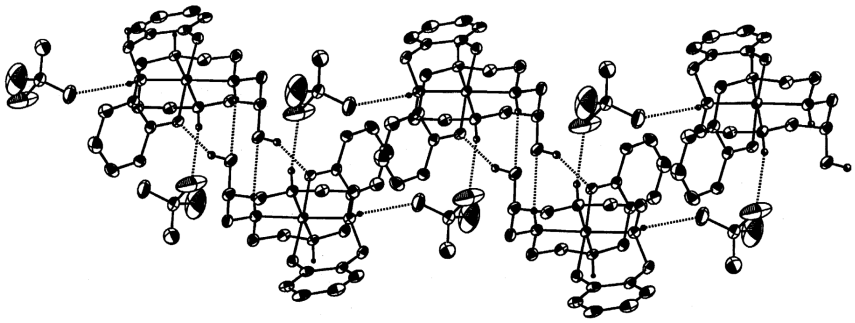

Figure 1.16. Alcoholic hydrogen bonded 1D supramolecular assembly of cobalt complexes.

Mn(IV) and Co(III) complexes of tridentate ONO donor Schiff base ligands made up of achiral amino alcohol have been reported.[12(g)] Supramolecular interactions of both C–H···O and O–H···O type in the case of Co complex lead to the stacking of molecular units resulting in the formation of cavities in the crystal lattice as shown in Figure 1.17.

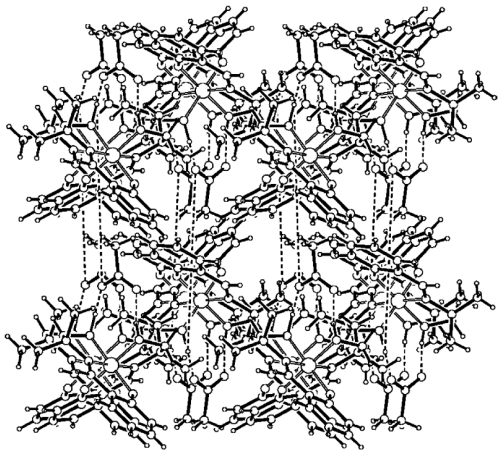

Figure 1.17. C–H···O and O–H···O interactions in a cobalt complex leading to the formation of cavities in the crystal lattice.

Rao *et al* reported a series of mono- di- and tri-nuclear Ni(II) complexes of N, O donating Schiff base ligands derived from achiral amino alcohols. All these complexes exhibited interesting crystal structures due to O–H···O interactions and some of these led to the formation of channels in the crystal lattice filled with methanol or metal ion bound acetate moieties.[12(i)]

Liao *et al* reported a supramolecular octanuclear copper(II) complex derived from an achiral amino alcohol based Schiff base ligand 2-salicylideneamino-1-ethanol. The structure consists of two tetracopper(II) cubane units related by hydrogen bonds.[20(b)]

1.8. Aim of the present investigation

Chiral metal complexes are promising new materials in various branches of chemistry. Synthesis and structural characterization of enantiopure metal complexes are thus important tasks in modern chemistry. The chemistry of chiral amino alcohol based complexes is relevant in this context and they have found wide applications in asymmetric synthesis and bioinorganic chemistry. Although a number of chiral amino alcohol based complexes are employed as catalysts in asymmetric synthesis, structural

and coordination chemistry of such systems has not been explored much. The known chemistry is dominated by metal ions like Ti^{4+}, V^{5+} etc. Understanding the coordination properties - coordination mode, nuclearity, bridging properties, metal oxidation state etc. - of such systems will help to design new systems with desirable properties. Interest in ligands containing phenoxy and alkoxy groups also lies in their relevance to the coordination environments of active sites of metalloenzymes since some of the metalloenzymes are believed to contain oxo bridges in their active sites.

With respect to the supramolecular chemistry of inorganic complexes, introduction of chirality in to the ligand back bone may have tremendous influence on the resulting supramolecular organization. Chiral amino alcohol based Schiff bases are simple and efficient systems to study such effects. Also one can probe the effects of various hydrogen bonding substituents on the supramolecular chemistry of the resulting structures.

From the previous sections of this chapter, it can be seen that structural, supramolecular and coordination chemistry aspects of chiral amino alcohol based Schiff base complexes are not well addressed in the literature especially the case of Cu, Co and Mn metals which are of biological and catalytic relevance. In this study, attempts are made to discuss the structural, supramolecular and coordination chemistry aspects of these metal complexes with chiral amino alcohol based Schiff bases. Results are analyzed based on various structure-directing factors like the metal coordination preferences, hydrogen bonds, bridging groups, steric effects etc. Our interest also includes checking whether some of these Schiff base complexes are capable of catalyzing epoxidation reaction of simple olefins using PhIO as the oxidizing agent.

1.9. References

1. (a) J. March, *Advanced Organic Chemistry*, Wiley, New York, 1992; (b) S. Patai, in *The Chemistry of Carbon-Nitrogen Double Bond,* ed. S. Patai, Wiley, New York, 1970, 276; (c) K. Harada, in *The Chemistry of Carbon-Nitrogen Double Bond,* ed. S. Patai, Wiley, New York, 1970, 266; (d) C. Wittig, H. D. Frommeld and B. Suchanek, *Angew. Chem., Int. Ed. Engl.,* 1963, **2**, 683.
2. (a) H. Schiff, *Ann. Suppl.,* 1864, **3**, 343; (b) C. Ettling, *Ann.,* 1840, **35**, 241; (c) H. Schiff, *Ann.,* 1869, **150**, 193; (d) H. Schiff, *Ann.,* 1869, **151**, 186.
3. (a) S. Yamada, *Coord. Chem. Rev*., 1999, **190-192**, 537; (b) K. S. Murray, in *Advanced Inorganic Chemistry*, ed. A. G. Sykes, **vol. 43**, Academic Press, San Diego, CA, 1995, pp. 261-358; (c) R. Noyori, *Asymmetric Catalysis in Organic Synthesis,* Wiley, New York, 1994; (d) *Catalytic Asymmetric Synthesis,* ed. I. Ojima, VCH Publishers, New York, 1993; (e) *Comprehensive Asymmetric Catalysis*, eds. E. N. Jacobsen, A. Pfaltz and H. Yamamoto, Springer-Verlag, Berlin, 1999; (f) G. –Q. Lin, Y. –M. Li and A. S. C. Chan, *Principle and Application of Asymmetric Synthesis*, Wiley-Interscience, John Wiley and Sons, 2001.
4. (a) G. Wilkinson, *Comprehensive Coordination Chemistry*, **Vols. 4-6**, Pergamon Press, Oxford, 1987 (pp. 166-176, 494-495, 634, 638, 687); (b) P. H. Hang, J. G. Keck, E. J. Lien and M. Mc Lai, *J. Med. Chem.,* 1990, **608**, 33; (c) A. E. Tai, E. J. Lien, M. Mc Lai and T. A. Khwaja, *J. Med. Chem*., 1984, **236**, 27; (d) P. D. Beer and D. K. Smith, in *Progress in Inorganic Chemistrty,* ed K.D. Karlin, **vol. 39**, John Wiley & Sons, New York, USA, 1982, p. 1; (e) V. McKee, in *Advanced Inorganic Chemistry*, ed A.G. Sykes, **vol. 40**, Academic Press, S. Diego, USA, 1993, p. 323; (f) J. Nelson, V. McKee and G. Morgan, in *Progress in Inorganic Chemistry*, ed. K.D. Karlin, **vol. 47**, John Wiley & Sons, New York, USA, 1998, p. 167; (g) S. Brooker, *Coord. Chem. Rev.,* 2001, **222**, 33; (h) *Cation Binding by Macrocycles,* eds. Y. Inone and G. W. Gokel, Marcel Dekker Inc., New York, USA, 1990; (i) *Supramolecular*

Chemistry of Anions, eds. A. Branchi, K. Bowman-James and E. Garcia-Espan˜a, Wiley-VCH, New York, USA, 1997; (j) V. Amendola, L. Fabbrizzi, C. Mangano, P. Pallavicini, A. Poggi and A. Taglietti, *Coord. Chem. Rev.,* 2001, **219–221**, 821; (k) K. Bernauer, S. Ghizdavu and L. Verardo, *Coord. Chem. Rev.,* 1999, **190–192**, 357.

5. E. L. Eliel and S. H. Wilen, *Stereochemistry of Organic Compounds*, Wiley, New York, 1994.
6. G. M. Loudon, *Organic Chemistry*, Addison-Wesley Publishing Co., Massachusetts, 1984, 231.
7. L. Pasteur, *Am. Chim. Phys*., 1848, **24**, 442.
8. (a) A.Von Zelewsky and O.Mamula, *J. Chem. Soc., Dalton Trans.,* 2000, 219; (b) U. Knof and A. Von Zelewsky, *Angew. Chem., Int. Ed.,* 1999, **38**, 303; (c) M. Ziegler and A. Von Zelewsky, *Coord. Chem. Rev.,* 1998, **177**, 257; (d) A. Juris, V. Balzani, F. Barigelletti, S. Campagna, P. Belser and A. Von Zelewsky, *Coord. Chem. Rev.*, 1988, **84**, 85; (e) C. Provent, A. F. Williams, in *Transition Metals in Supramolecular Chemistry*, ed. J. P. Sauvage, John Wiley and Sons, New York, 1999, pp 135-191; (f) R. Büchner, J. S. Field and H. Raymond, *Inorg. Chem*., 1997, **36**, 3952; (g) V. H. Houlding and V. M. Miskowski, *Coord. Chem. Rev*., 1991, **111**, 145; (h) A. Von Zelewsky, P. Belser, P. Hayoz, R. Dux, X. Hua, A. Suckling *et al*, *Coord. Chem. Rev.,* 1994, **132**, 75; (i) J. Zyss, C. Dhenaut, T. Chauvan and I. Ledoux, *Chem. Phys. Lett.,* 1993, **206**, 409; (j) N. J. Long, *Angew. Chem., Int. Ed. Engl.,* 1995, **107**, 37; (k) *Supramolecular Chemistry,* eds. V. Balzani and L. De Cola, NATO ASI Series, Kluwer Academic Publishers, Dordrecht, 1992.
9. (a) M. A. Alam, M. Nethaji and M. Ray, *Angew. Chem., Int. Ed*., 2003, **42**, 1940; (b) X. –W Liu, N. Tang, Y. –H. Chang and M. –Y. Tan, *Tetrahedron Asymmetry,* 2004, **15**, 1269; (c) C. –T. Yang, M. Vetrichelvan, X. Yang, B. Moubaraki, K. S. Murray and J. J. Vittal, *Dalton Trans.,* 2004, 113; (d) K. –Y. Choi, Y. –M. Jeon, H. Ryu, J. –J. Oh, H. –H. Lim and M. –W. Kim,

Polyhedron, 2004, **23**, 903; (e) P. Deschamps, P. P. Kulkarni and B. Sarkar, *Inorg. Chem*., 2003, **42**, 7366; (f) C. –T. Yang, B. Moubaraki, K. S. Murray and J. J. Vittal, *Dalton Trans*., 2003, 880; (g) J. J. Vittal and X. Yang, *CrystGrowthDes.,* 2002, **2**, 259; (h) R. –M. Wang, C. –J. Hao, Y. –P. Wang and S. –B. Li, *J. Mol. Catal. A: Chem*., 1999, **147**, 173.

10. (a) A. Abiko and S. Masamune, *Tetrahedron Lett.,* 1992, **33**, 5517; (b) M. J. McKennon and A. I. Meyers, *J. Org. Chem.,* 1993, **58**, 3568.
11. (a) J. L. Vicario, D. Badía, L. Carrillo, E. Reyes and J. Etxebarria, *Curr. Org. Chem.,* 2005, **9**, 219; (b) G. Lu, Y. –M. Li, X. –S. Li and A. S. C. Chan, *Coord. Chem. Rev*., 2005, **249**, 1736; (c) L. Pu and H. –B Yu, *Chem. Rev*., 2001, **101**, 757; (d) D. J. Ager, I. Prakash and D. R. Schaad, *Chem. Rev*., 1996, **96**, 835.
12. (a) C. R. Cornman, G. J. Colpas, J. D. Hoeschele, J. Kampf and V. L. Pecoraro, *J. Am. Chem. Soc.,* 1992, **114**, 9925; (b) C. J. Carrano, C. M. Nunn, R. Quan, J. A. Bonadies and V. L. Pecoraro, *Inorg. Chem.*, 1990, **29**, 944; (c) D. C. Crans, H. Chen, O. P. Anderson and M. M. Miller, *J. Am. Chem. Soc*., 1993, **115**, 6769; (d) D. C. Crans, P. M. Ehde, P. K. Shin and L. Pettersson, *J. Am. Chem. Soc*., 1993, **113**, 3728; (e) Y. Xie, Q. Liu, H. Jiang and J. Ni, *Eur. J. Inorg. Chem*., 2003, 4010; (f) Y. –S. Xie, X. –T. Liu, M. Zhang, K. –J. Wei and Q. –L. Liu, *Polyhedron*, 2005, **24**, 165; (g) M. Dey, C. P. Rao, P. K. Saarenketo, K. Rissanen, E. Kolehmainen and P. Guionneau, *Polyhedron*, 2003, **22**, 3515; (h) M. Dey, C. P. Rao, P. Saarenketo, K. Rissanen and E. Kolehmainen, *Eur. J. Inorg. Chem.,* 2002, 2207; (i) M. Dey, C. P. Rao, P. K. Saarenketo and K. Rissanen, *Inorg. Chem. Commun*., 2002, **5**, 924.
13. (a) T. D. Owens, A. J. Souers and J. A. Ellman, *J. Org. Chem*., 2003, **68**, 3; (b) E. N. Jacobsen, *Acc. Chem. Res*., 2000, **33**, 421.
14. (a) M. Hayashi, Y. Miyamoto, T. Inoue and N. Oguni, *J. Org. Chem.,* 1993, **58**, 1515; (b) M. Hayashi, T. Inoue, Y. Miyamoto and N. Oguni, *Tetrahedron,* 1994, **50**, 4385; (c) Á. Gama, L. Z. Flores-López, G. Aguirre, M.

Parra-Hake, R. Somanathan and T. Cole, *Tetrahedron: Asymmetry,* 2005, **16**, 1167; (d) L. Z. Flores-Lopéz., M. Parra-Hake, R. Somanathan and P. J. Walsh, *Organometallics*, 2000, **19**, 2153; (e) Q. Tian, C. Jiang, Y. Li , C. Jiang and T. You, *J. Mol. Catal. A: Chem.,* 2004, **219**, 315; (f) V. Banphavichit, W. Mansawat, W. Bhanthumnavin and T. Vilaivan, *Tetrahedron*, 2004, **60**, 10559; (g) R. Fleischera, H. Wunderlich and M. Braun, *Eur. J. Org. Chem.,* 1998, 1063; (h) C. K. Hoa, A. D. Schuler, C. B. Yoo, S. R. Herron, K. A. Kantardjieff and A. R. Johnson, *Inorg. Chim. Acta*, 2002, **431**, 71; (i) J. M. Hoover, J. R. Petersen, J. H. Pikul and A. R. Johnson, *Organometallics,* 2004, **23**, 4614; (j) J. R. Petersen, J. M. Hoover, W. S. Kassel, A. L. Rheingold and A. R. Johnson, *Inorg. Chim. Acta,* 2005, **358**, 687.

15. (a) C. Bolm and F. Bienewald, *Angew. Chem., Int. Ed. Engl.,* 1995, **34**, 2640; (b) G. Liu, D. A. Cogan and J. A. Ellman, *J. Am. Chem. Soc.*, 1997, **119**, 9913; (c) D. A. Cogan, G. Liu, K. Kim, B. J. Backes and J. A. Ellman, *J. Am. Chem. Soc.,* 1998, **120**, 8011; (d) S. A. Blum, R. G. Bergman and J. A. Ellmann, *J. Org. Chem.*, 2003, **68**, 150; (e) Á. Gama, L. Z. Flores-López, G. Aguirre, M. Parra-Hake, L. H. Hellberg and R. Somanathan, *ARKIVOC* 2003, **11**, 4; (f) A. Barbarini, R. Maggi, M. Muratori, G. Sartori and R. Sartorio, *Tetrahedron: Asymmetry,* 2004, **15**, 2467; (g) J. Hartung, S. Drees, M. Greb, P. Schmidt, I. Svoboda, H. Fuess, A. Murso and D. Stalke, *Eur. J. Org. Chem.,* 2003, 2388.
16. (a) T. Aratani, Y. Yoneyoshi and T. Nagase, *Tetrahedron Lett.*, 1975, 1707; (b) T. Aratani, Y. Yoneyoshi and T. Nagase, *Tetrahedron Lett.*, 1977, 2599; (c) T. Aratani, *Pure Appl. Chem.*, 1985, **57**, 1839; (d) Z. Li, G. Liu, Z. Zheng and H. Chen, *Tetrahedron,* 2000, **56**, 7187; (e) Z. Li, Z. Zheng, B. Wan and H. Chen, *J. Mol. Catal. A: Chem.,* 2001, **165**, 67; (f) L. Cai, H. Mahmoud and Y. Han, *Tetrahedron: Asymmetry,* 1999, **10**, 411; (g) C. Jiang, Z. Ming, Q. Tan, D. Qian and T. You, *Enantiomer*, 2002, **7**, 287; (h) M. Itagaki, K. Hagiya, M. Kamitamari, K. Masumoto, K. Suenobu and Y. Yamamoto,

Tetrahedron, 2004, **60**, 7835; (i) K. Yanagi and M. Minobe, *Acta Cryst.,* 1987, **C43**, 2060; (j) K. Yanagi and M. Minobe, *Acta Cryst*., 1987, **C43**, 1045; (k) Y. Yuan, J. Yao, J. Lu, Y. Zhang and R. Gu, *Inorg. Chem. Commun*., 2005, **8**, 1014; (l) N. Oi, H. Kitahara, R. Kira and F. Aoki, *Anal. Sci*., 1991, **7**, 151.

17. (a) H. –L. Kwong, W. –S. Lee, T. –S. Lai and W. –T. Wong, *Inorg. Chem. Commun.,* 1999, **2**, 66; (b) H. –L. Kwong, L. –S Cheng and W. –S. Lee, *J. Mol. Catal. A: Chem.,* 1999, **150**, 23; (c) Z. Li, M. Fernández and E. N. Jacobsen, *Org. Lett.,* 1999, **1**, 1611; (d) R. Tümerdem, G. Topal and Y. Turgut, *Tetrahedron: Asymmetry*, 2005, **16**, 865; (e) A. Bøgevig, I. M. Pastor and H. Adolfsson, *Chem. Eur. J.*, 2004, **10**, 294; (f) P. Västilä, J. Wettergren and H. Adolfsson, *Chem. Commun.,* 2005, 4039; (g) J. K. Park, H. G. Lee, C. Bolm and B. M. Kim, *Chem. Eur. J.,* 2005, **11**, 945; (h) S. G. Telfer, R. Kuroda and T. Sato, *Chem. Commun.,* 2003, 1064; (i) S. G. Telfer, T. Sato, R. Kuroda, J. Lefebvre, and D. B. Leznoff, *Inorg. Chem.,* 2004, **43**, 421; (j) S. Malfait, L. Pélinski and J. Brocard, *Tetrahedron: Asymmetry,* 1996, **7**, 653.
18. (a) S. V. Luis, B. Altava, M. I. Burguete, M. Collado, J. Escorihuela, E. García-Verdugo, M. J. Vicent and J. Martens, *Ind. Eng. Chem. Res*., 2003, **42**, 5977; (b) A. Vidal-Ferran, N. Bampos, A. Moyano, M. A. Pericás, A. Riera, and J. K. M. Sanders, *J. Org. Chem.,* 1998, **63**, 6309; (c) J. M. Fraile, J. A. Mayoral, J. Serrano, M. A. Pericàs, L. Solà, and D. Castellnou, *Org. Lett.,* 2003, **5**, 4333; (d) S. Itsuno, Y. Sakurai, K. Ito, T. Maruyama, S. Nakahama and J. M. J. Fréchet, *J. Org. Chem.,* 1990, **55**, 304.
19. (a) J. C. Brown and J. G. Wardeska, *Inorg. Chem.,* 1982, **21**, 1530; (b) D. P. Kessissoglou, X. Li, W. M. Butler and V. L. Pecoraro, *Inorg. Chem.,* 1987, **26**, 2487; (c) M. Dey, C. P. Rao, P. K. Saarenketo and K. Rissanen, *Inorg. Chem. Commun.,* 2002, **5**, 380; (d) G. Asgedom, A. Sreedhara, J. Kivikoski, J. Valkonen, E. Kolehmainen and C. P. Rao, *Inorg. Chem.,* 1996, **35**, 5674.

20. (a) G. Baum, E. C. Constable, D. Fenske, C. E. Housecroft and T. Kulke, *Chem. Eur. J.,* 1999, **5**, 1862 and references therein; (b) S. –F. Si, J. –K. Tang, D. –Z. Liao, Z. –H. Jiang and S. –P. Yan, *Inorg. Chem. Commun.,* 2002, **5**, 76.

Chapter 2

Materials and experimental methods

2.1. Abstract

Synthetic procedures and characterization data for the chiral Schiff base ligands H_2L^1-H_2L^8 and their Mn, Co and Cu complexes used in this study are provided in this chapter. Spectral properties of all the ligands are discussed along with the single crystal X-ray structural characterization of one of the chiral Schiff bases H_2L^8. A listing of all the chemicals and other materials used and a brief discussion of the various physicochemical techniques employed during the course of the investigation are also presented.

2.2. Materials

Salicylaldehyde, 5-bromosalicylaldehyde, 5-nitrosalicylaldehyde, (S)-(+)-2-phenylglycinol and (S)-(−)-2-Amino-3-phenyl-1-propanol (L-phenylalaninol) were purchased from Lancaster (India) and used as received. Styrene, *trans*-stilbene and iodosobenzene diacetate used for epoxidation studies were purchased from Lancaster (India) and used without further purifications. Styrene oxide and *trans*-stilbene oxide were procured from Aldrich Chemical Company Inc. USA. Tetrabutylammoniumperchlorate (TBAP), used as the supporting electrolyte in electrochemical measurements, $CDCl_3$ and 5-methoxysalicylaldehyde were purchased from Acros (India). L. R. Grade solvents were purchased from Leonid Chemicals, Pvt Ltd. Bangalore, India and used as received. Solvents used for UV, CD and GC analyses were of HPLC grade and procured from E. Merck (India). The metal salts used were of analytical grade and purchased from S. D. Fine Chem. Ltd (India). All other chemicals used were of analytical grade.

2.3. Physical measurements

Microanalytical (C, H, N) data were obtained with a Perkin-Elmer Model 240C elemental analyzer. A Shimadzu 3101- PC UV/VIS/NIR spectrophotometer was used to record the electronic spectra. Infrared spectra were recorded by using KBr pellets on a Jasco-5300 FT-IR spectrophotometer. ^1H NMR spectra in $CDCl_3$ solution were recorded on a Bruker DRX-400 spectrometer using $Si(CH_3)_4$ as an internal standard. Room temperature solid state magnetic susceptibilities were measured by using a Sherwood Scientific magnetic susceptibility balance. A CH-Instruments model 620A electrochemical analyzer was used for cyclic voltammetric experiments with acetonitrile solutions of the complexes containing TBAP as supporting electrolyte. The three-electrode measurements were carried out at 298 K under a dinitrogen atmosphere with a platinum disc working electrode, a platinum wire auxiliary electrode and an Ag/AgCl reference electrode. Optical rotations were

measured with an AUTOPOL-II automatic polarimeter (readability ±0.01°). The CD spectra were measured in solution phase with a JASCO J-810 spectropolarimeter. EPR spectra were recorded on a Jeol JES-FA200 spectrometer.

Gas chromatographic analyses were carried out on a Shimadzu GC 14B instrument equipped with a stainless steel packed column (5 m, 5 % SE 30), a chiral capillary column (Supelco α-DEX 325, 30m length, 0.25mm id, 0.25μm film thickness) and a flame ionization detector.

2.4. Synthesis and characterization of Schiff bases (H_2L^1-H_2L^8)

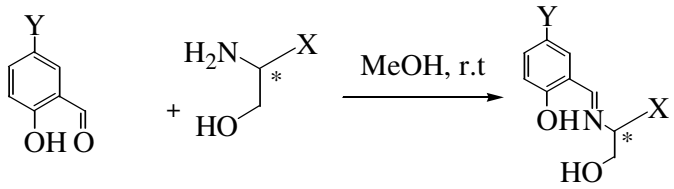

H_2L^1. X = Ph, Y = H
H_2L^2. X =CH_2-Ph, Y = H
H_2L^3. X = Ph, Y = OMe
H_2L^4. X = CH_2-Ph, Y = OMe
H_2L^5. X = Ph, Y = Br
H_2L^6. X = CH_2-Ph, Y = Br
H_2L^7. X = Ph, Y = NO_2
H_2L^8. X = CH_2-Ph, Y = NO_2

Scheme 2.1. Synthetic scheme for chiral Schiff bases H_2L^1-H_2L^8.

All the chiral ligands H_2L^1-H_2L^8 (Scheme 2.1) are synthesized in good yields by the Schiff base condensation of one equivalent of salicylaldehyde/substituted salicylaldehyde with one equivalent of the respective chiral amino alcohol in methanol at room temperature. They are characterized by elemental, IR, ^{1}H NMR, UV-Vis and circular dichroism spectroscopy techniques. Synthesis and characterization details for each ligand are given below.

H_2L^1

(S)-(+)-2-phenylglycinol (0.137 g, 1 mmol) and salicylaldehyde (0.122 g, 1 mmol) were stirred together in methanol (15 mL) for 1 h at room temperature. The resulting yellow solution was filtered and the filtrate was kept for 2 days in an open beaker for slow evaporation. Yellow, needle-shaped crystals, precipitated during this time, were collected by filtration, washed with hexane and dried at room temperature.

MF: $C_{15}H_{15}NO_2$, MW: 241.29, Yield: 97 %.

Anal. calcd. (found) for $C_{15}H_{15}NO_2$: C, 74.67 (75.02); H, 6.27 (6.16); N, 5.81 (5.79) %.

IR (KBr, cm^{-1}): 3214, 2852, 1626, 1577, 1491, 1458, 1383, 1273, 1211, 1153, 1118, 1062, 916, 857, 806, 754, 692, 636, 520, 457.

^{1}H NMR (400 MHz, $CDCl_3$): δ 3.95 (d, J = 6.12 Hz, 2H, CH_2), δ 4.49 (t, J = 6.49 Hz, 1H, CH), δ 6.864-7.008 (m, 2H, Ar), δ 7.269-7.403 (m, 7H, Ar), δ 8.5 (s, 1H).

UV/Vis (CH_3CN); λ_{max}/nm ($\varepsilon/M^{-1}cm^{-1}$): 315 (4290), 255 (14180).

CD (CH_3CN, 10^{-4}M); λ_{max}/nm (mdeg): 315 (–5.92), 255 (–10.57).

H_2L^2

L-phenylalaninol [(S)-(–)-2-Amino-3-phenyl-1-propanol] (0.151 g, 1 mmol) and salicylaldehyde (0.122 g, 1 mmol) were stirred together in methanol (15 mL) for 1 h at room temperature. The resulting yellow solution was filtered and the filtrate was kept for 2 days in an open beaker for slow evaporation. Yellow precipitate of H_2L^2 thus obtained was washed with hexane and dried at room temperature.

MF: $C_{16}H_{17}NO_2$, MW: 255.31, Yield: 77 %.

Anal. calcd. (found) for $C_{16}H_{17}NO_2$: C, 75.27 (74.98); H, 6.71 (6.67); N, 5.49 (5.65) %.

IR (KBr, cm^{-1}): 3256, 2922, 2868, 1631, 1579, 1494, 1460, 1412, 1334, 1280, 1194, 1149, 1114, 1097, 1039, 970, 914, 833, 775, 756, 702, 655, 567, 474, 457.

^{1}H NMR (400 MHz, $CDCl_3$): δ 2.94 (m, 2H, CH_2-Ph), 3.54 (m, 1H, CH), 3.814 (m, 2H, CH_2-OH), 6.838-7.340 (m, 9H, Ar), 8.1 (s, 1H, HC=N).

UV/Vis (CH_3CN); λ_{max}/nm (ε/$M^{-1}cm^{-1}$): 315 (4689), 255 (13647).

CD (CH_3CN, 10^{-4}M); λ_{max}/nm (mdeg): 315 (−4.05), 255 (−8.6).

H_2L^3

(S)-(+)-2-phenylglycinol (0.137 g, 1 mmol) and 5-methoxysalicylaldehyde [2-hydroxy-5-methoxybenzaldehyde] (0.152 g, 1 mmol) were stirred together in methanol (15 mL) for 3 h at room temperature. The resulting yellow solution was filtered and the filtrate was kept for slow evaporation. A yellow solid obtained was washed with hexane and dried at room temperature.

MF: $C_{16}H_{17}NO_3$, MW: 271.31, Yield: 92 %.

Anal. calcd. (found) for $C_{16}H_{17}NO_3$: C, 70.83 (70.77); H, 6.32 (6.25); N, 5.16 (5.11) %.

IR (KBr, cm^{-1}): 3485, 2860, 1635, 1589, 1491, 1272, 1157, 1068, 1028, 902, 831, 790, 761, 700, 534, 457.

^{1}H NMR (400 MHz, $CDCl_3$): 3.77 (s, 3H, OCH_3), 3.92-3.94 (d, *J* = 6.5 Hz, 2H, CH_2), 4.46-4.49 (t, *J* = 6.44 Hz, 1H, CH), 6.78-6.94 (m, 3H, Ar), 7.26-7.39 (m, 5H, Ar), 8.45 (s, 1H, HC=N).

UV/Vis (CH_3CN); λ_{max}/nm (ε/$M^{-1}cm^{-1}$): 343 (5039), 258 (10309).

CD (CH_3CN, 10^{-4}M); λ_{max}/nm (mdeg): 343 (−12.70), 258 (−19.80).

H_2L^4

L-phenylalaninol (0.151 g, 1 mmol) and 5-methoxysalicylaldehyde (0.152 g, 1 mmol) were stirred together in methanol (15 mL) for 3 h at room temperature. The resulting yellow solution was filtered and the filtrate was kept for slow evaporation. A yellow solid obtained was washed with hexane and dried at room temperature.

MF: $C_{17}H_{19}NO_3$, MW: 285.34, Yield: 90 %.

Anal. calcd. (found) for $C_{17}H_{19}NO_3$: C, 71.56 (71.3); H, 6.71 (6.56); N, 5.01 (4.91) %.
IR (KBr, cm^{-1}): 3422, 1635, 1591, 1493, 1379, 1334, 1271, 1224, 1159, 1037, 908, 821, 761, 702.
^1H NMR (400 MHz, $CDCl_3$): 2.8-3.0 (m, 2H, CH_2), 3.51 (m, 1H, CH), 3.73 (s, 3H, OCH_3), 3.77-3.82 (m, 2H, CH_2-OH), 6.57-6.95 (m, 3H, Ar), 7.13-7.27 (m, 5H, Ar), 8.03 (s, 1H, HC=N).
UV/Vis (CH_3CN); λ_{max}/nm ($\varepsilon/M^{-1}cm^{-1}$): 343 (5025), 258 (7916), 230 (20892).
CD (CH_3CN, 10^{-4}M); λ_{max}/nm (mdeg): 343 (−11.6), 258 (−19.2).

H_2L^5

(S)-(+)-2-phenylglycinol (0.137 g, 1 mmol) and 5-bromosalicylaldehyde [5-bromo-2-hydroxybenzaldehyde] (0.201 g, 1 mmol) were stirred together in methanol (15 mL) for 1 h at room temperature. The resulting yellow solution was filtered and the filtrate was kept for 2 days in an open beaker for slow evaporation. Yellow solid of H_2L^5 thus obtained was washed with hexane and dried at room temperature.
MF: $C_{15}H_{14}BrNO_2$, MW: 320.18 Yield: 87 %.
Anal. calcd. (found) for $C_{15}H_{14}BrNO_2$: C, 56.27 (56.33); H, 4.41 (4.35); N, 4.37 (4.44) %.
IR (KBr, cm^{-1}): 3414, 3026, 2920, 1630, 1568, 1475, 1452, 1371, 1278, 1205, 1182, 1128, 1057, 1028, 914, 893, 852, 823, 761, 698, 638, 625, 559, 530, 459.
^1H NMR (400 MHz, $CDCl_3$): δ 3.95 (d, 2H, J = 6.54 Hz, CH_2-OH), 4.5 (t, 1H, J = 6.55 Hz, CH), 7.28-7.44 (m, 7H, Ar), 6.89 (d, 1H, Ar, *ortho* to OH), 8.43 (s, 1H, HC=N).
UV/Vis (CH_3CN); λ_{max}/nm ($\varepsilon/M^{-1}cm^{-1}$): 327 (4685), 255 (12801).
CD (CH_3CN, 10^{-4}M); λ_{max}/nm (mdeg): 327 (−5.08), 255 (−20.02).

H_2L^6

L-phenylalaninol (0.151 g, 1 mmol) and 5-bromosalicylaldehyde (0.201 g, 1 mmol) were stirred together in methanol (15 mL) for 1 h at room temperature. The resulting

yellow solution was filtered and the filtrate was kept for 2 days in an open beaker for slow evaporation. Yellow solid of H_2L^6 thus obtained was washed with hexane and dried at room temperature.

MF: $C_{16}H_{16}NO_2Br$, MW: 334.21, Yield: 85 %.

Anal. calcd. (found) for $C_{16}H_{16}NO_2Br$: C, 57.5 (57.1); H, 4.83 (4.77); N, 4.19 (4.11) %.

IR (KBr, cm^{-1}): 3364, 3024, 2922, 2870, 1633, 1599, 1570, 1510, 1477, 1365, 1275, 1186, 1072, 1035, 968, 925, 825, 750, 704, 625, 557, 472.

^1H NMR (400 MHz, $CDCl_3$): δ 2.95 (m, 2H, CH_2-Ph), 3.55 (m, 1H, CH), 3.82 (m, 2H, CH_2-OH), 6.86 (d, 1H, Ar, *ortho* to OH), 7.13-7.404 (m, 7H, Ar), 8.01 (s, 1H, HC=N).

UV/Vis (CH_3CN); λ_{max}/nm ($\varepsilon/M^{-1}cm^{-1}$): 326 (4751), 255 (12135).

CD (CH_3CN, $10^{-4}M$); λ_{max}/nm (mdeg): 326 (–6.72), 255 (–18.06).

H_2L^7

(S)-(+)-2-phenylglycinol (0.137 g, 1 mmol) and 5-nitrosalicylaldehyde [2-hydroxy-5-nitrobenzaldehyde] (0.167 g, 1 mmol) were stirred together in methanol (15 mL) for 3 h at room temperature. The resulting yellow solution was filtered and the filtrate was kept for slow evaporation. The resulting yellow solid was collected, washed with hexane and dried at room temperature.

MF: $C_{15}H_{14}N_2O_4$, MW: 286.28, Yield: 87 %.

Anal. calcd. (found) for $C_{15}H_{14}N_2O_4$: C, 62.93 (63.11); H, 4.93 (4.76); N, 9.79 (9.87) %.

^1H NMR (400 MHz, $CDCl_3$): δ = 4.00 (d, J = 7.2 Hz, 2H, CH_2), 4.61 (t, J = 6.4 Hz, 1H, CH), 7.00-7.45 (m, 6H, Ar), 8.20-8.27 (m, 2H, Ar), 8.52 (s, 1H, H-C=N).

IR (KBr, cm^{-1}): 3271, 1649, 1614, 1545, 1350, 1224, 1070, 900, 835, 696.

UV/Vis (CH_3CN); λ_{max}/nm ($\varepsilon/M^{-1}cm^{-1}$): 401 (5611), 320 (12501), 260 (24269), 240 (25881).

CD (CH_3CN, 10^{-4}M); λ_{max}/nm (mdeg): 401 (−0.67), 320 (−3.45), 260 (−2.92), 240 (−1.82).

H_2L^8

L-phenylalaninol (0.151 g, 1 mmol) and 5-nitrosalicylaldehyde (0.167 g, 1 mmol) were stirred together in methanol (15 mL) for 3 h at room temperature. The resulting yellow solution was filtered and the filtrate was kept for 2 days in an open beaker for slow evaporation. Yellow precipitate of H_2L^8 thus obtained was washed with hexane and dried at room temperature.

MF: $C_{16}H_{16}N_2O_4$, MW: 300.31, Yield: 90 %.

Anal. calcd. (found) for $C_{16}H_{16}N_2O_4$: C, 63.99 (64.05); H, 5.37 (5.29); N, 9.33 (9.18) %.

IR (KBr, cm^{-1}): 3470, 1649, 1618, 1543, 1487, 1446, 1404, 1346, 1226, 1134, 1064, 941, 904, 835, 756, 729, 700, 630.

^{1}H NMR (400 MHz, $CDCl_3$): δ 2.97 (m, 2H, CH_2-Ph), 3.65 (m, ^{1}H, CH), 3.86 (m, 2H, CH_2-OH), 6.92 (d, 1H, Ar, *ortho* to OH), 7.2 (m, 5H, Ar), 8.04 (s, 1H, HC=N), 8.06 (d, 1H, Ar, *ortho* to NO_2), 8.15 (m, 1H, Ar, *ortho* to NO_2).

UV/Vis (CH_3CN); λ_{max}/nm (ε/$M^{-1}cm^{-1}$): 401 (6950), 325 (9931), 260 (17447), 240 (17111).

CD (CH_3CN, 10^{-4}M); λ_{max}/nm (mdeg): 401 (−2.66), 320 (−4.66), 260 (−5.85), 240 (−3.85).

2.4.1. Spectral properties of the Schiff bases H_2L^1-H_2L^8

The IR spectra of the ligands show broad peaks in the range of 3210-3500 cm^{-1} due to the phenolic and alcoholic OH groups. The peaks observed at ~2920 and ~2870 cm^{-1} are assigned to aliphatic C−H stretch. Peaks around 1600, 1490 and 1450 cm^{-1} are most probably due to aromatic C=C stretch. These Schiff bases exhibit the ν(C=N) band in the range of 1626-1649 cm^{-1}. The peaks in the range 1028-1070 cm^{-1}

are assigned to alcoholic C–O stretching. The IR band at 625 cm^{-1} in the case of ligands H_2L^5 and H_2L^6 is indicative of the presence of the –Br group. ν_{asym} and ν_{sym} stretches of the $-NO_2$ group present in ligands H_2L^7 and H_2L^8 appears at 1545, 1350 and 1543, 1346 cm^{-1} respectively.[1] The ^1H NMR spectra of the ligands show azomethine proton signal in the range δ 8.0-8.5 ppm. Detailed NMR peak assignments are given in synthetic details (Section 2.4). Representative ^{1}HNMR spectra are given in Figure 2.1.

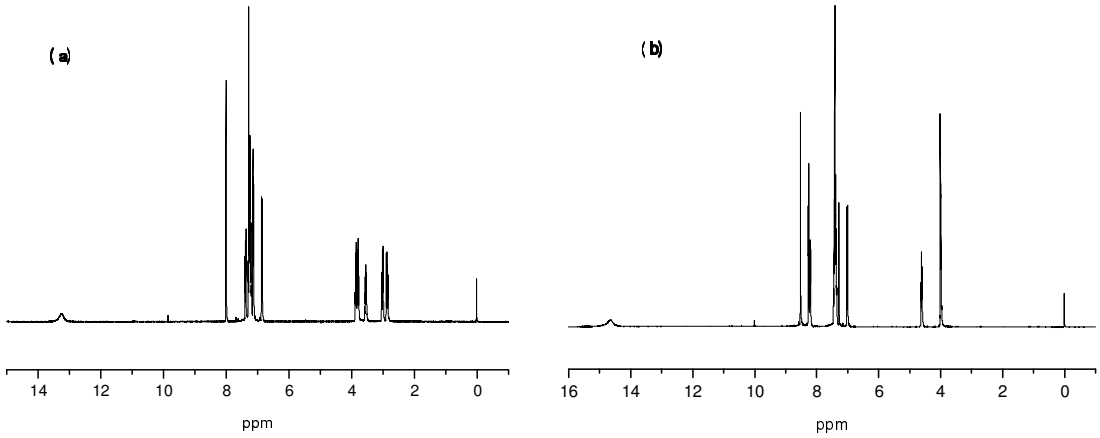

Figure 2.1. ^1H NMR spectra of Schiff bases (a) H_2L^6 and (b) H_2L^7 in $CDCl_3$ solutions.

The electronic absorption spectra of the chiral Schiff base ligands H_2L^1-H_2L^8 in acetronitrile exhibit characteristic absorption bands at ~320 and ~255 nm which are assigned to transitions of the intramolecularly hydrogen-bonded salicylidenimino chromophore (Scheme 2.2(a)). These ligands show circular dichroism spectra with multiple Cotton effects corresponding to the electronic absorption maxima. The negative sign of these Cotton effect bands can be correlated with the absolute configuration of the amino alcohol moiety.[2] In some cases especially nitro substituted Schiff bases, a broad band near 400 nm and one another band near 260 nm become evident. The additional bands are tentatively assigned to the quinoid tautomer present in solution (Scheme 2.2(b)).[2,3] This assumption is further confirmed by the X-ray crystallographic analysis of one of the nitro substituted Schiff base H_2L^8, where

intramolecular proton transfer is observed from phenolic O to imine N due to hydrogen bonding (*vide infra*). Representative electronic and CD spectra are given in Figure 2.2.

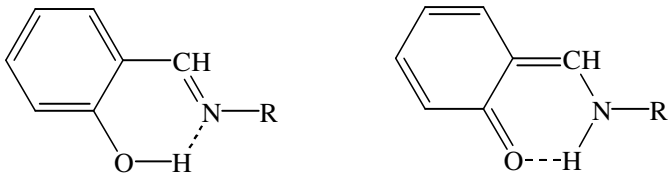

(a) **(b)**

Scheme 2.2. Tautomers of a Schiff base.

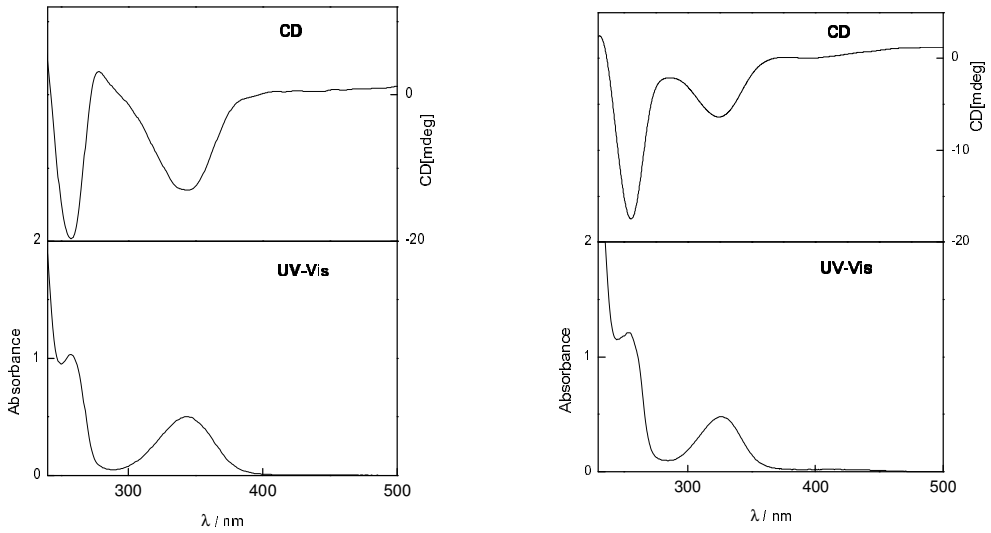

(a) **(b)**

Figure 2.2. Electronic and CD spectra of Schiff bases (a) H_2L^3 and (b) H_2L^6 in acetonitrile solutions of 10^{-4}M concentrations.

2.4.2. X-ray structure of H_2L^8

X-ray quality crystals of H_2L^8 were grown from a toluene solution by slow evaporation method and the data were collected on a Bruker-Nonius SMART APEX CCD single crystal diffractometer using graphite monochromated Mo-Kα radiation (0.71073Å). The SMART software[4] was used for intensity data acquisition and the SAINTPLUS[8] software was used for data extraction. Absorption correction was performed with help of SADABS[4] program. The SHELX-97[5] was used for structure solution and least-square refinement on F^2. The phenolic H atoms were located in a difference Fourier map, close to the imine-N atoms and refined with free coordinates and isotropic U parameters. Other H atoms were placed in idealized positions and constrained to ride on their parent atoms. Although a non-crystallographic inversion center close to (0.25, 0, 0.25) relates the two independent molecules in the asymmetric unit, emulating a space group $P2_1/n$, the actual space group is $P2_1$ which is consistent with the fact that the H_2L^8 is an enantiomerically pure compound. Similar examples are reported in the literature.[6]

The Schiff base crystallizes in Monoclinic $P2_1$ space group with two molecules in the asymmetric unit. Relevant crystallographic details are presented in Table 2.1. ORTEP drawing of the molecule showing the atom labeling scheme is given in Figure 2.3. The asymmetric unit contains two molecules of H_2L^8 as shown in Figure 2.3. Some important bond lengths and angles are given in Table 2.2.

Table 2.1. Crystal and structure refinement data for H_2L[8]

Molecular formula	$C_{16}H_{16}N_2O_4$
Formula weight	300.31
Crystal system	Monoclinic
Space group	$P2_1$
a / Å	5.8623(8)
b / Å	8.1322(10)
c / Å	30.674(4)
β / °	91.450(2)
V / Å^3	1461.9(3)
Z	4
μ / mm^{-1}	0.099
ρ_{calcd} / gcm^{-3}	1.364
Independent reflections	15286 (R_{int} = 0.030)
Observed reflections	3102
Parameters	407
Final R indices ($I > 2\sigma(I)$)	R1[a] = 0.0414, wR2[b] = 0.1014
Goodness-of-fit[c]	1.031
Largest peak and hole e/ Å^3	0.163 and -0.137 e.Å^{-3}

[a] $R1 = \sum||F_o| - |F_c||/\sum|F_o|$. [b] $wR2 = \{\sum[(F_o^2 - F_c^2)^2]/\sum[w(F_o^2)^2]\}^{1/2}$.
[c] $GOF = \{\sum[w(F_o^2 - F_c^2)^2]/(n - p)\}^{1/2}$ where 'n' is the number of reflections and 'p' is the number of parameters refined; $w = 1/[\sigma^2(F_o^2) + (aP)^2 + bP]$ where a = 0.0619 and b = 0.0475.

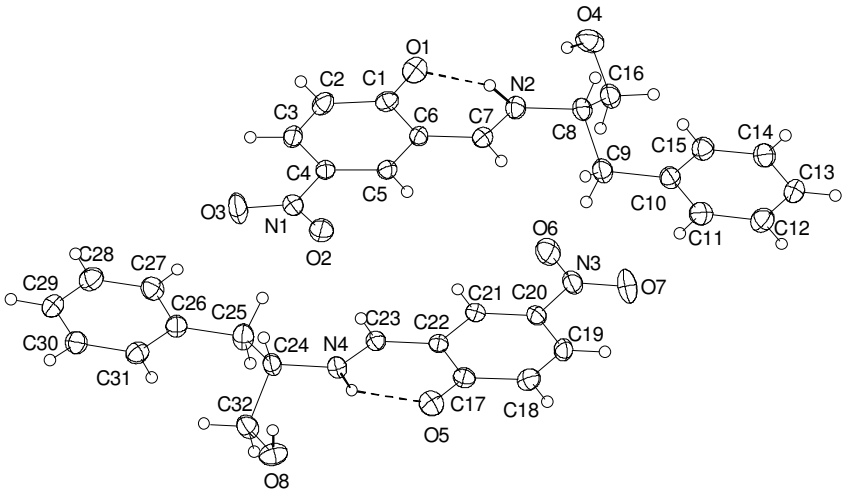

Figure 2.3. The structure of the asymmetric unit of H_2L^8, showing the atom-numbering scheme. Thermal ellipsoids are drawn at the 20 % probability level. The intra-molecular hydrogen bonds are shown as dashed lines.

Table 2.2 Selected bond distances (Å) and bond angles (°) for H_2L^8

O(1)-C(1)	1.266(3)	O(5)-C(17)	1.267(3)
C(1)-C(2)	1.422(4)	C(17)-C(18)	1.432(4)
C(2)-C(3)	1.351(4)	C(18)-C(19)	1.359(4)
C(4)-C(3)	1.403(4)	C(20)-C(19)	1.394(4)
C(5)-C(4)	1.370(3)	C(21)-C(20)	1.358(4)
C(5)-C(6)	1.395(4)	C(21)-C(22)	1.398(4)
C(6)-C(7)	1.422(4)	C(22)-C(17)	1.436(4)
C(6)-C(1)	1.444(4)	C(22)-C(23)	1.420(3)
N(2)-C(7)	1.287(4)	N(4)-C(23)	1.286(3)
N(2)-C(8)	1.478(3)	N(4)-C(24)	1.460(3)
O(1)-C(1)-C(2)	122.2(3)	O(5)-C(17)-C(22)	121.3(2)
O(1)-C(1)-C(6)	121.1(3)	C(18)-C(17)-C(22)	115.5(3)
C(2)-C(1)-C(6)	116.7(3)	C(18)-C(19)-C(20)	120.2(3)
C(3)-C(2)-C(1)	122.5(3)	C(19)-C(18)-C(17)	122.2(3)
C(4)-C(5)-C(6)	120.3(3)	C(20)-C(21)-C(22)	120.3(3)
C(5)-C(6)-C(1)	119.8(2)	C(21)-C(22)-C(23)	117.7(2)
C(5)-C(6)-C(7)	119.4(3)	C(21)-C(20)-C(19)	120.8(3)
C(5)-C(4)-C(3)	121.1(3)	C(21)-C(22)-C(17)	120.9(2)
C(7)-C(6)-C(1)	120.8(3)	C(23)-C(22)-C(17)	121.3(2)
C(7)-N(2)-C(8)	125.7(3)	C(23)-N(4)-C(24)	123.5(3)

The structure of the molecule reveals an intra-molecular proton transfer from the hydroxyl-O atom to the imine-N atom, through an O–H···N intramolecular hydrogen bond. The hydrogen-bonding parameters are given in Table 2.3; these are comparable to those reported for similar systems.[7]

Table 2.3. Hydrogen bonding parameters (Å, °) for H_2L[8]

Donor –H···Acceptor	D – H	H···A	D···A	D–H···A
N2–H1A···O1	0.97(4)	1.77(3)	2.611(3)	143(3)
N4–H1B···O5	0.91(3)	1.93(3)	2.638(3)	134(3)

The short distances noticed for the bonds C2–C3 [1.351(4) Å], C4–C5 [1.370(3) Å], C18–C19 [1.359(4) Å] and C20–C21 [1.358(4) Å], in comparison with the regular aromatic distances, suggest a contribution from a quinoid structure as expected for NH tautomers.[7,8] The short distances of O1–C1 = 1.266 (3) Å and O5–C17 1.267(3) Å also supports the same. The presence of $–NO_2$ group in the *para* position is expected to have a role in stabilizing the present tautomeric form of the molecule.

The intramolecular hydrogen transfer from the *o*-hydroxy group to the imine-N atom is important with respect to the solvato-, thermo- and photochromic properties exhibited by *o*-hydroxy Schiff bases.[9] Such proton exchanging materials can be utilized for the design of various molecular electronic devices.[10]

2.5. Synthetic procedure and characterization data for Mn complexes

All the eight Mn complexes **1-8** (Scheme 2.3) were prepared using the following general procedure given for complex **1**. Some variations applied from this common procedure are mentioned separately in the case of respective complexes.

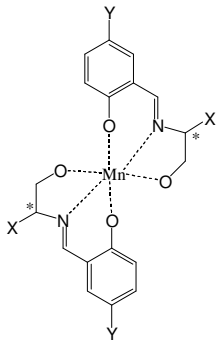

1. X = Ph Y = H
2. X = CH_2-Ph Y = H
3. X = Ph Y = OMe
4. X = CH_2-Ph Y = OMe
5. X = Ph Y = Br
6. X = CH_2-Ph, Y = Br
7. X = Ph Y = NO_2
8. X = CH_2-Ph Y = NO_2

Scheme 2.3. Schematic representation of manganese complexes **1-8**.

Complex 1

To a methanolic solution (15 mL) of ligand H_2L^1 (0.241 g, 1 mmol) was added $(CH_3COO)_2Mn{\cdot}4H_2O$ (0.245 g, 1 mmol). The mixture was allowed to stir at room temperature in air for six hours. The resultant dark brown solution was evaporated to dryness using rotavapor and vacuum pump. The solid, thus obtained, was dissolved in dichloromethane, washed twice with water, once with brine solution (using separating funnel) and dried over anhydrous Na_2SO_4. The resulting dark brown solution, on slow evaporation, gave brown microcrystalline solid of complex **1**.

Recrystallized from ethanol. MF: $[MnL^1{}_2]$, MW: 533.48, Yield: 74 %.

Anal. calcd. (found) for $C_{30}H_{26}N_2O_4Mn$: C, 67.54 (67.16); H, 4.91 (4.83); N, 5.25 (5.33) %.

IR (KBr, cm^{-1}): 1616, 1535, 1440, 1312, 1200, 1148, 1022, 943, 897, 802, 756, 700, 640, 611, 579, 540, 457.

UV/Vis (CH_3CN); λ_{max}/nm ($\varepsilon/M^{-1}cm^{-1}$): 296sh (17967), 340sh (12316), 410 (6079), 473sh (3891), 550sh (1836).

CD (CH_3CN, 10^{-4}M); λ_{max}/nm (mdeg): 282 (–5.57), 340 (–11.70), 408 (–0.92).

Complex 2

Recrystallized from DMF. MF: $[MnL^2_2]\cdot 2DMF$, MW: 707.72, Yield: 68 %.

Anal. calc. (found) for $C_{38}H_{44}N_4O_6Mn$: C, 64.49 (64.17); H, 6.27 (6.21); N, 7.92(8.01) %.

IR (KBr, cm^{-1}): 1616, 1606, 1539, 1493, 1464, 1413, 1269, 1222, 1159, 1030, 819, 758, 702, 653, 553.

UV/Vis (CH_3CN); λ_{max}/nm ($\varepsilon/M^{-1}cm^{-1}$): 294sh (22387), 344 (13200), 404 (8252), 470sh (4432), 540 (2538).

CD (CH_3CN, 10^{-4}M); λ_{max}/nm (mdeg): 280 (–17.6), 358 (–10.01), 415 (–20.24).

Complex 3

Recrystallized from ethanol. MF: $[MnL^3_2]$, MW: 593.5, Yield: 73 %.

Anal. calcd. (found) for $C_{32}H_{30}MnN_2O_6$: C, 64.76 (64.53); H, 5.09 (5.13); N, 4.72 (4.83) %.

IR (KBr, cm^{-1}): 1616, 1606, 1535, 1444, 1383, 1309, 1197, 1145, 1089, 1076, 1047, 902, 868, 760, 742, 696, 601, 532, 468, 426.

UV/Vis (CH_3CN); λ_{max}/nm ($\varepsilon/M^{-1}cm^{-1}$): 254 (28155), 282sh (14834), 345 (7077), 437 (3509), 520sh (1465), 620 (682).

CD (CH_3CN, 10^{-4}M); λ_{max}/nm (mdeg): 283 (–3.17), 357 (–10.01), 430 (–5.08).

Complex 4

Recrystalized from ethanol. MF: $[MnL^4_2]$, MW: 621.58, Yield: 70 %.

Anal. calcd. (found) for $C_{34}H_{34}MnN_2O_6$: C, 65.70 (65.33); H, 5.51 (5.47); N, 4.51 (4.6) %.

IR (KBr, cm^{-1}): 1616, 1606, 1539, 1493, 1462, 1419, 1354, 1294, 1269, 1222, 1157, 1035, 817, 761, 700, 659, 578, 518, 455.

UV/Vis (CH_3CN); λ_{max}/nm ($\varepsilon/M^{-1}cm^{-1}$): 250 (34024), 285sh (15234), 350 (7654), 441 (4548), 515sh (2286), 615 (1225).

CD (CH_3CN, $10^{-4}M$); λ_{max}/nm (mdeg): 289 (–13.53), 356 (–5.07), 437 (–10.00).

Complex 5

Recrystallized from DMF. MF: $[MnL^5_2]$, MW: 691.27, Yield: 76 %.

Anal. calcd. (found) for $C_{30}H_{24}N_2O_4Br_2Mn$: C, 52.12 (51.95); H, 3.50 (3.61); N, 4.05 (4.17) %.

IR (KBr, cm^{-1}): 1616, 1558, 1521, 1454, 1417, 1298, 1172, 1024, 943, 821, 761, 702, 653, 542, 420.

UV/Vis (CH_3CN): λ_{max}/nm ($\varepsilon/M^{-1}cm^{-1}$): 292sh (17561), 354sh (8338), 410 (5188), 481sh (2697), 560 (1291).

CD (CH_3CN, $10^{-4}M$); λ_{max}/nm (mdeg): 275 (–3.42), 345 (–5.32), 405 (–9.56).

Complex 6

Recrystallized from DMF. MF: $[MnL^6_2]\cdot 0.5DMF$, MW: 755.87, Yield: 73 %.

Anal. calc. (found) for $C_{32}H_{28}N_2O_4Br_2Mn\cdot 0.5C_3H_7NO$: C, 53.23 (53.60); H, 4.20 (4.01); N, 4.63 (4.88) %.

IR (KBr, cm^{-1}): 1610, 1520, 1452, 1369, 1300, 1170, 1045, 798, 746, 700, 644, 574, 520, 455.

UV/Vis (CH_3CN); λ_{max}/nm ($\varepsilon/M^{-1}cm^{-1}$): 292sh (17710), 350sh (9794), 400 (5703), 470sh (2719), 550sh (1384).

CD (CH_3CN, 10^{-4}M); λ_{max}/nm (mdeg): 288 (–10.1), 345 (–3.01), 413 (–8.3).

Complex 7

The reaction of H_2L^7 with manganese acetate initially yielded a yellow precipitate which was filtered and dissolved in dimethylformamide to give a dark brown solution. This dark brown solution kept in an open beaker on slow evaporation yielded brown needle shaped cryatals of complex **7**.

Recrystallized from DMF. MF: $[MnL^7_2]\cdot DMF$, MW: 696.57, Yield: 68 %.

Anal. calcd. (found) for $C_{33}H_{31}N_5O_9Mn$: C, 56.90 (56.61); H, 4.49 (4.37); N, 10.05 (9.93) %.

IR (KBr, cm^{-1}): 1626, 1601, 1550, 1498, 1454, 1377, 1313, 1242, 1194, 1130, 1099, 1016, 951, 842, 804, 754, 694, 657, 597, 551, 474, 434.

UV/Vis (CH_3CN); λ_{max}/nm ($\varepsilon/M^{-1}cm^{-1}$): 230sh (35720), 251 (31154), 348 (26320), 387sh (18591), 461sh (4565), 515 (2174).

CD (CH_3CN, 10^{-4}M); λ_{max}/nm (mdeg): 276 (–5.87), 345 (–5.96), 393 (–3.32).

Complex 8

The reaction of H_2L^8 with manganese acetate initally yielded a brown Mn(III) complex probably due to the incomplete oxidation at earlier reaction conditions. Extended reaction time (24h) in alkaline medium (2 equivalents of NaOH) to ensure complete deprotonation of the ligand was employed to get the corresponding Mn(IV) complex.

Recrystallized from DMF. MF: $[MnL^8_2]$, MW: 651.52, Yield: 72 %.

Anal. calcd. (found) for $C_{32}H_{28}MnN_4O_8$: C, 58.99 (58.26); H, 4.33 (4.24); N, 8.60 (8.72) %.

IR (KBr, cm^{-1}): 1670, 1626, 1602, 1543, 1496, 1456, 1383, 1313, 1130, 1097, 949, 833, 796, 750, 700, 650, 578, 516, 472, 418.

UV/Vis (CH_3CN); λ_{max}/nm ($\varepsilon/M^{-1}cm^{-1}$): 231 (36967), 247 (36625), 344 (29988), 380sh (22618), 460sh (5522), 515 (2853).

CD (CH_3CN, 10^{-4}M); λ_{max}/nm (mdeg): 280 (–6.88), 340 (–6.46), 390 (–3.63).

2.6. Synthetic procedure and characterization data for Co complexes

All the eight cobalt complexes **9-16** reported in this thesis were prepared using the following general procedure given for complex **9**.

To a methanolic solution (25 mL) of ligand H_2L^1 (0.241 g, 1 mmol) was added $(CH_3COO)_2Co{\cdot}4H_2O$ (0.249 g, 1 mmol). The mixture was allowed to stir at room temperature in air overnight. The resultant dark reddish brown solution was evaporated to dryness using rotavapor and vacuum pump. The solid, thus obtained, was extracted with dichloromethane and evaporated to give a reddish brown microcrystalline solid which was recrystallized from a solution of dimethyl formamide.

Complex 9

MF: $[Co(CoL^1{}_2)_2{\cdot}H_2O]{\cdot}2DMF{\cdot}2H_2O$, MW: 1334.11, Yield: 77 %.

Anal calcd. (found) for $C_{66}H_{72}N_6O_{13}Co_3$: C, 59.42 (59.05); H, 5.44 (5.15); N, 6.30 (6.11) %.

IR (KBr, cm^{-1}): 3416, 3051, 2918, 2854, 1633, 1597, 1533, 1493, 1454, 1439, 1385, 1344, 1317, 1253, 1195, 1147, 1124, 1095, 1028, 945, 896, 831, 752, 704, 650, 628, 592, 534.

UV/Vis (CH_3CN); λ_{max}/nm ($\varepsilon/M^{-1}cm^{-1}$): 252(87930), 317 (13220), 398 (9402), 525 (867), 690 (138).

CD (CH_3CN, 10^{-4}M); λ_{max}/nm (mdeg): 262 (–24.88), 282 (–18.84), 394 (–27.62), 535 (4.19), 668(4.55).

Complex 10

MF: $[Co(CoL^{2}_{2})_2 \cdot H_2O] \cdot 2DMF \cdot H_2O$, MW: 1372.20, Yield: 76 %.

Anal calcd. (found) for $C_{70}H_{78}N_6O_{12}Co_3$: C, 61.27 (61.69); H, 5.73 (5.53); N, 6.12 (5.98) %.

IR (KBr, cm^{-1}): 3024, 2916, 1635, 1599, 1535, 1448, 1388, 1315, 1195, 1147, 1082, 956, 844, 748, 700, 580, 524, 468.

UV/Vis (CH_3CN); λ_{max}/nm ($\varepsilon/M^{-1}cm^{-1}$): 251 (76170), 322 (10950), 394 (8070), 526 (1284), 705 (400).

CD (CH_3CN, $10^{-4}M$); λ_{max}/nm (mdeg): 280 (–4.19), 394 (–13.27), 516 (0.22), 675 (3.48).

Complex 11

MF: $[CoL^{3}(HL^{3})] \cdot 0.25DMF$, MW: 616.81, Yield: 74 %.

Anal calcd. (found) for $C_{32}H_{31}N_2O_6Co \cdot 0.25C_3H_7NO$: C, 63.77 (64.06); H, 5.35 (5.29); N, 5.11 (5.23) %.

IR (KBr, cm^{-1}): 2928, 1635, 1539, 1469, 1423, 1298, 1259, 1219, 1157, 1033, 947, 819, 769, 702, 528, 418.

UV/Vis (CH_3CN); λ_{max}/nm ($\varepsilon/M^{-1}cm^{-1}$): 255 (35880), 315 (7686), 418 (3803), 535 (423), 700 (88).

CD (CH_3CN, $10^{-4}M$); λ_{max}/nm (mdeg): 275 (–21.6), 417 (–26.13), 535 (4.14), 692 (8.05).

Complex 12

MF: $[CoL^{4}(HL^{4})] \cdot 0.25DMF$, MW:644.86, Yield: 69 %.

Anal calcd. (found) for $C_{34}H_{35}N_2O_6Co \cdot 0.25C_3H_7NO$: C, 64.72 (64.48); H, 5.74 (5.39); N, 4.89 (4.44) %.

IR (KBr, cm^{-1}): 3414, 3028, 2924, 1635, 1537, 1464, 1385, 1304, 1255, 1217, 1157, 1084, 1035, 814, 744, 700, 532, 466.

UV/Vis (CH_3CN); λ_{max}/nm ($\varepsilon/M^{-1}cm^{-1}$): 255 (35471), 315 (7544), 420 (3914), 535 (435), 700 (96).

CD (CH_3CN, 10^{-4}M); λ_{max}/nm (mdeg): 292 (–9.15), 415 (–10.14), 520 (0.62), 685 (6.40).

Complex 13

MF: $[Co(CoL^5{}_2)_2 \cdot DMF]$, MW:1522.55, Yield: 72 %.

Anal calcd. (found) for $C_{63}H_{55}N_5O_9Br_4Co_3$: C, 49.7 (49.33); H, 3.64 (3.77); N, 4.60 (4.41) %.

IR (KBr, cm^{-1}):1635, 1589, 1520, 1458, 1417, 1385, 1311, 1305, 1172, 1134, 1028, 945, 819, 761, 688, 650, 597, 536, 418.

UV/Vis (CH_3CN); λ_{max}/nm ($\varepsilon/M^{-1}cm^{-1}$): 290 (29600), 330 (12350), 411 (8600), 530 (836), 682 (187).

CD (CH_3CN, 10^{-4}M); λ_{max}/nm (mdeg): 261 (–25.4), 293 (–17.66), 403 (–34.30), 527 (5.00), 670 (7.83).

Complex14

MF: $[Co(CoL^6{}_2)_2 \cdot DMF]$, MW:1578.66 , Yield: 66 %.

Anal calcd. (found) for $C_{67}H_{63}N_5O_9Br_4Co_3$: C, 50.97 (51.16); H, 4.02 (3.93); N, 4.44 (4.20) %.

IR (KBr, cm^{-1}): 3024, 2920, 1637, 1591, 1521, 1454, 1377, 1311, 1172, 1082, 819, 746, 700, 646, 580, 468.

UV/Vis (CH_3CN): λ_{max}/nm ($\varepsilon/M^{-1}cm^{-1}$): 244 (66340), 285 (21630), 324 (8610), 399 (6360), 530 (754), 692 (250).

CD (CH_3CN, 10^{-4}M); λ_{max}/nm (mdeg): 291 (–4.43), 405 (–7.01), 527 (1.00), 690 (2.20).

Complex 15

MF: $H[Co(CoL^{7}_{2})_3]\cdot H_2O$, MW: 1960.36, Yield: 68 %.

Anal calcd. (found) for $C_{90}H_{75}N_{12}O_{25}Co_4$: C, 55.14 (55.01); H, 3.86 (3.92); N, 8.57 (8.23) %.

IR (KBr, cm^{-1}): 3566, 2924, 1647, 1602, 1548, 1473, 1383, 1313 (nitro), 1132, 1101, 1026, 951, 827, 756, 696, 655, 540.

UV/Vis (CH_3CN); λ_{max}/nm ($\varepsilon/M^{-1}cm^{-1}$): 243 (120830), 315 (38660), 387 (92940), 520 (1560), 650 (478).

CD (CH_3CN, 10^{-4}M); λ_{max}/nm (mdeg): 262 (–45.73), 383 (–40.37), 530 (8.25), 660 (11.00).

Complex 16

MF: $[Co(CoL^{8}_{2})_2\cdot DMF]\cdot 2DMF\cdot H_2O$, MW: 1607.27 , Yield: 70 %.

Anal calcd. (found) for $C_{73}H_{79}N_{11}O_{20}Co_3$: C, 54.55 (54.78); H, 4.95 (4.83); N, 9.59 (9.13) %.

IR (KBr, cm^{-1}): 2922, 1647, 1601, 1545, 1473, 1386, 1313, 1097, 947, 831, 754, 702, 659, 489.

UV/Vis (CH_3CN); λ_{max}/nm ($\varepsilon/M^{-1}cm^{-1}$): 240 (72860), 317 (21190), 385 (50960), 520 (1013), 650 (350).

CD (CH_3CN, 10^{-4}M); λ_{max}/nm (mdeg): 259 (–12.26), 390 (–13.17), 522 (1.96), 660 (4.83).

2.7. Synthetic procedure and characterization data for Cu complexes

All the eight complexes **17-24** were prepared using the following general procedure given for complex **17**.

Complex 17

To a methanolic solution of the ligand H_2L (0.241 g, 1 mmol) was added $CuCl_2 \cdot 2H_2O$ (0.179 g, 1 mmol). The mixture was allowed to stir at room temperature in air overnight. The resultant green solution was evaporated to dryness using rotavapor and vacuum pump. The green colored solid thus obtained was recrystallized from ethanol/methanol.

Recrystallized from ethanol. MF: $[Cu_2(\mu\text{-}Cl)_2(HL^1)_2] \cdot H_2O$, MW: 696.57, Yield: 47 %.

Anal. calc. (found) for $C_{30}H_{30}N_2O_5Cl_2Cu_2$: C, 51.73 (53.26); H, 4.34 (4.2); N, 4.02 (4.09) %.

IR (KBr, cm^{-1}): 1626, 1541, 1467, 1442, 1294, 1199, 1149, 1126, 1068, 1006, 945, 896, 761, 700, 590, 528, 430.

UV/Vis (MeOH); λ_{max}/nm ($\varepsilon/M^{-1}cm^{-1}$): 682.00 (172), 372.00 (9567), 271.00 (23649).

CD (MeOH, 10^{-4}M); λ_{max}/nm (mdeg): 379 (−5.45), 290 (−1.57).

Complex 18

Recrystallized from ethanol. MF: $[Cu_2(\mu\text{-}Cl)_2(HL^2)_2] \cdot C_2H_5OH$, MW: 752.67, Yield: 56 %.

Anal. calc. (found) for $C_{34}H_{38}N_2O_5Cl_2Cu_2$: C, 54.26 (53.94); H, 5.09 (5.11); N, 3.72 (3.66) %.

IR (KBr, cm^{-1}): 3749, 3026, 1635, 1601, 1541, 1446, 1394, 1288, 1197, 1151, 1082, 1028, 904, 790, 748, 700, 584, 516, 445.

UV/Vis (MeOH); λ_{max}/nm ($\varepsilon/M^{-1}cm^{-1}$): 680 (190), 372 (9816), 270 (24011).

CD (CH_3CN, 10^{-4}M); λ_{max}/nm (mdeg): 380 (−5.92), 290 (−1.8).

Complex 19

Recrystallized from methanol. MF: $[Cu_2(\mu\text{-}Cl)_2(HL^3)_2]\cdot CH_3OH$, MW: 770.65, Yield: 59 %.

Anal. calc. (found) for $C_{33}H_{36}N_2O_7Cu_2Cl_2$: C, 51.43 (51.28); H, 4.71 (4.66); N, 3.64 (3.65) %.

IR (KBr, cm^{-1}): 3414, 2937, 1631, 1541, 1469, 1269, 1221, 1159, 1033, 827, 771, 700, 532.

UV/Vis (MeOH); λ_{max}/nm ($\varepsilon/M^{-1}cm^{-1}$): 670 (198), 404 (8008), 275 (23649).

CD (CH_3CN, $10^{-4}M$); λ_{max}/nm (mdeg): 410 (−6.2), 280 (−1.9).

Complex 20

Recrystallized from methanol. MF: $[Cu_2(\mu\text{-}Cl)_2(HL^4)_2]\cdot CH_3OH$, MW: 798.70. Yield: 62 %.

Anal. calc. (found) for $C_{35}H_{40}N_2O_7Cu_2Cl_2$: C, 52.63 (52.15); H, 5.05 (4.88); N, 3.51 (3.39) %.

IR (KBr, cm^{-1}): 3414, 2935, 1633, 1545, 1471, 1385, 1277, 1224, 1159, 1084, 1033, 808, 746, 700, 576, 516, 451.

UV/Vis (MeOH); λ_{max}/nm ($\varepsilon/M^{-1}cm^{-1}$): 670 (215), 400 (9434), 271 (20869).

CD (MeOH, $10^{-4}M$); λ_{max}/nm (mdeg): 405 (−3.82), 276 (−1.63).

Complex 21

Recrystallized from methanol. MF: $[Cu_2(\mu\text{-}Cl)_2(HL^5)_2]\cdot CH_3OH$. MW: 868.39, Yield: 63 %.

Anal. calc. (found) for $C_{31}H_{30}Br_2N_2O_5Cu_2Cl_2$: C, 42.88 (42.60); H, 3.48 (3.49); N, 3.23 (3.30) %.

IR (KBr, cm^{-1}): 3468, 1633, 1577, 1521, 1456, 1294, 1172, 1132, 1055, 833, 761, 698, 644, 528, 457.

UV/Vis (MeOH); λ_{max}/nm ($\varepsilon/M^{-1}cm^{-1}$): 706 (166), 383 (5011), 271 (13476).

CD (MeOH, 10^{-4}M); λ_{max}/nm (mdeg): 388 (–4.1), 274 (–0.97).

Complex 22

Recrystallized from methanol. MF: $[Cu_2(\mu\text{-}Cl)_2(HL^6)_2]\cdot CH_3OH$, MW: 896.44, Yield: 56 %.

Anal. calc. (found) for $C_{33}H_{34}N_2O_5Br_2Cu_2Cl_2$: C, 44.21 (44.33); H, 3.82 (3.93); N, 3.12 (3.16) %.

IR (KBr, cm^{-1}): 3402, 3024, 2918, 1633, 1593, 1527, 1458, 1375, 1278, 1174, 1084, 974, 821, 746, 700, 646, 569, 545, 516, 449.

UV/Vis (MeOH); λ_{max}/nm ($\varepsilon/M^{-1}cm^{-1}$): 685 (171), 381 (9052), 270 (18608).

CD (MeOH, 10^{-4}M); λ_{max}/nm (mdeg): 385 (–3.92), 290 (–1.7).

Complex 23

Recrystallized from methanol. MF: $[Cu(HL^7)Cl]$, MW: 384.27, Yield: 69 %.

Anal. calc. (found) for $C_{15}H_{13}N_2O_4CuCl$: C, 46.88 (47.02); H, 3.41 (3.49); N, 7.29 (7.18) %.

IR (KBr, cm^{-1}): 1634, 1600, 1549, 1468, 1387, 1308, 1094.

Diffuse reflectance electronic (KBr pellet): λ_{max} = 270, 375, 700 nm.

UV/Vis (MeOH); λ_{max}/ nm ($\varepsilon/M^{-1}cm^{-1}$): 252 (20271), 355 (18137), 690 (104).

CD (MeOH, 10^{-4}M); λ_{max}/nm (mdeg): 356 (–2.9), 289 (–0.57).

Complex 24

Recrystallized from methanol, MF: $[Cu(HL^8)Cl]$, MW: 398.30, Yield: 66 %.

Anal. calc. (found). for $C_{16}H_{15}N_2O_4CuCl$: C, 48.25 (48.39); H, 3.80 (3.88); N, 7.03 (6.98) %.

IR (KBr, cm^{-1}): 3427, 1643, 1604, 1554, 1466, 1390, 1311, 1101, 833, 700, 516.

UV/Vis (MeOH); λ_{max}/ nm ($\varepsilon/M^{-1}cm^{-1}$): 680 (229), 356 (28328), 251 (32630).

CD (MeOH, 10^{-4}M); λ_{max}/nm (mdeg): 365 (–3.2), 275 (–0.67).

2.8. Catalytic epoxidation procedure

2.8.1. Preparation of PhIO

The iodosobenzene (PhIO) used in the catalytic study as oxidant is prepared using a reported procedure.[11] Finely ground iodosobenzene diacetate (32.2 g, 0.10 mol) is placed in a 250 ml beaker, and 150 ml of 3N sodium hydroxide is added over a 5 minute period with vigorous stirring. The lumps of solid that form are triturated with a stirring rod or spatula for 15 minutes, and the reaction mixture stands for an additional 45 minutes to complete the reaction. 100 ml of water is added, the mixture is stirred vigorously, and the crude solid iodosobenzene is collected on a Büchner funnel, washed there with 200 ml of water, and dried by maintaining suction. Final purification is effected by triturating the dried solid in 75 ml of chloroform in a beaker. The iodosobenzene is separated by filtration and air-dried; weighed (Yield 85-90 %).

2.8.2. Epoxidation of *trans*-stilbene catalyzed by 1-8

trans-Stilbene (0.2 g, 1.1 mmol) and iodosobenzene (0.49 g, 2.2 mmol) were added to a solution of the complex (60 μmol) in acetonitrile (5 mL) at room temerature. After stirring for two days, the mixture was concentrated in vacuum and purified with column chromatography (SiO_2, hexane-ethylacetate 1:0 ~19:1) to give stilbene oxide as colorless solid. The product was identified as *trans*-stilbene oxide by comparing its NMR spectrum (δ ~ 3.85 in $CDCl_3$) with that of reported *trans*-stilbene oxide.[12]

2.8.3. Epoxidation of styrene catalyzed by 1-8

Styrene (0.114 g, 1.1 mmol) and iodosobenzene (0.49 g, 2.2 mmol) were added to a solution of the complex (60 μmol) in acetonitrile (5 mL) and stirred at room temperature under nitrogen atmosphere. After completion of the reaction, the

solvent was removed under vacuum and the residue was treated with Et_2O (6 × 5 mL). The Et_2O washings were combined together and concentrated to a small volume. Bromobenzene (0.075 g) was added as an internal standard to it and the volume was made up to 10 mL. The resulting solution was analyzed by gas chromatography and the product was identified as styrene oxide by camparing the retention time with that of the authentic sample.

Both epoxidation products, (E)-stilbene oxide and styrene oxide were found to be recemic mixtures, as evidenced by polarimetric studies (for stilbene oxide) and chiral GC analysis (for styrene oxide).

2.9. References

1. R. M. Silverstein and F. X. Webster, *Spectroscopic Identification of Organic Compounds,* John Wiley & Sons Inc., New York, 1998.
2. H. E. Smith, J. R. Neergaard, E. P. Burrows and F. –M.Chen, *J. Am. Chem. Soc.,* 1974, **96**, 2908.
3. H. E. Smith, B. G. Padilla, J. R. Neergaard and F. –M. Chen, *J. Org. Chem.*, 1979, **44**, 1690.
4. Bruker, *SADABS, SMART, SAINTPLUS and SHELXTL.* Bruker AXS Inc., Madison, Wisconsin, USA, 2003.
5. G. M. Sheldrick, *Programs for Crystal Structure Solution and Analysis,* University of Göttingen, Göttingen, Germany, 1997.
6. J. W. Bats, M. A. Grundl and A. S. K. Hashmi, *Acta Cryst*., 2001, **C57**, 208.
7. P. M. Dominiak, E. Grech, G.Barr, S. Teat, P. Mallinson and K. Woźniak, *Chem. Eur. J.,* 2003, **9**, 963.
8. G. Asgedom, A. Sreedhara, J. Kivikoski, J. Valkonen, E. Kolehmainen and C. P. Rao, *Inorg. Chem*., 1996, **35**, 5674.
9. (a) E. Hadjoudis and I. M. Mavridis, *Chem. Soc. Rev.,* 2004, **33**, 579; (b) A. Filarowski, *J. Phys. Org. Chem.*, 2005, **18**, 686.
10. S. H. Alarcón, D. Pagani, J. Bacigalupo and A. C. Olivieri, *J. Mol. Struct.,* 1999, **75**, 233.
11. H. Saltzman and J. G. Sharefkin, *Org. Synth.,* 1973, **Coll. Vol. V**, 658.
12. D. Das and C. P. Cheng, *J. Chem. Soc., Dalton Trans.,* 2000, 1081.

Synthesis, structure, catalytic properties and supramolecular chemistry of a series of chiral mononuclear Mn(IV) complexes derived from chiral amino alcohol based Schiff bases

3.1. Abstract

A series of optically active mononuclear Mn(IV) complexes have been synthesized by reacting the chiral Schiff base ligands (H_2L^1-H_2L^8) derived from salicylaldehyde/substituted salicylaldehydes and chiral amino alcohols with manganese(II) acetate. Reactions of one mole equivalent of $Mn(CH_3COO)_2 \cdot 4H_2O$ with one mole equivalent of the respective Schiff base ligands in MeOH under aerobic condition produce the complexes **1-8** in reasonable yields. All the complexes have been characterized by using analytical, spectroscopic and electrochemical techniques. Four of these are characterized by single crystal X-ray analysis. X-ray analyses revealed that complexes are slightly distorted octahedral in geometry. The bond parameters are consistent with Mn(IV) oxidation state. In all these complexes, the chiral ligands H_2L^1-H_2L^8 act as meridional ONO donors in their doubly deprotonated state. The chirality of the complexes has been confirmed by solution CD studies. The electronic absorption spectra of the complexes in acetonitrile solution display two d-d bands in the visible region and absorptions in UV and near UV regions due to charge transfer transitions. The EPR spectra (g values ~4.5-5.5 and ~2) displayed by the complexes in frozen methanol/DMF solutions are consistent with Mn(IV) oxidation state. In the cyclic voltammograms, complexes exhibit quasi-reversible responses corresponding to the Mn(IV)/Mn(III) reduction in the range $E_{1/2}$ = –0.54 - –0.27 V (vs Ag/AgCl). Room temperature magnetic moments observed for these complexes are in the range 3.8-4.2 B.M consistent with a high spin d^3 system.

All these complexes are found to catalyze the epoxidation of styrene and *trans*-stilbene in presence of PhIO as terminal oxidant in acetonitrile solutions.

3.2. Introduction

In chapter I the chemistry of amino alcohol containing chiral Schiff base ligands with various metal ions has been discussed. Tridentate ligands derived from substituted salicylaldehydes and chiral amino alcohols are among the 'privileged' ligand templates generally employed for various asymmetric transformations. Complexes of this ligand system with metal ions such as Ti^{4+}, V^{5+} etc. have been successfully applied as chiral catalysts. But the manganese chemistry of such ligands has not been explored much.

The chemistry of higher valent manganese, especially Mn(IV) has been the subject of considerable research for the past couple of decades.[1] This is because of the importance of higher valent manganese in various biological systems like oxygen evolving complex (OEC) of photosystem II.[2] The S_2 state of the OEC exhibits a g = 2 multiline and, under certain conditions, g = 4.1 EPR signals, which are associated with the manganese center. EPR evidence led Hansson *et al* to propose a model that involves a trinuclear Mn complex adjacent to a mononuclear Mn(IV) one.[3] Recent 3.8, 3.7, 3.5 Å resolution X-ray structures of PSII also support a 3+1 motif.[4] Because of the new structural data, renewed attention is being paid to both trinuclear manganese complexes and mono nuclear Mn(IV) compounds.

In addition to their biological interest, Mn(IV) systems are also important with respect to asymmetric catalysis.[5] The role of chiral Mn(IV) species in the catalytic asymmetric epoxidation of olefins has been the subject of some current papers.[6] In many olefin oxidation reactions, monomeric Mn(III) compounds that use chiral ligands are used as catalysts. But in these reactions, Mn(IV) complexes (which are formed during reactions) are found to be responsible for radical type epoxidation.[6(b)] Therefore, monomeric Mn(IV) complexes which use chiral ligands are of considerable interest from catalytic point of view also.

Although there are some references of higher valent manganese complexes prepared from achiral amino alcohol based Schiff bases,[1(m)] there is no report on manganese complexes derived from chiral amino alcohol based ligands in the literature. Considering the above facts, we have used the Schiff base ligands H_2L^1-H_2L^8 derived from chiral amino alcohols and substituted salicylaldehydes to prepare new Mn(IV) complexes and explore their physical, structural, supramolecular and catalytic properties.

3.3. Experimental

3.3.1. Materials

As described in section **2.2**

3.3.2. Physical measurements

Details are given in section **2.3**

3.3.3. Synthesis of Schiff base ligands H_2L^1-H_2L^8

Synthesis and characterization of chiral Schiff base ligands H_2L^1-H_2L^8 are described in section **2.4**

3.3.4. Synthesis of complexes 1-8

Synthetic details and characterization data for manganese complexes **1-8** are given in section **2.5**

3.3.5. X-ray crystallography

X-ray diffraction data for complex **1** were collected at room temperature (25 ºC) on a Siemens P4 Diffractometer equipped with a molybdenum tube and a graphite monochromator. A dark brown crystal of approximate dimensions $0.62 \times 0.50 \times 0.42$ mm was mounted on a glass fiber using epoxy resin. Unit-cell dimensions were determined from several accurately centered reflections using XSCANS program.[7] Three standard reflections measured after every 97 reflections exhibited no significant loss of intensity. The data were corrected for Lorentz-polarization effects and absorption. The structure was solved by direct methods and refined by least-squares techniques adapting the full-matrix weighted least-squares scheme using SHELXS-97 and SHELXL-97 programs respectively.[8] All atoms were located in the difference maps during successive cycles of least-squares. The sites of the non-hydrogen atoms were refined anisotropically, whereas those of the hydrogen atoms were refined isotropically.

X-ray data for complexes **2**, **6** and **7** were collected on a Bruker-Nonius SMART APEX CCD single crystal diffractometer using graphite monochromated Mo-Kα radiation (0.71073Å). The SMART software[9] was used for intensity data acquisition and the SAINTPLUS software[9] was used for data extraction. In each case, absorption correction was performed with help of SADABS program.[9] The SHELX-97 was used for structure solution and least-square refinement on F^2. All the non hydrogen atoms were refined anisotropically. The hydrogen atoms were included in the structure factor calculation by using a riding model. The DIAMOND[10] software was used for molecular graphics. The absolute configurations for all the complex molecules were successfully determined by refining the Flack parameters.[11]

Crystallographic data for the complexes **1** and **2** are presented in Table 3.1 and that for complexes **6** and **7** in Table 3.2.

Table 3.1. Crystal and structure refinement data for complexes **1** and **2**

Complex	**1**	**2**
Empirical formula	$C_{30}H_{26}MnN_2O_4$	$C_{38}H_{44}MnN_4O_6$
Formula weight	533.47	707.71
Crystal system	Monoclinic	Orthorhombic
Space group	*C2*	$P2_12_12_1$
a / Å	23.052(7)	9.8290(11)
b / Å	8.9826(8)	10.2640(12)
c / Å	12.684(3)	36.308(4)
β / °	107.504(12)	
V / Å ^{3}	2504.8(10)	3663.0(7)
Z	4	4
μ / mm^{-1}	0.567	0.410
ρ_{calcd} / gcm^{-3}	1.415	1.283
Independent reflections	2637 (0.0138)	22714 (0.0582)
Observed reflections	2552	8520
Parameters	439	446
*R*1,[a] w*R*2[b] [($I > 2\sigma(I)$)]	0.0236 and 0.0622	0.0668 and 0.1453
Goodness-of-fit[c]	1.073	1.043
Flack parameter	0.028(15)	0.03(3)
Largest peak and hole e/ Å^3	+ 0.112 and – 0.153	+ 0.690 and – 0.434

[a] $R1 = \sum||F_o| - |F_c||/\sum|F_o|$. [b] $wR2 = \{\sum[(F_o^2 - F_c^2)^2]/\sum[w(F_o^2)^2]\}^{1/2}$.
[c] GOF = $\{\sum[w(F_o^2 - F_c^2)^2]/(n - p)\}^{1/2}$ where 'n' is the number of reflections and 'p' is the number of parameters refined; $w = 1/[\sigma^2(F_o^2) + (aP)^2 + bP]$ where a = 0.0341 and b = 0.5347 for complex **1**; and a = 0.0757 and b = 0.2840 for complex **2.**

Table 3.2. Crystal and structure refinement data for complexes **6** and **7**

Complex	**6**	**7**
Empirical formula	$C_{32}H_{28}N_2O_4Br_2Mn\cdot0.5DMF$	$C_{33}H_{31}N_5O_9Mn$
Formula weight	755.87	696.57
Crystal system	Monoclinic	Orthorhombic
Space group	$P2_1$	$P2_12_12_1$
a / Å	19.677(6)	9.7284(15)
b / Å	21.013(7)	17.005(3)
c / Å	24.573(8)	18.999(3)
β / °	105.123(6)	
V / Å^3	9808(6)	3143.1(8)
Z	6	4
μ / mm^{-1}	2.890	0.485
ρ_{calcd} / gcm^{-3}	1.536	1.472
Independent reflections	115256	36187
	(R_{int} = 0.0834)	(Rint = 0.1032)
Observed reflections	46128	7375
Parameters	2352	431
$R1$,[a] w$R2$[b] [($I > 2\sigma(I)$)]	0.0563 and 0.1018	0.0642 and 0.0862
Goodness-of-fit[c]	0.929	1.001
Flack parameter	0.005(5)	0.00(2)
Largest peak and hole e/ Å^3	0.988 and – 0.672	0.474 and – 0.268

[a] $R1 = \sum||F_o| - |F_c||/\sum|F_o|$. [b] $wR2 = \{\sum[(F_o^2 - F_c^2)^2]/\sum[w(F_o^2)^2]\}^{1/2}$.
[c] GOF = $\{\sum[w(F_o^2 - F_c^2)^2]/(n - p)\}^{1/2}$ where 'n' is the number of reflections and 'p' is the number of parameters refined; $w = 1/[\sigma^2(F_o^2) + (aP)^2 + bP]$ where a = 0.0374 and b = 0 for complex **6**; and a = 0.0349 and b = 0 for complex **7.**

3.4. Results and discussion

3.4.1. Synthesis and properties

Reactions of Mn(II) acetate with optically pure Schiff base ligands H_2L^1- H_2L^8 afforded the neutral and optically active complexes $[Mn^{IV}L_2^{1-8}]$ in good yields. The elemental analyses and spectral data for complexes **1-8** are consistent with the expected mononuclear structure. Atmospheric oxygen is the possible oxidizing agent here, which oxidizes Mn(II) to Mn(IV). This oxidation is also assisted by the fact that the tridentate ligands $(L^{1-8})^{2-}$, containing phenolate and alkoxide oxygens, effectively stabilize the +4 oxidation state of manganese. Such stabilization of Mn(IV) species by phenolate and alkoxide oxygens is reported in the literature.[1(m)] In some cases, extended reaction time and use of NaOH to ensure the complete deprotonation of ligands were needed for the complete oxidation of Mn(II).

3.4.2. Infrared spectral properties

The infrared spectra of the complexes were collected in the range of 4000-400 cm^{-1}. Selected IR data for the complexes **1-8** are given in the experimental section. The IR band which conveys important information is the peak due to ν(OH) vibration occurring as a broad feature in the IR spectrum. For the free ligands there is a strong peak around 3400 cm^{-1} present before complexation. This band is absent in the IR spectrum of complexes which indicates the deprotonation of the ligand on complexation/coordination with the Mn(IV) center. The peaks observed in the range of 2800-3000 cm^{-1} are most likely due to the aliphatic and aromatic C─H stretches.

The C=N stretching is observed in the range 1610-1626 cm^{-1}, which is substantially lower than that displayed by the corresponding Schiff base ligands (1626-1649 cm^{-1}) indicating the coordination of azomethine N to metal. The strong

bands in the region 1433-1527 cm^{-1} are assigned to the C=C stretching vibrations of the aromatic rings.

3.4.3. Electronic and circular dichroism spectra

The electronic and circular dichroism spectra of the complexes **1-8** measured in acetonitrile solutions show a red shift in the band positions compared to the bands of the free ligands. In the visible region, an octahedral Mn(IV) d^3 system is expected to exhibit two electronic absorption bands due to d-d transitions viz $^4A_{2g} \rightarrow {}^4T_{2g}$ and $^4A_{2g} \rightarrow {}^4T_{1g}$. A shoulder at ~460-520 nm and a broad band at ~515-620 nm observed for the complexes in acetonitrile solutions are probably due to the d-d transitions. The comparatively large extinction coefficients for these transitions might be due to the intense tail from the UV absorptions. The intense bands observed in the high energy portions of the absorption spectra can be assigned to charge transfer transitions judging from their molar extinction coefficient values. The electronic spectrum of all these complexes are in good agreement with those reported for the hydroxyl-rich mononuclear Mn(IV) Schiff base complexes in the literature.[1(m)] A general blue shift in band positions is observed with electron withdrawing substituents on the ligands. Such a blue-shift originating from the electron withdrawing nature of the ligand substituents has been reported previously.[12]

The CD spectra of the manganese complexes **1-8** measured in acetonitrile solutions show peaks as negative Cotton effects, corresponding to the electronic (charge transfer) transitions at ~404, ~350 and ~290 nm, but to slightly shifted positions compared to their respective free ligands. The slight red shift in the band positions in CD spectra of the complexes and the free ligands is also consistent with the respective electronic spectra. Deprotonation of ligands during complex formation might produce this slight shift in the band positions. It may be noted that the present circular dichroism is of a "Type II" nature, as described by Moscowitz[13]. Representative electronic and circular dichroism spectra of two complexes **2** and **6** are shown in Figure 3.1.

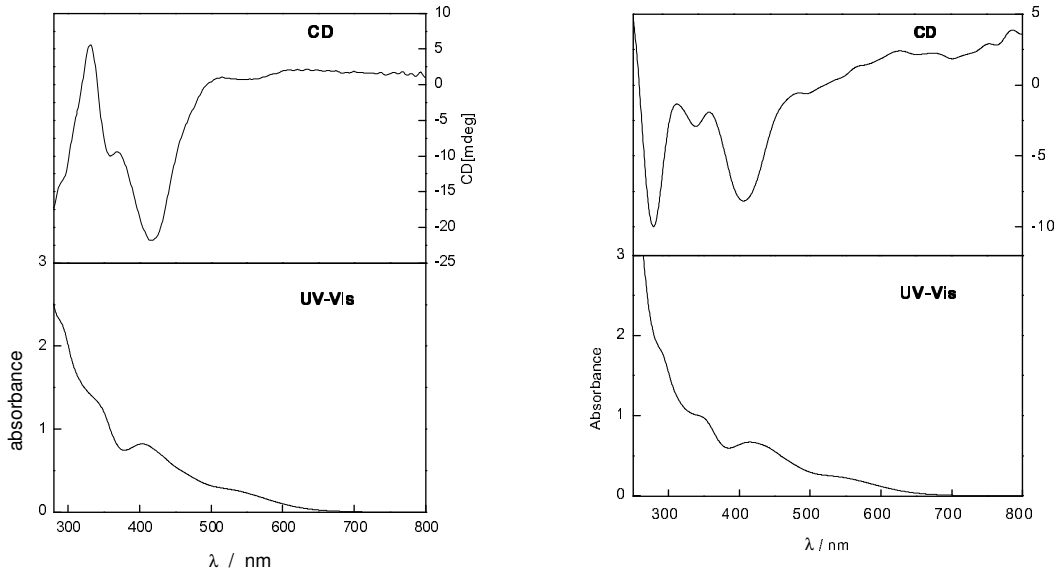

(2) **(6)**

Figure 3.1. Electronic and CD spectra of complexes **2** and **6** in acetonitrile solutions.

3.4.4. EPR and magnetic studies

The EPR measurements of complexes **1**-**6** were done in X-band frequency at -150^{o} C in methanol solutions. For solubility reasons, the spectra of complexes **7** and **8** were recorded in dimethylformamide (DMF) solutions. Some representative spectra are given in Figure 3.2. As expected, all the spectra correspond to paramagnetic d^3 system.

The EPR features of a d^3 system depend upon the axial (D) and rhombic (E) zero-field splitting parameters. In an axial field (E/D = 0), the spectrum is dependent on the magnitude of the zero-field splitting parameters. Two limiting cases are defined when the value of 2D is either much larger than or much smaller than the

microwave quantum hν (0.31 cm^{-1}). In the first case a strong signal at g ~4 and a weak signal at g ~2 are observed. Whereas in the second case a weak signal at g ~4 and a strong signal at g ~2 are found.[14]

The X-band EPR spectra of the complexes **1-8** in methanol/DMF solutions at −150° C display a strong absorption near g ~4.5-5.5 and a weak response at g ~2. This type of spectral profile is characteristic of a d^3 system in which the zerofield splitting parameter D is much larger than the microwave frequency hν, [2D >> hν]. In some cases (complexes **1** and **2**) the resonance at g ~2 are well resolved and the magnitudes of the ^{55}Mn hyperfine coupling of 90 G (complex **1**) and 87.7 G (complex **2**) observed for these complexes are consistent with that of the previous reports for Mn(IV) complexes.[1(n)] Table 3.3 gives the EPR g values and room temperature magnetic moments for the complexes **1-8**.

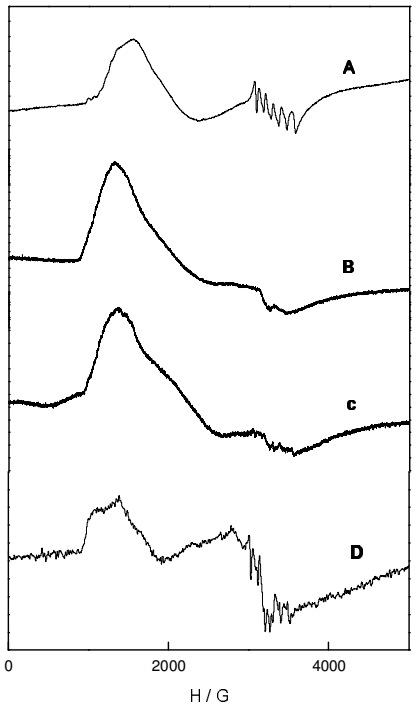

Figure 3.2. EPR spectra of complexes at −150° C. (A) complex **2** in methanol, (B) complex **6** in methanol, (C) complex **8** in DMF, (D) complex **7** in DMF.

Table 3.3. EPR g values and room temperature magnetic moments for complexes **1-8**

Complex	g values	μ_{eff}/μ_B
1	4.1, 2.1	4.20
2	3.9, 2.0	3.90
3	5.2, 2.4	3.98
4	5.2, 2.4	4.10
5	5.4, 2.4	4.07
6	5.5, 2.4	4.00
7	4.7, 2.0	3.80
8	4.7, 1.9	3.83

The room temperature magnetic susceptibilities of the complexes in solid state are found to be in the range of 3.8-4.2 μ_B, which are close to the spin only value (3.87) for a high spin d^3 system. These experimental μ_{eff} values clearly indicate the +4 oxidation state of manganese in the complexes **1-8** in agreement with the other characterization data.

3.4.5. Electrochemistry

Acetonitrile solutions of the complexes **1-8** were used to study the redox behavior with the help of cyclic voltammetry. The cyclic voltammograms of the complexes in 0.1M TBAP/CH_3CN (platinum disc working electrode, 298 K) show quasi-reversible reduction responses (Figure 3.3) at around $E_{1/2}$ = − 0.54-–0.27 V (*vs* Ag/AgCl) with peak to peak separation of 0.110-0.140 V (Table 3.4) which can be assigned to the $[Mn^{IV}L_2] + e^- \leftrightarrows [Mn^{III}L_2]^{1-}$ couple. Another quasi-reversible reduction is observed in the case of complex **2** at $E_{1/2}$ = –0.89 V, which is assigned to the Mn^{III}/Mn^{II} reduction (ΔE = 182 mV).

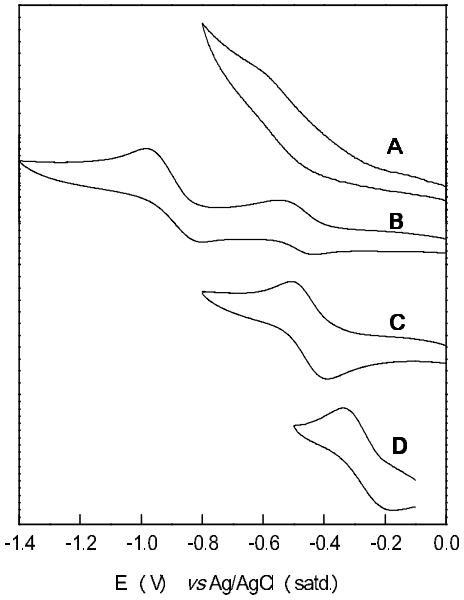

Figure 3.3.

Complex	Mn^{IV}/Mn^{III}
1	–0.45
2	–0.47
3	–0.52
4	–0.54
5	–0.43
6	–0.44
7	–0.26
8	–0.27

Table 3.4.

Figure 3.3 displays representative cyclic voltammograms (scan rate 100 mVs^{-1}) of ~10^{-3} M solutions (0.1 M TBAP) of complexes **4** (A), **2** (B), **6** (C) and **7** (D) in acetonitrile at a platinum disc electrode at 298 K. The **Table 3.4** presents the $E_{1/2}$ values for Mn^{IV}/Mn^{III} reduction responses for complexes **1**-**8.**

The one electron stoichiometry of the Mn(IV)/Mn(III) reduction response is confirmed for each complex by comparison of peak currents with that of ferrocene under identical conditions. The potential of this response is sensitive to substitution on salicylaldehyde. The potential increases with increasing electron releasing nature of the substituents on the ligands. Thus as the electron density on the phenolate-O decreases, Mn(IV) to Mn(III) reduction becomes more easy.

The negative reduction wave observed for all these complexes for Mn^{IV}/Mn^{III} couple indicates a relatively stable Mn(IV) complex and the ability of hydroxyl rich ligands to stabilize the high oxidation states of Mn. This observation justifies the rather easy formation of complexes **1-8** from ligands H_2L^{1-8} and Mn(II) salt in presence of air at ambient conditions.

3.4.6. Description of molecular structures

3.4.6.1. Crystal structure of complex 1

X-ray quality crystals of complex **1** were grown from ethanol solution by slow evaporation method. The complex crystallizes in chiral space group *C*2. The asymmetric unit contains two independent MnL (half of the complex) units, in which each manganese occupy a special position lying on a crystallographic C_2 axis. Therefore, in the crystal structure, two independent mononuclear Mn(IV) complexes are paired and both have same enantiomeric configuration. The overall geometry about the central manganese ion is octahedral with an N_2O_4 core, whereby two chiral ligands coordinate through ONO donor atoms. The tridentate ligands are meridionally coordinated to the manganese center in complex **1**. The four oxygen atoms locate at four corners of an approximate square plane (equator) and two N donors occupy *trans* (axial) positions and complete the octahedron (Figure 3.4). Crystallographic data for complex **1** is given in Table 3.1.

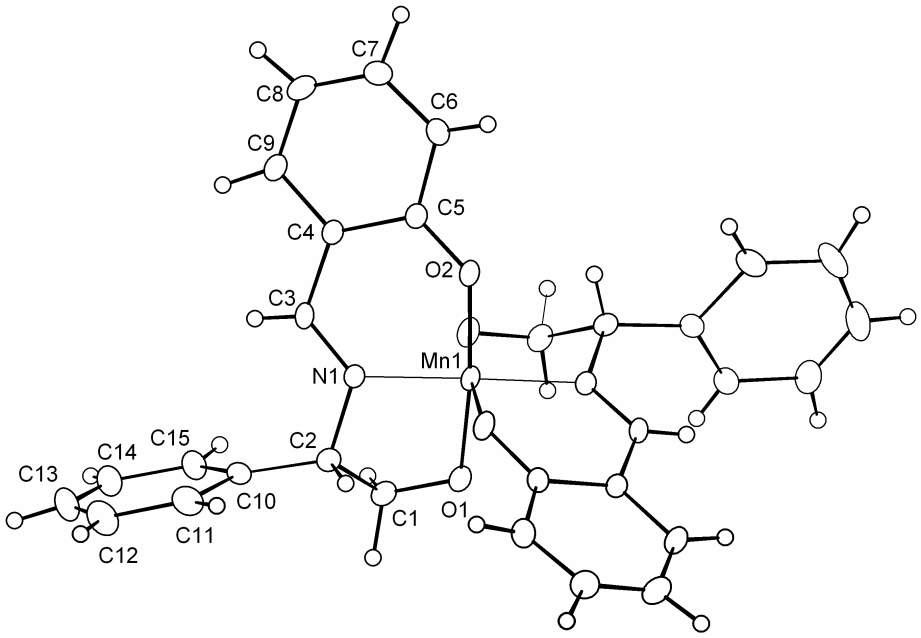

Figure 3.4. Thermal ellipsoid plot (20 % probability) and atom labeling for complex **1.** Only one of the two independent half molecules present in the asymmetric unit is shown (with labels) along with its symmetry generated part (unlabeled).

Selected bond lengths and angles for complex **1** are presented in Table 3.5. The average Mn–N and Mn–O bond lengths for complex **1** are 1.975(2) and 1.879(2) Å, respectively. In MnN_2O_4 coordination sphere, the O-Mn-O and O-Mn-N angles are close to 90^o (within $\pm 5^o$). The average Mn–N and Mn–O bond distances are comparable to those for various reported Mn(IV) complexes with similar ligation.[1(b)] The optical activity of the Mn complex **1** is induced by the enantiopure ligand, H_2L.

There is a weak intermolecular C–H···O hydrogen bonding interaction in the molecule between the alcoholic oxygen O1 and aromatic carbon C9. The relevant hydrogen bonding parameters are [C9–H9···O1#1 0.97 2.51 3.2867 137, #1 = x, 1+y, -1+z]. These interactions propagate through the crystal lattice resulting in the formation of one-dimensional chain like arrangement.

Table 3.5. Selected bond lengths (Å) and angles (°) for complex **1**

Mn(1)-O(1)	1.867(2)	N(1)-C(2)	1.484(3)
Mn(1)-O(2)	1.900(2)	O(2)-C(5)	1.316(3)
Mn(1)-N(1)	1.9696(18)	C(1)-C(2)	1.524(4)
O(1)-C(1)	1.403(3)	C(2)-C(10)	1.513(3)
N(1)-C(3)	1.285(3)	C(3)-C(4)	1.423(3)
O(1)-Mn(1)-O(2)	173.78(10)	N(1)-C(2)-C(10)	115.9(2)
O(1)-Mn(1)-N(1)	84.97(10)	N(1)-C(2)-C(1)	102.7(2)
O(2)-Mn(1)-N(1)	89.60(9)	C(10)-C(2)-C(1)	117.2(2)
C(1)-O(1)-Mn(1)	112.54(17)	N(1)-C(3)-C(4)	124.8(2)
C(3)-N(1)-C(2)	126.8(2)	C(9)-C(4)-C(3)	118.9(2)
C(3)-N(1)-Mn(1)	124.97(17)	C(3)-C(4)-C(5)	122.1(2)
C(2)-N(1)-Mn(1)	108.09(14)	O(2)-C(5)-C(6)	119.3(2)
C(5)-O(2)-Mn(1)	125.15(17)	O(2)-C(5)-C(4)	122.9(2)
O(1)-C(1)-C(2)	108.2(2)	C(15)-C(10)-C(2)	122.1(3)

3.4.6.2. Crystal structure of complex 2

Single crystals of complex **2**, suitable for X-ray crystallography, were grown by slow evaporation of a 1:1 mixture of dimethylformamide (DMF) and acetonitrile solution of the compound. The relevant crystallographic details are given in Table 3.1. Complex **2** crystallizes in the non-centrosymmetric orthorhombic space group $P2_12_12_1$. The asymmetric unit contains one molecule of the complex and two molecules of DMF. The thermal ellipsoid plot of the complex with atom labeling scheme is shown in Figure 3.5. The metal has six coordinate geometry with an N_2O_4 core. The chiral H_2L^2 ligand is dianionic in the complex and acts as a meridional ONO donor using imine nitrogen, phenolate and alkoxide oxygen atoms to bind the metal. The resulting MnN_2O_4 coordination sphere has nearly planar O_4 equator with respect to which the N atoms are located in *trans* positions.

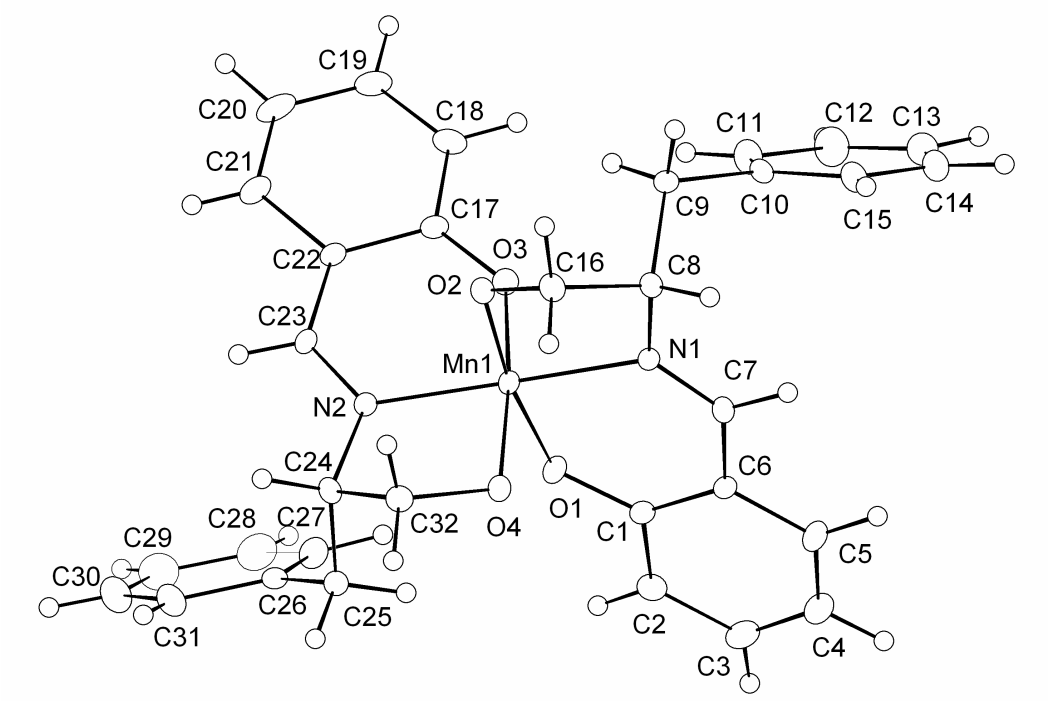

Figure 3.5. Thermal ellipsoid plot for complex **2** (20 % probability). Solvent molecules are omitted for clarity.

Selected bond lengths and angles for complex **2** are listed in Table 3.6. The angles at the metal center show deviations from the ideal octahedral values of 90° and 180° resulting in a distorted octahedral geometry around Mn. The distortion from octahedral geometry is reflected in the acute bite angles between the alkoxide O atom and the imine N atom of the $[ONO]^{2-}$ ligand: [O2-Mn-N1 , 82.79(13) and O4-Mn-N2, 83.89(13)°]. This deviation can be attributed mainly to the rigidity of the Schiff base ligand. Similar distortions from ideal octahedral geometry have been reported by Chakravorty *et al.* in Mn(IV) complexes of tridentate ONO donor Schiff base ligands.[1(i)] Thus the overall geometry around the manganese ion is best described as a distorted meridional octahedron. The average Mn–O_{phe}, Mn–O_{alk} and Mn–N bond distances of 1.9105(3), 1.884(3) and 1.974(3) Å respectively, fall in the range of those, reported for the structurally characterized mononuclear Mn(IV) complexes.[1(b)]

Table 3.6. Selected bond lengths (Å) and angles (°) for complex **2**

Mn(1)-O(1)	1.906(3)	Mn(1)-N(2)	1.975(3)
Mn(1)-O(2)	1.834(3)	N(1)-C(7)	1.297(5)
Mn(1)-N(1)	1.973(3)	N(2)-C(23)	1.275(5)
Mn(1)-O(3)	1.915(3)	O(1)-C(1)	1.319(5)
Mn(1)-O(4)	1.854(3)	O(3)-C(17)	1.290(5)
O(2)-Mn(1)-O(1)	172.48(13)	O(1)-Mn(1)-N(1)	90.81(13)
O(4)-Mn(1)-O(3)	172.27(14)	O(3)-Mn(1)-N(1)	96.52(13)
O(2)-Mn(1)-O(4)	93.50(14)	O(2)-Mn(1)-N(2)	89.58(14)
O(4)-Mn(1)-O(1)	90.49(14)	O(4)-Mn(1)-N(2)	83.89(13)
O(2)-Mn(1)-O(3)	90.70(14)	O(1)-Mn(1)-N(2)	97.19(14)
O(1)-Mn(1)-O(3)	86.09(14)	O(3)-Mn(1)-N(2)	89.66(13)
O(2)-Mn(1)-N(1)	82.79(13)	N(1)-Mn(1)-N(2)	170.22(15)
O(4)-Mn(1)-N(1)	90.45(13)		

In the crystal structure, there are intermolecular C–H···O hydrogen bonding interactions among [MnL_2] complexes resulting in a supramolecular hydrogen bonded network. This consists of hydrogen bonded chain-like arrangements *via* C13 –H13···O2 bonds (relevant H-bonding parameters: 0.93, 2.33, 3.195(7), 155.3), that are further interlinked *via* C9–H9B···O4 bonds (relevant H-bonding parameters: 0.97, 2.57, 3.350(5), 137.0) into an intricate hydrogen bonded framework as shown in Figure 3.6.

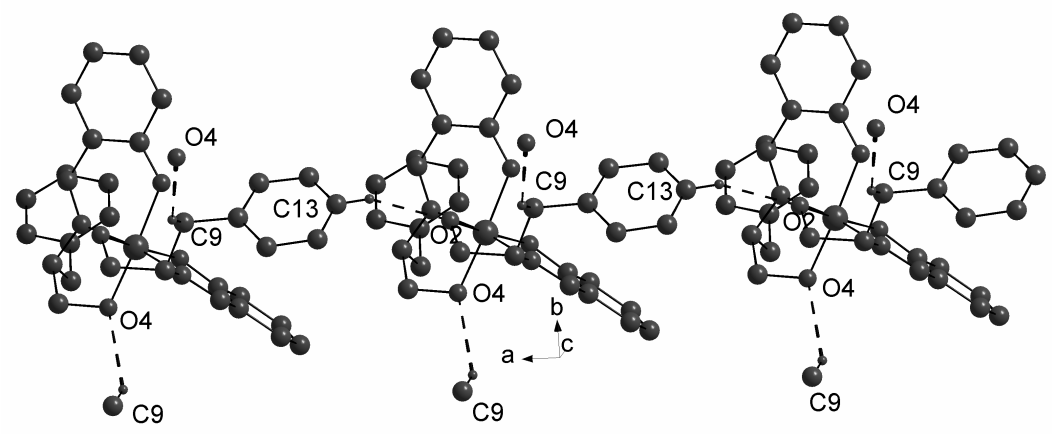

Figure 3.6. Intermolecular association *via* C–H···O hydrogen bonds in complex **2** to form chain-like structure and its mode of linking to adjacent chains.

Along the chain, each complex MnL_2 is additionally hydrogen bonded to a DMF solvent molecule (not shown in Figure 3.6 for clarity). Interestingly, the packing of the chiral complexes in the crystal results in the formation of channels, when viewed down the crystallographic *a* axis (Figure 3.7). DMF solvent molecules are accommodated in the alternate channels. We believe that the chirality of the complex **2** has some role in inducing the formation of such channels.

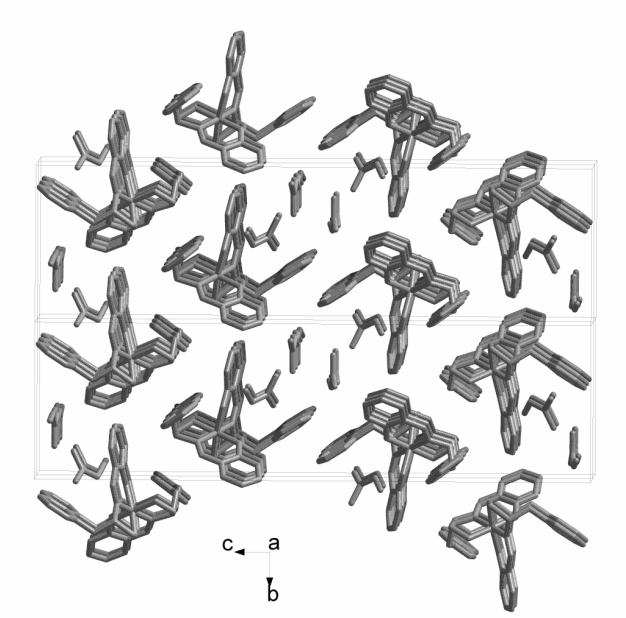

Figure 3.7. Packing diagram of complex **2** showing channels when viewed down crystallographic *a* axis. The channels are alternatively filled by the solvent DMF molecules.

3.4.6.3. Crystal structure of complex 6

Single crystals of complex **6** suitable for X-ray analysis were grown from dimethylformamide solution by slow evaporation method. Crystallographic data for complex **6** are given in Table 3.2.

The molecule crystallizes in the chiral space group monoclinic $P2_1$. The asymmetric unit contains six mononuclear Mn(IV) complexes along with three DMF molecules. In each of these mononuclear complexes present in the asymmetric unit, Mn is hexacoordinated with N_2O_4 coordination sphere. Two tridentate ONO donor ligands satisfy the coordination sites of the metal in a meridional manner. Each ligand coordinates through deprotonated phenolic and alcoholic groups along with an imine nitrogen. The thermal ellipsoid plot of a representative mononuclear unit of complex **6** with the atom labeling scheme is shown in Figure 3.8.

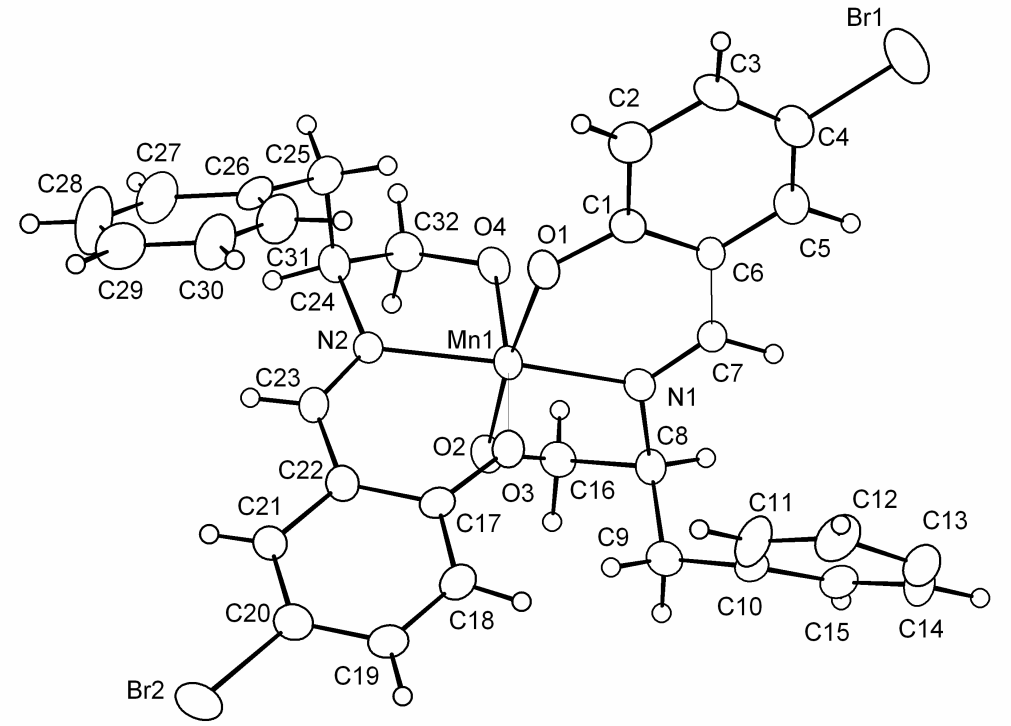

Figure 3.8. Thermal ellipsoid plot (20 % probability) of a representative mononuclear unit of complex **6**.

The coordination geometry around the Mn in each mononuclear unit present in the asymmetric unit can be considered as distorted octahedron. Four oxygen atoms can be taken as constituting a square plane and the two imine nitrogens are situated at axial *trans* positions. The Mn–O_{phe}, Mn–O_{alk}, and Mn–N_{imi} distances vary in the range 1.878(5)-1.913(5), 1.835(5)-1.862(5) and 1.964(6)-1.989(6) Å respectively. The average Mn–O_{phe} (1.896(5) Å), Mn–O_{alk} (1.849(5) Å) and Mn–N_{imi} (1.976(6) Å) distances observed are comparable to those reported for Mn(IV) complexes with similar ligation.[1(b)] Selected bond lengths and angles are given for a representative mononuclear unit in Table 3.7.

Table 3.7. Selected bond lengths (Å) and angles(°) for complex **6**

Mn(1)-O(1)	1.892(5)	Mn(1)-N(2)	1.989(5)
Mn(1)-O(2)	1.859(5)	N(1)-C(7)	1.287(7)
Mn(1)-N(1)	1.981(5)	N(2)-C(23)	1.287(8)
Mn(1)-O(3)	1.913(5)	O(1)-C(1)	1.334(8)
Mn(1)-O(4)	1.839(5)	O(3)-C(17)	1.303(8)
O(2)-Mn(1)-O(1)	173.7(2)	O(1)-Mn(1)-N(1)	91.0(2)
O(4)-Mn(1)-O(3)	171.7(2)	O(3)-Mn(1)-N(1)	95.0(2)
O(4)-Mn(1)-O(2)	92.2(2)	O(2)-Mn(1)-N(2)	87.6(2)
O(4)-Mn(1)-O(1)	89.9(2)	O(4)-Mn(1)-N(2)	84.0(2)
O(2)-Mn(1)-O(3)	92.9(2)	O(1)-Mn(1)-N(2)	98.5(2)
O(1)-Mn(1)-O(3)	85.7(2)	O(3)-Mn(1)-N(2)	89.7(2)
O(2)-Mn(1)-N(1)	83.1(2)	N(1)-Mn(1)-N(2)	169.7(2)
O(4)-Mn(1)-N(1)	92.1(2)		

All six mononuclear Mn(IV) complexes, present in the asymmetric unit, are involved in hydrogen bonding interactions in forming an intricate three-dimensional hydrogen bonded network. These six Mn(IV) complexes can be identified as Mn(1), Mn(2), Mn(3), Mn(4), Mn(5) and Mn(6). In the asymmetric unit, Mn(1) and Mn(2) complexes are hydrogen bonded to form a Mn(1)-Mn(2) dimer (Figure 3.9a). This is formed by the acceptance of C–H protons of Mn(2) complex by O2 oxygen of Mn(1) complex. The Mn(3) complex, which is not hydrogen bonded to any asymmetric unit components, is attached to Mn(1) and Mn(2) units *via* two respective C–H···O bonds (Figure 3.9b). Mn(4), Mn(5) and Mn(6) units are linked *via* hydrogen bonds in the asymmetric unit forming a hydrogen bonded trimer (Mn(4)-Mn(5)-Mn(6)) as shown in figure 3.9c. The formation of this trimer can be described by the bifurcated C–H···O hydrogen bonding interactions between Mn(5) and Mn(6) complexes followed by the interaction of Mn(5) complex with Mn(4) complex. This trimer, formed in the asymmetric unit, is additionally hydrogen bonded to three surrounding Mn complexes namely Mn(5), Mn(6) and Mn(6) in the crystal structure. The hydrogen bonded dimer is further hydrogen bonded to four Mn complexes, three Mn(3) and one Mn(4). These interactions result in the formation of multifaceted hydrogen bonding network as shown in Figure 3.10. Packing of these manganese complexes result in the formation of channels in the crystal lattice when viewed down

to the crystallographic *a* axis (Figure 3.10). The chirality of the complex $[Mn^{IV}L^{6}{}_{2}]$ plays an important role in forming such channels. The relevant C–H···O hydrogen bonding parameters are described in Table 3.8.

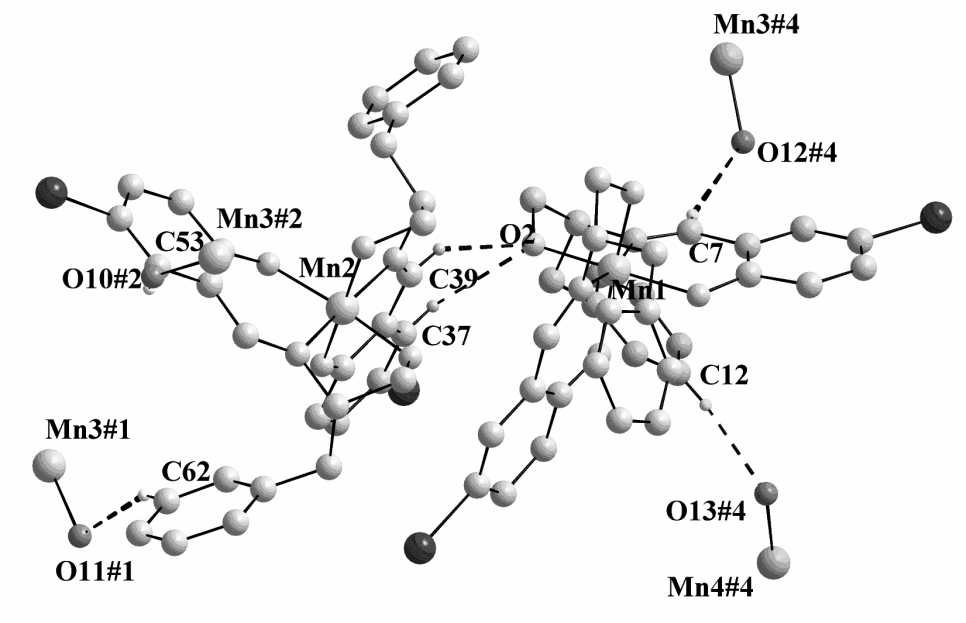

Figure 3.9a

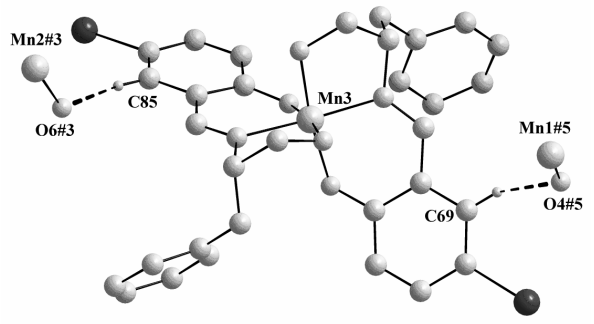

Figure 3.9b

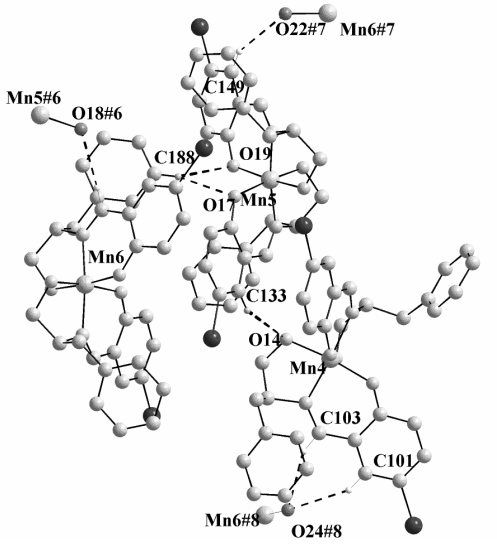

Figure 3.9c

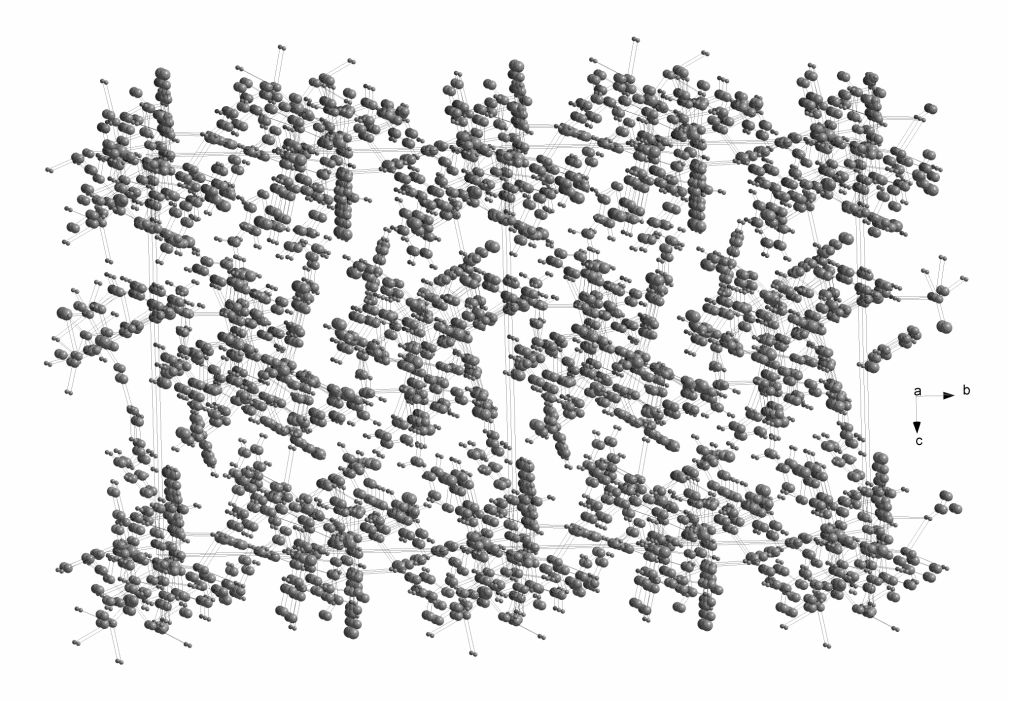

Figure 3.10. Hydrogen bonded network in the crystal lattice of complex **6.**

Table 3.8. Hydrogen-bonding parameters (Å, °) for complex **6**

Donor–H···Acceptor	D – H	H···A	D···A	D – H···A	Symmetry operator of A
C(7)–H(7)···O(12)	0.93	2.57	3.413(8)	151.6	1-x, 0.5+y, 1-z
C(12)–H(12)···O(13)	0.93	2.37	3.294(10)	172.7	1-x, 0.5+y, 1-z
C(37)–H(37)···O(2)	0.93	2.62	3.371(9)	138.6	x, y, z
C(39)–H(39)···O(2)	0.93	2.40	3.223(8)	147.4	x, y, z
C(53)–H(53)···O(10)	0.93	2.46	3.237(9)	141.6	-x, 0.5+y, 1-z
C(62)–H(62)···O(11)	0.93	2.47	3.316(10)	151.0	x, 1+y, z
C(69)–H(69)···O(4)	0.93	2.41	3.193(8)	141.7	1-x, -0.5+y, 1-z
C(85)–H(85)···O(6)	0.93	2.53	3.392(9)	155.2	-x, -0.5+y, 1-z
C(101)–H(101)···O(24)	0.93	2.51	3.367(9)	153.3	1-x, -0.5+y, 2-z
C(103)–H(103)···O(24)	0.93	2.59	3.433(8)	151.1	1-x, -0.5+y, 2-z
C(133)–H(133)···O(14)	0.93	2.63	3.471 (9)	151.0	x, y, z
C(149)–H(149)···O(22)	0.93	2.41	3.259(9)	151.8	-x, -0.5+y, 2-z
C(183)–H(183)···O(18)	0.93	2.55	3.296(8)	137.4	-x, 0.5+y, 2-z
C(188)–H(188)···O(17)	0.93	2.42	3.288(11)	156.1	x, y, z

3.4.6.4. Crystal structure of complex 7

Complex **7** crystallizes in orthorhombic chiral space group $P2_12_12_1$. The asymmetric unit contains one molecule of the mononuclear complex and one solvent DMF molecule. Crystallographic data are given in Table 3.2. The thermal ellipsoid plot of the complex with the atom labeling scheme is shown in Figure 3.11. As observed in the previous examples, here also the doubly deprotonated chiral Schiff base (H_2L^7) acts as tridentate ONO donor ligand and binds the metal in a meridional manner. The N_2O_4 coordination sphere of the resulting Mn center can be better described as a slightly distorted octahedron. The distortion from the ideal octahedral geometry is reflected in the bond lengths and angles given in Table 3.9.

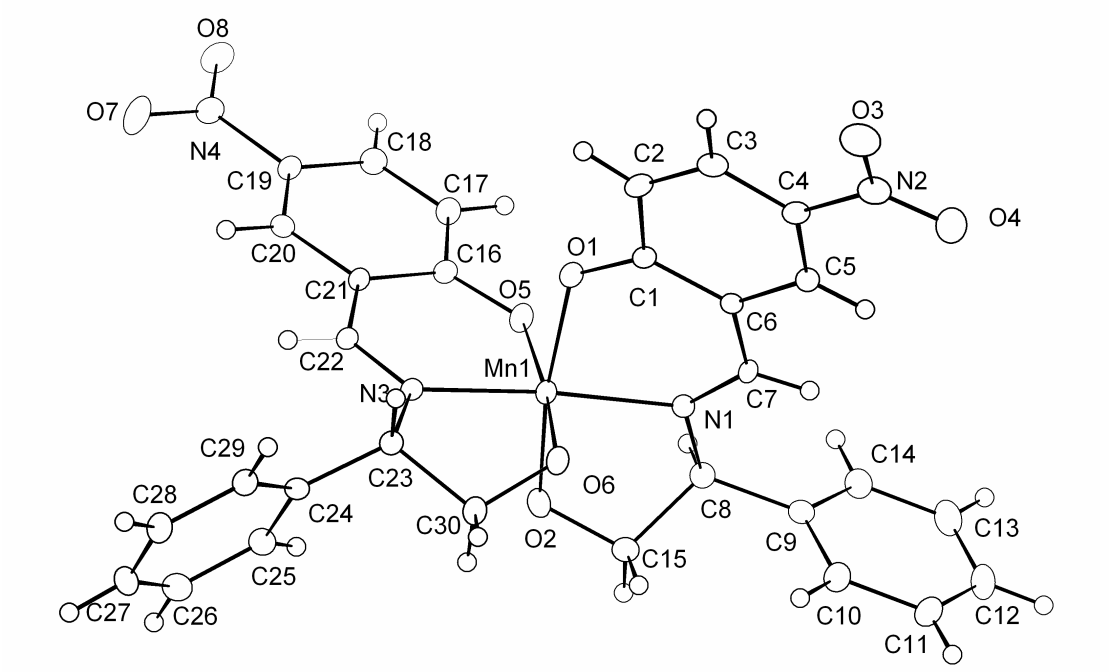

Figure 3.11. Thermal ellipsoid plot of complex **8** (10 % probability) showing atom labeling scheme.

Table 3.9. Selected bond lengths (Å) and angles (°) for complex **7**

Mn(1)-O(1)	1.934(3)	Mn(1)-N(3)	1.972(3)
Mn(1)-O(2)	1.898(3)	N(1)-C(7)	1.283(4)
Mn(1)-N(1)	1.987(3)	N(3)-C(22)	1.287(4)
Mn(1)-O(5)	1.928(3)	O(1)-C(1)	1.303(4)
Mn(1)-O(6)	1.843(3)	O(5)-C(16)	1.307(4)
O(2)-Mn(1)-O(1)	170.72(12)	O(1)-Mn(1)-N(1)	88.70(12)
O(6)-Mn(1)-O(5)	174.06(12)	O(6)-Mn(1)-N(1)	89.66(11)
O(2)-Mn(1)-O(5)	89.43(12)	O(2)-Mn(1)-N(3)	95.77(12)
O(6)-Mn(1)-O(1)	92.21(12)	O(5)-Mn(1)-N(3)	90.49(11)
O(6)-Mn(1)-O(2)	92.26(12)	O(1)-Mn(1)-N(3)	92.80(11)
O(5)-Mn(1)-O(1)	86.94(11)	O(6)-Mn(1)-N(3)	83.68(11)
O(2)-Mn(1)-N(1)	83.20(12)	N(3)-Mn(1)-N(1)	173.22(12)
O(5)-Mn(1)-N(1)	96.19(11)		

The Mn–O_{phe} bond lengths of 1.934(3) and 1.928(3) Å are slightly longer than that of the previous examples. This may be due to the presence of electron withdrawing nitro group at the *para* position of the phenolate oxygen. The electron withdrawing –NO_2 group reduces the electron density on phenolate oxygen causing an increase in the bond length compared to unsubstituted and bromo substituted complexes.

Interestingly, this complex acts as the well defined building unit in forming a helical-like structure that is constructed from unusual ONO···ONO non-covalent, non hydrogen bonded interactions (O···O distance is 3.245(6) Å). Such O···O (non-covalent) interactions is recently reported in organic molecules.[15]

3.4.7. Catalytic studies

In order to determine the catalytic activity of the monomeric Mn(IV) complexes, oxidation reactions of *trans*-stilbene and styrene were performed in acetonitrile solutions using iodosobenzene (PhIO) as the oxidant. Details of catalytic experiments and product analyses are given in section 2.8. The results are summarized in Table 3.10. In these oxidation reactions, the complexes were found to activate PhIO at room temperature to give corresponding epoxidation products, *trans*-stilbene and

styrene oxides in moderate yields. No appreciable reactions took place in the absence of catalysts. The products of oxidation reactions were found to be mainly epoxides.

Table 3.10. Epoxidation data for complexes **1-8**

Complex	Yield of Epoxide (%)	
	Styrene oxide	Stilbene oxide
1	53	37
2	48	33
3	41	27
4	38	29
5	45	33
6	47	35
7	55	40
8	57	42

For *trans*-stilbene, the product was isolated and characterized by NMR spectroscopy and the percentage yield was in the range of 37-42. For styrene, the epoxidation reaction was monitored by GC using bromobenzene as an internal standard to quantify the final yield. The percentage yield was in the range of 38-57. A representative GC profile of the analysis of the epoxidation reaction products of styrene is presented in Figure 3.12. The peaks are assigned by comparing the retention time of each peak with that of standard samples under identical conditions.

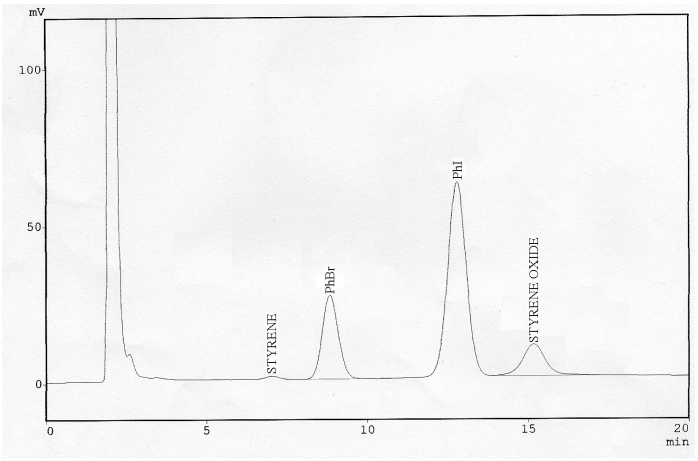

Figure 3.12. A representative G. C. profile for the analysis of styrene epoxidation product.

It is important to note that, in both epoxidation reactions, the oxidized products were identified as racemic mixtures, although the manganese complexes used as catalysts contain chiral centres. The possible reason for this non-enantioselectivity might be the degradation of the catalyst (detaching the enantiopure ligands) during the binding process of the substrate to the manganese centre, since there are no vacant sites on metal center due to its octahedral geometry.

3.5. Conclusion

A series of chiral mononuclear Mn(IV) complexes are synthesized from chiral amino alcohol based Schiff bases with N_2O_4 coordination environment. The oxidation state of manganese was confirmed by IR, CV, EPR studies and magnetic moment determination. The chirality of the complexes was evidenced by circular dichroism spectroscopy. The EPR spectral feature (an absorption near g ~4 and a weak response at g ~2) is consistent with a Mn(IV) complex. Four of the complexes are characterized by single crystal X-ray structure determination. The alkoxide and phenolate oxygens are not acting as bridging groups in these complexes thus giving only mononuclear

complexes. The complexes exhibit a negative redox wave in the cyclic voltammogram corresponding to Mn^{IV}/Mn^{III} couple indicating the ability of the Schiff bases H_2L^1-H_2L^8 to stabilize the higher oxidation states of manganese. Some of the complexes show weak hydrogen bonding interactions in their crystal structures. These interactions lead to the formation of interesting supramolecular architectures including one dimensional chains, channels etc. in the crystal lattice. Formation of such structures emphasizes the potential of chiral amino alcohol based Schiff bases in supramolecular chemistry as desirable ligand systems. The complexes **1-8** were found to catalyze the oxidation reactions of *trans*-stilbene and styrene to their corresponding epoxides in presence of iodosobenzene as the oxidant. The non-enantioselectivity of these reactions can be attributed to the octahedral structure of the complexes.

3.6. References

1. (a) R. P. John, A. Sreekanth, M. R. P. Kurup and H. –K. Fun, *Polyhedron,* 2005, **24**, 601; (b) T. Weyhermuller, T. K. Paine, E. Bothe, E. Bill and P. Chaudhuri, *Inorg. Chim. Acta,* 2002, **337**, 344; (c) T. M. Rajendiran, J. W. Kampf and V. L. Pecoraro, *Inorg. Chim. Acta,* 2002, **339**, 497; (d) P. Perez-Lourido, J. Romero, L. Rodriguez, J. A. Garcia-Vazquez, J. Castro, A. Sousa, J. R. Dilworth and O. R. Nascimento, *Inorg. Chem. Commun.,* 2002, **5**, 337; (e) H. Asada, M. Ozeki, M. Fujiwara and T. Matsushita, *Chem. Lett.,* 1999, 525; (f) M. Mikuriya, D. Jie, Y. Kakuta and T. Tokii, *Bull. Chem. Soc. Jpn.,* 1993, **66**, 1132; (g) R. O. C. Hart, S. G. Bott, J. L. Atwood and S. R. Cooper, *J. Chem. Soc., Chem. Commun.,* 1992, 894; (h) S. M. Saadeh, M. S. Lah and V. L. Pecoraro, *Inorg. Chem.,* 1991, **30**, 8; (i) S. Dutta, P. Basu and A. Chakravorty, *Inorg. Chem.,* 1991, **30**, 4031; (j) S. K. Chandra, S. B. Choudhury, D. Ray and A. Chakravorty, *J. Chem. Soc., Chem. Commun.,* 1990, 474; (k) S. K. Chandra, P. Basu, D. Ray, S. Pal and A. Chakravorty, *Inorg. Chem.,* 1990, **29**, 2423; (l) P. Deplano, E. F. Trogu, F. Bigoli and M. A. Pellingheli, *J. Chem. Soc., Dalton Trans.,* 1987, 2407; (m) D. P. Kessissoglou, X. Li, W. M. Butler and V. L. Pecoraro, *Inorg. Chem.,* 1987, **26**, 2487; (n) D. P. Kessissoglou, W. M. Butler and V. L. Pecoraro, *J. Chem. Soc., Chem. Commun.,* 1986, 1253; (o) P. S. Pavacik, J. C. Huffman and G. Christou, *J. Chem. Soc., Chem. Commun.,* 1986, 43; (p) M. Tirant and T. D. Smith, *Inorg. Chim. Acta,* 1986, **121**, 5.
2. (a) *Manganese Redox Enzymes*, ed. V. L. Pecoraro, VCH Publishers, New York, 1992; (b) V. K. Yachandra, V. J. DeRose, M. J. Latimer, I. Mukerji, K. Sauer and M. P. Klein, *Science,* 1993, **260**, 675; (c) R. Manchanda, G. W. Brudvig and R. H. Crabtree, *Coord. Chem. Rev.,* 1995, **144**, 1; (d) R. J. Debus, *Biochim. Biophys. Acta,* 1992, **1102**, 269; (e) J. Cole, Y. K. Yachandra, R. D. Guiles, A. E. McDermott, R. D. Britt, S. L. Dexheimer, K. Sauer and M. P.

Klein, *Biochim. Biophys. Acta,* 1987, **890**, 395; (f) J. L. Zimmermann and A. W. Rutherford, *Biochemistry,* 1986, **25**, 395.

3. O. R. Hansson, R. Aasa and T. Vanngard, *Biophys. J.,* 1987, **51**, 825.
4. (a) A. Zouni, H. T. Witt, J. Kern, P. Fromme, N. Kraub, W. Saenger and P. Orth, *Nature*, 2001, **409**, 739; (b) N. Kamiya and J. R. Shen, *Proc. Natl. Acad. Sci. U.S.A.,* 2003, **100**, 98; (c) K. N. Ferreira, T. M. Iverson, K. Maghlaoui, J. Barber and S. Iwata, *Science,* 2004, **303**, 1831.
5. (a) *Comprehensive Asymmetric Catalysis*, eds. E. N. Jacobsen, A. Pfaltz and H.Yamamoto, Springer-Verlag, New York, 1999; (b) T. Katsuki, in *Catalytic Asymmetric Synthesis*, ed. I. Ojima, VCH Publishers, New York, 2000.
6. (a) K. P. Bryliakov, O. A. Kholdeeva, M. P. Vanina and E. P. Talsi, *J. Mol. Catal. A: Chem.,* 2002, **178**, 47; (b) W. Adam, C. Mock-Knoblauch, C. R. Saha-Möller and M. Herderich, *J. Am. Chem. Soc.,* 2000, **122**, 9685.
7. *XSCANS* Version 2.31, Siemens Energy and Automation, Inc., Madison, WI, USA, 1997.
8. G. M. Sheldrick, SHELX-97, *Program for Crystal Structure Solution and Analysis*, University of Göttingen, Göttingen, Germany, 1997.
9. Bruker. *SADABS, SMART, SAINTPLUS and SHELXTL*, Bruker AXS Inc., Madison, Wisconsin, USA, 2003.
10. K. Brandenburg, *DIAMOND Version 2.1e*, Crystal Impact GbR, Bonn, Germany, 2001.
11. H. D. Flack, *Acta Crystallogr. Sect A,* 1983, **39**, 876.
12. R. J. P. Williams, *J. Chem. Soc.,* 1955, 137; R. N. Mukherjee, O. A. Rajan and A. Chakravorty, *Inorg. Chem.*, 1982, **21**, 785; J. W. Pyrz, A. L. Roe, L. J. Stern and L. Que Jr., *J. Am. Chem. Soc.,* 1985, **107**, 614; A. V. Lakshmi, N. R. Sangeetha and S. Pal, *Ind. J. Chem.*, 1997, **36A**, 844; A. Choudhury, B. Geetha, N. R. Sangeetha, V. Kavita, V. Susila and S. Pal, *J. Coord. Chem.*, 1999, **48**, 87; N. R. Sangeetha, V. Kavita, S. Wocadlo, A. K. Powell and S. Pal, *J. Coord. Chem.*, 2000, **51**, 55.

13. A. Moscowitz, *Tetrahedron*, 1961, **13**, 48.
14. (a) E. Pederson and H. Toftlund, *Inorg. Chem.,* 1974, **13**, 1603; (b) D. C. Bradley, R. G. Copperthwaite, S. A. Cotton, K. D. Sales and J. F. Gibson, *J. Chem. Soc., Dalton Trans.,* 1973, 191; (c) J. C. Hempel, L. O. Morgan and W. B. Lewis, *Inorg. Chem.,* 1970, **9**, 2064; (d) L. S. Singer, *J. Chem. Phys.,* 1955, **23**, 379.
15. R. K. R. Jetti, P. K. Thallapally, A. Nangia, C. –K. Lam and T. C. W. Mak, *Chem. Commun.,* 2002, 952.

Synthesis and characterization of mono, tri- and tetranuclear cobalt complexes derived from chiral amino alcohol based Schiff bases

4.1. Abstract

A series of cobalt complexes **(9-16)** has been synthesized by the reaction of chiral Schiff bases H_2L^1-H_2L^8 (Scheme 2.1), derived from substituted salicylaldehydes and chiral amino alcohols, with cobalt acetate in methanol at room temperature. All these complexes are characterized by elemental analysis, IR, UV-Vis, CD spectroscopy and room temperature magnetic moment measurements. Four of these complexes (**9**, **12**, **15**, **16**) are characterized by single crystal X-ray structure determination as well. The complexes show considerable structural diversity in their crystal structures, depending on the steric and electronic factors of the ligands. The ligands H_2L^3 and H_2L^4 derived from 5-methoxy (5-MeO) salicylaldehyde gave mononuclear Co(III) complexes having octahedral geometry. At the same time, complexes derived from H_2L^1, H_2L^2, H_2L^5, H_2L^6 and H_2L^8 (5-H, 5-Br and 5-NO_2 salicylaldehyde derivatives) are found to be alkoxo bridged trinuclear complexes with mixed oxidation states Co(III)-Co(II)-Co(III). In these complexes the two terminal Co(III) centers are octahedral while the middle Co(II) is in distorted trigonal bipyramidal/square pyramidal geometry. Ligand H_2L^7 gave an interesting tetranuclear cobalt complex in which three octahedral Co(III) complexes act as chelating units for a central Co(II), which adopts a distorted trigonal prismatic geometry. The mononuclear cobalt complex **12** obtained from 5-methoxy salicylaldehyde derivative shows intermolecular O–H···O interactions leading to the formation of helical supramolecular arrangement in the relevant crystal lattice.

4.2. Introduction

Multinuclear cobalt complexes have rich coordination chemistry that has been investigated at length. Such complexes reported in the literature with various ligand systems show a great deal of structural diversity and variations in their oxidation states. Among these, mixed valent tri- and tetra- nuclear cobalt complexes are of special interest since the study of such systems contributes immensely to the overall understanding of the coordination chemistry of cobalt.[1]

The bioinorganic interest of cobalt complexes has increased during the past two decades because of the discovery and characterization of new cobalt containing proteins. Since the mid 1980s more than eight new cobalt dependent proteins (for eg. methionine aminopeptidase (MetAP)) have been discovered, which led to the enhanced inclusion of cobalt coordination compounds in bioinorganic modeling studies.[2] In addition to their biological relevance cobalt complexes, especially chiral cobalt complexes, are widely employed as catalysts for various organic transformations.[3]

Inorganic supramolecular chemistry is an emerging area of modern coordination chemistry. A major goal in inorganic supramolecular chemistry is to develop well defined polynuclear coordination arrays through proper design strategies which include the selection of suitable ligand systems and metal ions. Various cobalt complexes are reported as building blocks to give interesting supramolecular architectures in their crystal lattices.[4]

The chiral amino alcohol based Schiff bases are suitable ligands for the preparation of complexes with structural, biomimetic and supramolecular relevance. Presence of alcoholic and phenolic OH groups, azomethine C=N group and chirality of such systems enhances the biological relevance of the resulting complexes. The hydrogen bonding groups present in the ligand backbone can stabilize the overall structure and may lead to some interesting supramolecular assemblies. The alcoholic and phenolic hydroxyl groups are known to promote multinuclear complex formation

through alkoxide and phenoxide bridging. Present chapter describes the coordination chemistry of cobalt with the chiral Schiff bases H_2L^1-H_2L^8 (Scheme 2.1).

4.3. Experimental

4.3.1. Materials

As given in section **2.2**

4.3.2. Physical measurements

Details are given in section **2.3**

4.3.3. Synthesis and characterization of the Schiff bases H_2L^1-H_2L^8

Synthesis and characterization of chiral Schiff base ligands H_2L^1-H_2L^8 are described in section **2.4**

4.3.4. Synthesis of complexes 9-16

Synthetic details and characterization data for cobalt complexes **9-16** are given in section **2.6**

4.3.5. X-ray crystallography

Data for complexes **9**, **12** and **15** were collected at room temperature on a Bruker SMART APEX CCD area detector system [λ(Mo-Kα) = 0.71073 Å], graphite monochromator, 2400 frames were recorded with an ω scan width of 0.3°, crystal-detector distance 60 mm, collimator 0.5 mm. The data were reduced using SAINTPLUS[5] and a multi-scan absorption correction using SADABS[5] was performed. Structure solution and refinement were done using programs of SHELX-97[6]. Hydrogen atoms were introduced on calculated positions and included in the refinement riding on their respective parent atoms. The absolute configurations for the complex molecules were successfully determined by refining the Flack parameter.[7]

For complex **9** all the non-hydrogen atoms except that of the uncoordinated solvent molecules are refined anisotropically. Some of the benzene rings show disorder and some restraints were applied. Hydrogen atoms were not located in association with coordinated and solvent water molecules.

In the case of complex **12** all the non-hydrogen atoms are refined anisotropically. The hydrogen atoms associated with some of the alcoholic oxygens are not located.

For complex **15**, the R_{int} value was high (0.1235). Such a high R_{int} value is probably due to the long *c* axis (46.257(3) Å) and the subsequent difficulty in neatly resolving adjacent reflections and to the low diffraction power of the crystal characterized by a large fraction of weak intensities. Also the complex contains a large amount of void space. All the non-hydrogen atoms except the water oxygen are refined anisotropically. The hydrogen atoms associated with the solvent water molecule are not located in the difference Fourier maps.

Single crystals of the complex **16** were grown by slow evaporation of a dimethylformamide solution. Unit cell determination and the data collection were performed on an Enraf-Nonius Mach3 single crystal diffractometer using graphite monochromated Mo $K\alpha$ radiation (λ = 0.71073 Å). An empirical absorption correction was applied to the data based on the ψ-scans of three reflections.[8] Programs of WinGX[9] were used for data reduction and absorption correction. The structure was solved by direct methods and refined on F^2 by full-matrix least squares procedures using SHELX-97 programs.[6] All the non-hydrogen atoms except the uncoordinated solvent molecules are refined anisotropically. Some benzene rings show disorder and some restraints were applied. Hydrogen atoms were not located in association with water molecule oxygen atom. A high R_{int} value (0.1510) observed is probably due to the low diffraction power of the crystal characterized by a large fraction of weak intensities.

Crystallographic data for the complexes **9** and **12** are presented in Table 4.1 and for complexes **15** and **16** in Table 4.2.

Table 4.1. Crystal and structure refinement data for complexes **9** and **12**

Complex	**9**	**12**
Empirical formula	$C_{66}H_{72}N_6O_{13}Co_3$	$C_{139}H_{147}N_9O_{25}Co_4$
Formula weight	1334.09	2579.38
Crystal system	Triclinic	Orthorhombic
Space group	*P*1	$P2_12_12_1$
λ / Å	0.71073	0.71073
a / Å	11.4737(7)	21.5421(11)
b / Å	12.4004(8)	25.5084(13)
c / Å	13.2286(8)	25.6047(13)
α / °	105.0090(10)	
β / °	92.7810(10)	
γ / °	93.7460(10)	
V / Å^3	1809.87(19)	14069.9(12)
Z	1	4
μ / mm^{-1}	0.739	0.532
ρ_{calcd} / gcm^{-3}	1.224	1.218
T / ºC	25	25
Scan type	ω	ω
Independent reflns	18905 (R_{int}= 0.0228)	147193 (R_{int}= 0.0982)
Observed reflections	13920	27690
Number of parameters	735	1598
Goodness-of-fit[c]	1.033	0.992
*R*1,[a] w*R*2[b] [($I > 2\sigma(I)$]	0.0716, 0.1790	0.0783, 0.1831
Largest diff. peak and hole e Å^{-3}	0.795 and -0.319	1.048 and -0.326
Absolute structure parameter	0.036(17)	-0.001(16)

[a] $R1 = \sum||F_o| - |F_c||/\sum|F_o|$. [b] $wR2 = \{\sum[(F_o^2 - F_c^2)^2]/\sum[w(F_o^2)^2]\}^{1/2}$.
[c] $GOF = \{\sum[w(F_o^2 - F_c^2)^2]/(n - p)\}^{1/2}$ where 'n' is the number of reflections and 'p' is the number of parameters refined; $w = 1/[\sigma^2(F_o^2) + (aP)^2 + bP]$ where a = 0.1163 and b = 0 for complex **9**; and a = 0.1212 and b = 0 for complex **12**.

Table 4.2. Crystal and structure refinement data for complexes **15** and **16**

Complex	**15**	**16**
Empirical formula	$C_{90}H_{75}Co_4N_{12}O_{25}$	$C_{73}H_{79}Co_3N_{11}O_{20}$
Formula weight	1960.34	1607.26
Crystal system	Tetragonal	Monoclinic
Space group	$P4_12_12$	$P2_1$
λ / Å	0.71073	0.71073
a / Å	18.5054(5)	12.352(11)
b / Å	18.5054(5)	24.736(19)
c / Å	46.257(3)	13.085(5)
β / °		90.22(6)
V / Å^3	15840.7(11)	3998(5)
Z	4	2
μ / mm^{-1}	0.459	0.690
ρ_{calcd} / gcm^{-3}	0.822	1.335
T / ºC	25	25
Scan type	ω	ω
Independent reflns.	183227 (R_{int}= 0.1235)	9308 (R_{int}= 0.1582)
Observed reflections	19330	9304
Number of parameters	591	909
Goodness-of-fit[c]	0.916	1.019
$R1$,[a] w$R2$[b] [($I > 2\sigma(I)$)]	0.0820, 0.2087	0.0830, 0.1758
Largest diff. peak and hole e Å^{-3}	0.966 and –0.424	0.572 and –0.609
Absolute structure parameter	–0.02(2)	–0.02(3)

[a] $R1 = \sum||F_o| - |F_c||/\sum|F_o|$. [b] $wR2 = \{\sum[(F_o^2 - F_c^2)^2]/\sum[w(F_o^2)^2]\}^{1/2}$.
[c] GOF = $\{\sum[w(F_o^2 - F_c^2)^2]/(n - p)\}^{1/2}$ where 'n' is the number of reflections and 'p' is the number of parameters refined; $w = 1/[\sigma^2(F_o^2) + (aP)^2 + bP]$ where a = 0.1500 and b = 0 for complex **15**; and a = 0.1090 and b = 0 for complex **16**.

4.4. Results and discussion

4.4.1. Synthesis of complexes 9-16

The complexes **9-16** were synthesized by reacting one mole equivalent of the corresponding Schiff base with one mole equivalent of cobalt acetate tetrahydrate in methanol. The dark brown/reddish brown solutions were evaporated completely and subsequently extracted with dichloromethane (DCM). The DCM solutions on evaporation gave dark brown/reddish brown solids which were recrystallized from dimethylformamide solutions. Elemental analytical data did not conform to general molecular formula for these complexes which was later confirmed by the single crystal X-ray analyses. Coordination of the imine center through nitrogen is seen in the υ(C=N) in the range 1651-1641 cm^{-1}. In some complexes this value is found to be slightly higher than that for the uncoordinated Schiff bases. Although this is quite uncommon, such observation has been reported in literature in the case of Mo complexes of amino alcohol based Schiff base complexes.[10] The strong band at ~1540 cm^{-1} is characteristic of the phenolic C–O stretching mode acquiring partial double bond character through conjugation with the imine system in chelate rings. The C=C stretch appears at around 1600 cm^{-1} as a shoulder band.

The complexes showed variations in their nuclearity and overall structural arrangements despite the fact that the experimental conditions were identical. It was found that all the complexes contain at least one Co(III) center formed by the oxidation of Co(II) to Co(III). Atmospheric oxygen is the possible oxidizing agent here and this oxidation is facilitated by alkoxide and phenoxide groups of the ligands. H_2L^3 and H_2L^4 gave mononuclear low spin Co(III) complexes, while ligands H_2L^1, H_2L^2, H_2L^5, H_2L^6 and H_2L^8 gave mixed valence trinuclear Co(III)-Co(II)-Co(III) complexes. The ligand H_2L^7 gave an interesting tetranuclear cobalt complex with rather uncommon trigonal prismatic geometry around the central cobalt. The elemental analytical data and magnetic moment measurements are in good agreement with the above conclusions later confirmed by the single crystal X-ray analyses.

Tetradentate Schiff base-oxovanadium complexes having electron donating or withdrawing groups at the 5-position of the salicylaldehyde moieties are reported to show similar structural diversity where in the 5-MeO substituted complex is monomeric while the 5-H, 5-Br and 5-NO_2 substituted complexes are found to be polymeric.[11]

4.4.2. Electronic and circular dichroism spectra

The electronic and circular dichroism spectra of complexes **9-16** were recorded in acetonitrile solutions. The electronic spectra show two weak bands in the 650-700 nm and 520-535 nm range. These bands are tentatively assigned to $^1A_{1g} \rightarrow {}^1T_{1g}$ and $^1A_{1g} \rightarrow {}^1T_{2g}$ ligand field transitions respectively for an octahedral Co(III) center.[12] The transitions due to Co(II) centers in mixed valent complexes might have been obscured by the intense absorption due to Co(III) portion of these complexes. Similar instances have been reported previously.[13] It appears that the relatively high intensities of these d-d bands are due to strong tail from charge transfer transitions. The intense band observed around 400 nm is assigned to phenolate (O^-) $p_\pi \rightarrow$ Co(III) charge transfer transition (LMCT). The other intense transitions are assigned to intraligand charge transfer transitions (ILCT).

A general blue shift in band positions is observed for these complexes with electron withdrawing substituents. Such blue-shift originating from the electron withdrawing nature of the substituents has been observed previously in some manganese, iron, vanadium and copper complexes.[14]

The circular dichroism spectra of these complexes show bands corresponding to the electronic absorptions. The bands due to the d-d transitions are positive while the charge transfer transitions appear as negative cotton effects. Some representative electronic and circular dichroism spectra are given in Figure 4.1. The electronic and CD spectra of the complexes **9-16** are similar despite the structural changes. The appearance of Co(III) d-d bands in all eight complexes confirm the presence of atleast one Co(III) center in each complex.

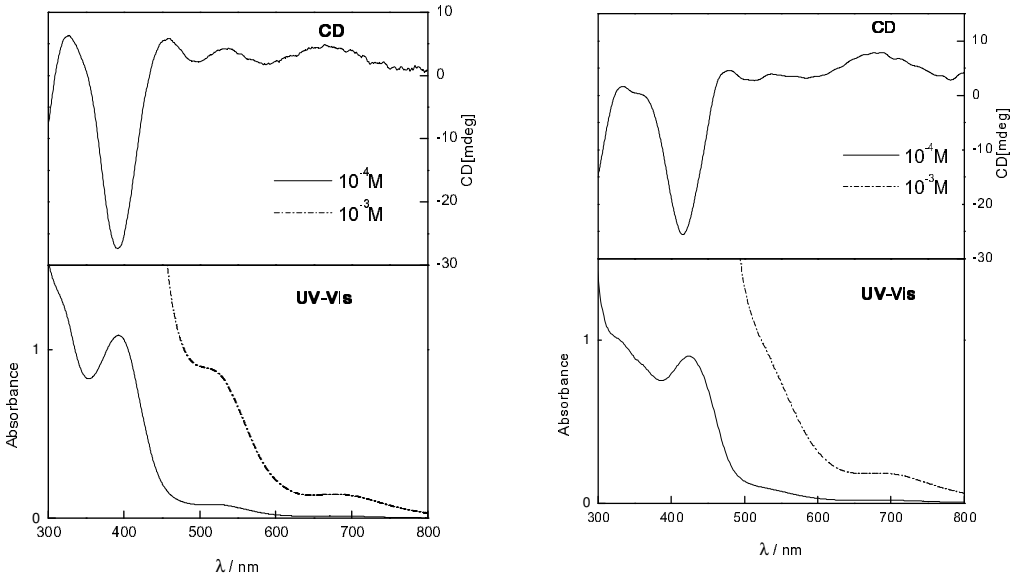

Figure 4.1. The electronic and circular dichroism spectra of complexes **9** (a) and **11**(b) in acetonitrile solutions.

4.4.3. Magnetic properties

The magnetic susceptibility measurements of the complexes were done on powdered samples at room temperature and the values are given in Table 4.3. These values in the range 3.4 - 5.1 BM are characteristic of high spin Co(II) configuration (S = 3/2) with three unpaired electrons. The magnetic properties of polynuclear complexes are extremely sensitive to structural modifications. The Co(II) center present in these complexes are found to exist in a variety of structural environments ranging from distorted trigonal bipyramidal in **9** to distorted trigonal prismatic in complex **15**. The large spread of μ_{eff} values is attributed to the geometric distortions that influence the magnitude of the ligand field splitting. The observed low effctive magnetic moment for complex **9** implies that the orbital contribution to the spin-only value (3.87 μB) is fairly small in that case. The complexes **11** and **12** were found to be diamagnetic as expected for a low spin Co(III) state.

Table 4.3. Summary of electronic spectra and room temperature magnetic moments for complexes **9-16**

Complex (All in MeCN solution)	Electronic band positions, nm	Extinction coeff, ε ($M^{-1}cm^{-1}$)	Proposed band assignment	Room temp magnetic moment, μ_{eff}/μ_B
9	690	138	d-d	3.40
	522	867	d-d	
	398	9402	CT	
	317	13220	CT	
	252	87930	CT	
10	705	400	d-d	4.35
	526	1284	d-d	
	394	8070	CT	
	322	10950	CT	
	251	76170	CT	
11	700	88	d-d	Diamagnetic
	535	423	d-d	
	418	3803	CT	
	315	7686	CT	
	255	35880	CT	
12	700	96	d-d	Diamagnetic
	535	435	d-d	
	420	3914	CT	
	315	7544	CT	
	255	35471	CT	
13	682	187	d-d	3.80
	530	836	d-d	
	411	8600	CT	
	330	12350	CT	
	290	29600	CT	

14	692	250	d-d	4.27
	530	754	d-d	
	399	6360	CT	
	324	8610	CT	
	285	21630	CT	
	244	66340	CT	
15	650	478	d-d	5.10
	520	1560	d-d	
	387	92940	CT	
	315	38660	CT	
	243	120830	CT	
16	650	350	d-d	4.25
	520	1013	d-d	
	385	50960	CT	
	317sh	21190	CT	
	240	72860	CT	

4.4.4.1. Crystal structure of complex 9

The crystals of complex **9** suitable for X-ray analysis were grown from dimethylformamide (DMF) solutions by slow evaporation. The relevant crystallographic parameters are given in the Table 4.1. X-ray analysis shows that the asymmetric unit of complex **9** contains one trinuclear cobalt complex, two solvent DMF molecules and two water molecules. The molecular structure with atom labeling scheme of the complex are shown in Figure 4.2. Selected bond lengths and angles are listed in Table 4.4.

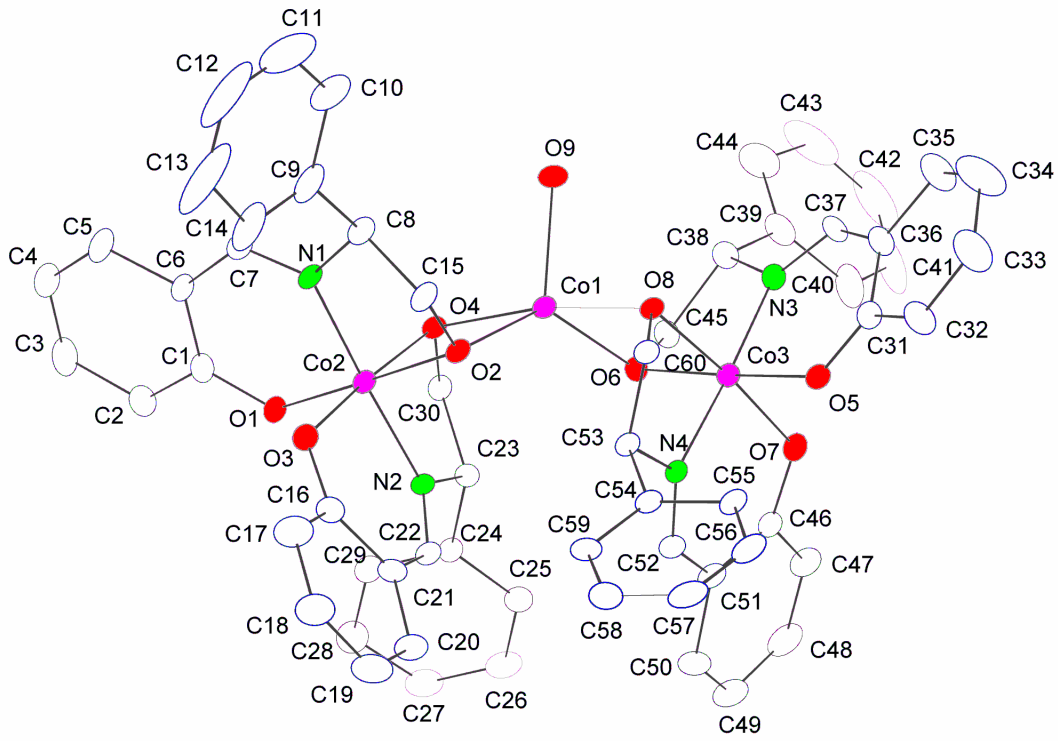

Figure 4.2. Structure of complex **9** with atom labeling scheme. Hydrogen atoms and solvent molecules are omitted for clarity. Thermal ellipsoids are represented by their 10 % probability level.

The complex crystallizes in the triclinic space group *P*1. The trinuclear cobalt complex lacks a crystallographic center of inversion. In this trinuclear geometry, the two terminal cobalt complexes are in distorted octahedral shape with N_2O_4 coordination sphere. The doubly deprotonated amino alcohol Schiff base ligands act as tridentate donors and bind the cobalt ions in a meridional manner. The square base of the octahedron is made up of two phenoxo oxygens and two alkoxide oxygens about which the two imine nitrogen are situated at *trans* positions.

Table 4.4 Selected bond distances (Å) and angles (°) for complex **9**

Co(1)-O(2)	1.983(5)	Co(2)-N(1)	1.904(5)
Co(1)-O(4)	2.093(5)	Co(2)-O(2)	1.904(5)
Co(1)-O(6)	1.995(5)	Co(2)-N(2)	1.913(5)
Co(1)-O(8)	2.133(4)	Co(3)-N(3)	1.901(6)
Co(1)-O(9)	2.004(5)	Co(3)-O(7)	1.896(4)
Co(1)-Co(2)	3.0016(11)	Co(3)-O(6)	1.898(4)
Co(1)-Co(3)	3.0194(11)	Co(3)-O(5)	1.903(5)
Co(2)-O(1)	1.877(5)	Co(3)-N(4)	1.907(5)
Co(2)-O(3)	1.883(5)	Co(3)-O(8)	1.909(4)
Co(2)-O(4)	1.924(5)		
O(2)-Co(1)-O(6)	130.74(17)	O(3)-Co(2)-O(4)	174.4(2)
O(2)-Co(1)-O(9)	116.5(2)	N(1)-Co(2)-O(4)	95.2(2)
O(6)-Co(1)-O(9)	112.5(2)	O(2)-Co(2)-O(4)	83.87(19)
O(2)-Co(1)-O(4)	77.69(18)	N(2)-Co(2)-O(4)	83.6(2)
O(6)-Co(1)-O(4)	100.55(18)	O(1)-Co(2)-Co(1)	137.24(16)
O(9)-Co(1)-O(4)	98.76(19)	O(3)-Co(2)-Co(1)	130.77(16)
O(2)-Co(1)-O(8)	96.91(18)	N(1)-Co(2)-Co(1)	94.83(17)
O(6)-Co(1)-O(8)	76.80(16)	O(2)-Co(2)-Co(1)	40.43(14)
O(9)-Co(1)-O(8)	90.77(18)	N(2)-Co(2)-Co(1)	83.09(16)
O(4)-Co(1)-O(8)	170.38(17)	O(4)-Co(2)-Co(1)	43.83(13)
O(2)-Co(1)-Co(2)	38.50(13)	N(3)-Co(3)-O(7)	87.4(2)
O(6)-Co(1)-Co(2)	119.02(13)	N(3)-Co(3)-O(6)	85.0(2)
O(9)-Co(1)-Co(2)	116.64(16)	O(7)-Co(3)-O(6)	91.1(2)
O(4)-Co(1)-Co(2)	39.55(13)	N(3)-Co(3)-O(5)	94.8(2)
O(8)-Co(1)-Co(2)	133.80(13)	O(7)-Co(3)-O(5)	91.7(2)
O(2)-Co(1)-Co(3)	117.75(13)	O(6)-Co(3)-O(5)	177.3(2)
O(6)-Co(1)-Co(3)	38.00(12)	N(3)-Co(3)-N(4)	176.8(2)
O(9)-Co(1)-Co(3)	106.95(16)	O(7)-Co(3)-N(4)	93.9(2)
O(4)-Co(1)-Co(3)	137.18(13)	O(6)-Co(3)-N(4)	92.0(2)
O(8)-Co(1)-Co(3)	38.92(12)	O(5)-Co(3)-N(4)	88.1(2)
Co(2)-Co(1)-Co(3)	136.33(3)	N(3)-Co(3)-O(8)	94.6(2)
O(1)-Co(2)-O(3)	91.4(2)	O(7)-Co(3)-O(8)	175.2(2)
O(1)-Co(2)-N(1)	94.3(2)	O(6)-Co(3)-O(8)	84.75(18)
O(3)-Co(2)-N(1)	86.5(2)	O(5)-Co(3)-O(8)	92.5(2)
O(1)-Co(2)-O(2)	177.6(2)	N(4)-Co(3)-O(8)	83.9(2)
O(3)-Co(2)-O(2)	91.0(2)	N(3)-Co(3)-Co(1)	92.11(17)
N(1)-Co(2)-O(2)	85.7(2)	O(7)-Co(3)-Co(1)	131.05(15)
O(1)-Co(2)-N(2)	87.5(2)	O(6)-Co(3)-Co(1)	40.31(14)
O(3)-Co(2)-N(2)	94.5(2)	O(5)-Co(3)-Co(1)	137.02 (17)
N(1)-Co(2)-N(2)	177.9(2)	N(4)-Co(3)-Co(1)	84.82(15)
O(2)-Co(2)-N(2)	92.5(2)	O(8)-Co(3)-Co(1)	44.57(13)
O(1)-Co(2)-O(4)	93.8(2)		

The observed distortions from an octahedral geometry could be caused by the small bite angle of the chelating Schiff base group [N2-Co2-O4 83.6(2)^{o} for Co2 and N4-Co3-O8 83.9(2)^{o} for Co3]. The average Co–N_{imi} [1.909(5) Å for Co2 and 1.904(6) Å for Co3], Co–O_{phe} [1.880(5) Å for Co2 and 1.900(5) Å for Co3] and Co–O_{alk} [1.914(5) Å for Co2 and 1.904(4) Å for Co3] distances observed are consistent with the corresponding values observed in related octahedral Co(III) systems.[15, 12(b)]

Two of these terminal octahedral complexes act as chelating ligands to the central cobalt through alkoxide oxygen bridging. The central cobalt atom is five coordinated with an O_5 coordination sphere. The coordination sites are satisfied by four bridging alkoxide oxygen atoms and a water molecule. The geometry around Co2 can be considered as distorted trigonal bipyramidal. The axial Co–O bond lengths Co1–O4 and Co1–O8 (av. 2.113(5) Å) are significantly longer than the other three which are considered as equatorials (av. 1.994(5) Å). The distortion along the axial direction can be seen from the O4-Co1-O8 angle of 170.38(17)^{o}. The τ value for complex **9** as explained by Addison *et al.*,[16] is calculated to be 0.66, confirming a distorted trigonal bipyramidal geometry [τ = 1 for trigonal bipyramidal geometry, τ = 0 for square pyramidal geometry]. The distortion from ideal tbp geometry can be rationalized due to the formation of two 4-membered rings around Co1 as a result of coordination of alkoxide oxygens. This fact can be viewed from the distortion of bond angles [O4-Co1-O2 (77.69(18)^{o}) O6-Co1-O8 (76.80(16)^{o}] from the ideal 90^{o} due to the 4-membered ring formation. Steric factors also may be contributing to the observed distortion. The two 4-membered rings attached to the central cobalt are inclined to each other at an angle of 54.33^{o}.

The Co–O bond lengths (av. 2.042(5) Å) around the central cobalt are significantly longer than those around the terminal cobalt atoms, indicating that the central cobalt is divalent while the terminal ones are trivalent (see Table 4.4). The variation in Co(III)–O and Co(II)–O bond lengths can be expected because of the larger Shannon radius of Co(II) (0.885 Å) as compared to that of Co(III) (0.75 Å).[17]

The net charge of 8– requires that there be two Co^{3+} ions and one Co^{2+} in complex **9**. The trimer is therefore, a Co(III)-Co(II)-Co(III) mixed-valence complex.

The average Co···Co separation is 3.011(11) Å which is considerably smaller than the Co···Co separations [3.821[1(a)], 3.872[1(c)] and 3.066[1(g)] Å] found in similar mixed valence trinuclear cobalt complexes. The Co2-Co1-Co3 angle is found to be 136.33(3)°.

There is an interesting hydrogen bonding interaction in the molecule between the coordinated water molecule and the solvent DMF molecules. The two DMF molecules are connected to the water molecule through O–H···O hydrogen bonding interactions. The O···O distances are O9···O10#1 = 2.591(9) Å and O9···O11#2 = 2.610(10) Å where #1 = x, 1+y, –1+z and #2 = x, 1+y, z.

4.4.4.2. Crystal structure of complex 16

X-ray analysis indicates that the asymmetric unit of complex **16** contains one trinuclear cobalt complex, two solvent DMF molecules and a water molecule. The complex crystallizes in the monoclinic space group $P2_1$. The molecular structure and the atom labeling scheme of the complex are shown in Figure 4.3. Crystallographic details are presented in Table 4.2.

Quite similar to the complex **9,** the molecular structure of complex **16** consists of a trinuclear cobalt geometry which lacks a crystallographic centre of inversion. The two terminal cobalt complexes are in distorted octahedral N_2O_4 coordination sphere with doubly deprotonated amino alcohol Schiff base ligands satisfying the coordination sites around cobalt in a meridional manner. The deviations of bond angles from ideal octahedral values are within ± 7°, see Table 4.5.

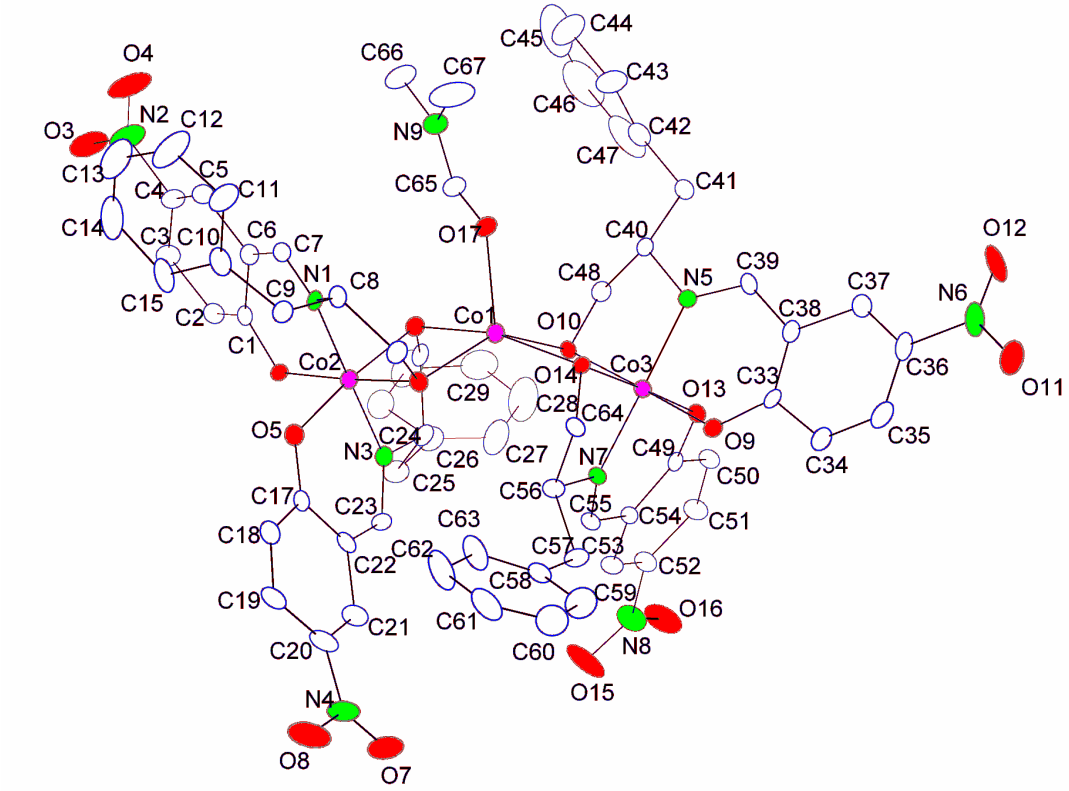

Figure 4.3. Structure of complex **16** with atom labeling scheme. Hydrogen atoms and solvent molecules are omitted for clarity. Thermal ellipsoids are represented by their 10 % probability level

The average Co–N_{imi} [1.887(10) Å for Co2 and 1.912(9) Å for Co3], Co–O_{phe} [1.884(8) Å for Co2 and 1.895(8)Å for Co3] and Co–O_{alk} [1.898(8) Å for Co2 and 1.901(7) Å for Co3] distances observed for the terminal cobalt centers are consistent with corresponding values observed in related octahedral Co(III) systems.[15]

The two terminal octahedral Co complexes act as chelating units for the central cobalt through alkoxide oxygen bridging. The central cobalt is five coordinated, the fifth coordination site being occupied by a solvent DMF molecule. Two 4-membered rings are formed around the central cobalt as a result of the chelation through alkoxide oxygens by the two terminal cobalt octahedral complexes. Due to this reason the central cobalt assumes a highly distorted geometry which is almost intermediate between trigonal bipyramidal and square pyramidal as evidenced from the τ value of 0.40.[16] It can be concluded that the distortion is more towards square pyramidal. The average Co–O distance for Co1 is 2.039(9) Å. The two 4-membered rings attached to the central cobalt are inclined to each other at an angle of 44.31°.

Here also the bond lengths about the central cobalt are significantly longer than those about the terminal cobalt centers, indicating that the central atom is divalent while the terminal ones are trivalent. Based on the bond length analysis, charge balance and magnetic moment measurement studies the trimer in complex **16** can be formulated as a Co(III)-Co(II)-Co(III) mixed-valence complex.

Similar to the complex **9**, the Co···Co separations 2.992(3) Å [Co2···Co1] and 2.969(3) Å [Co3···Co1] are found to be smaller than the Co···Co separations of 3.872(2), 3.066 and 3.821 Å reported for similar mixed valent systems. [1(a), 1(c), (g)] The Co2-Co1-Co3 angle is 140.01(8)°.

Table 4.5. Selected bond distances (Å) and angles (°) for complex **16**

Co(2)-N(1)	1.871(10)	Co(3)-O(14)	1.907(7)
Co(2)-O(1)	1.881(8)	Co(3)-O(13)	1.901(7)
Co(2)-O(5)	1.887(8)	Co(3)-N(5)	1.923(9)
Co(2)-N(3)	1.902(10)	Co(3)-Co(1)	2.969(3)
Co(2)-O(2)	1.893(7)	Co(1)-O(10)	1.992(7)
Co(2)-O(6)	1.903(8)	Co(1)-O(2)	2.006(8)
Co(2)-Co(1)	2.992(3)	Co(1)-O(14)	2.043(7)
Co(3)-O(9)	1.888(8)	Co(1)-O(17)	2.069(9)
Co(3)-O(10)	1.895(7)	Co(1)-O(6)	2.083(8)
Co(3)-N(7)	1.901(9)		
N(1)-Co(2)-O(1)	94.8(4)	O(10)-Co(3)-N(5)	86.7(4)
N(1)-Co(2)-O(5)	88.0(4)	N(7)-Co(3)-N(5)	177.8(4)
O(1)-Co(2)-O(5)	91.7(3)	O(14)-Co(3)-N(5)	96.0(3)
N(1)-Co(2)-N(3)	176.1(4)	O(13)-Co(3)-N(5)	86.0(3)
O(1)-Co(2)-N(3)	87.4(3)	O(9)-Co(3)-Co(1)	135.6(3)
O(5)-Co(2)-N(3)	95.1(4)	O(10)-Co(3)-Co(1)	41.4(2)
N(1)-Co(2)-O(2)	84.4(4)	N(7)-Co(3)-Co(1)	81.9(3)
O(1)-Co(2)-O(2)	176.2(3)	O(14)-Co(3)-Co(1)	43.0(2)
O(5)-Co(2)-O(2)	92.0(3)	O(13)-Co(3)-Co(1)	132.6(2)
N(3)-Co(2)-O(2)	93.2(4)	N(5)-Co(3)-Co(1)	96.1(3)
N(1)-Co(2)-O(6)	93.1(4)	O(10)-Co(1)-O(2)	142.1(3)
O(1)-Co(2)-O(6)	91.5(3)	O(10)-Co(1)-O(14)	78.2(3)
O(5)-Co(2)-O(6)	176.5(3)	O(2)-Co(1)-O(14)	99.7(3)
N(3)-Co(2)-O(6)	83.7(4)	O(10)-Co(1)-O(17)	112.0(3)
O(2)-Co(2)-O(6)	84.8(3)	O(2)-Co(1)-O(17)	105.3(4)
N(1)-Co(2)-Co(1)	91.4(3)	O(14)-Co(1)-O(17)	104.3(3)
O(1)-Co(2)-Co(1)	135.1(3)	O(10)-Co(1)-O(6)	95.6(3)
O(5)-Co(2)-Co(1)	133.0(2)	O(2)-Co(1)-O(6)	77.5(3)
N(3)-Co(2)-Co(1)	84.8(3)	O(14)-Co(1)-O(6)	166.2(3)
O(2)-Co(2)-Co(1)	41.3(2)	O(17)-Co(1)-O(6)	89.4(3)
O(6)-Co(2)-Co(1)	43.7(2)	O(10)-Co(1)-Co(3)	39.0(2)
O(9)-Co(3)-O(10)	177.0(3)	O(2)-Co(1)-Co(3)	125.1(2)
O(9)-Co(3)-N(7)	87.9(4)	O(14)-Co(1)-Co(3)	39.57(19)
O(10)-Co(3)-N(7)	91.2(4)	O(17)-Co(1)-Co(3)	117.5(3)
O(9)-Co(3)-O(14)	93.0(3)	O(6)-Co(1)-Co(3)	132.0(2)
O(10)-Co(3)-O(14)	84.1(3)	O(10)-Co(1)-Co(2)	122.7(2)
N(7)-Co(3)-O(14)	83.2(4)	O(2)-Co(1)-Co(2)	38.5(2)
O(9)-Co(3)-O(13)	91.1(3)	O(14)-Co(1)-Co(2)	135.6(2)
O(10)-Co(3)-O(13)	91.8(3)	O(17)-Co(1)-Co(2)	102.2(3)
N(7)-Co(3)-O(13)	94.6(4)	O(6)-Co(1)-Co(2)	39.1(2)
O(14)-Co(3)-O(13)	175.3(3)	Co(3)-Co(1)-Co(2)	140.01(8)
O(9)-Co(3)-N(5)	94.3(4)		

4.4.4.3. Crystal structure of complex 12

Single crystals of complex **12** suitable for X-ray crystallography were grown from DMF solution of the complex by slow evaporation method. The complex crystallizes in the chiral space group orthorhombic $P2_12_12_1$. The asymmetric unit consists of four mononuclear cobalt complexes and one solvent DMF molecule. The cobalt complexes are almost octahedral in shape. The tridentate ONO donor Schiff base ligand binds the metal in a meridional manner. The molecular geometry and the atom labeling scheme for a representative mononuclear unit is given in Figure 4.4. Selected bond lengths and bond angles are given in Table 4.6.

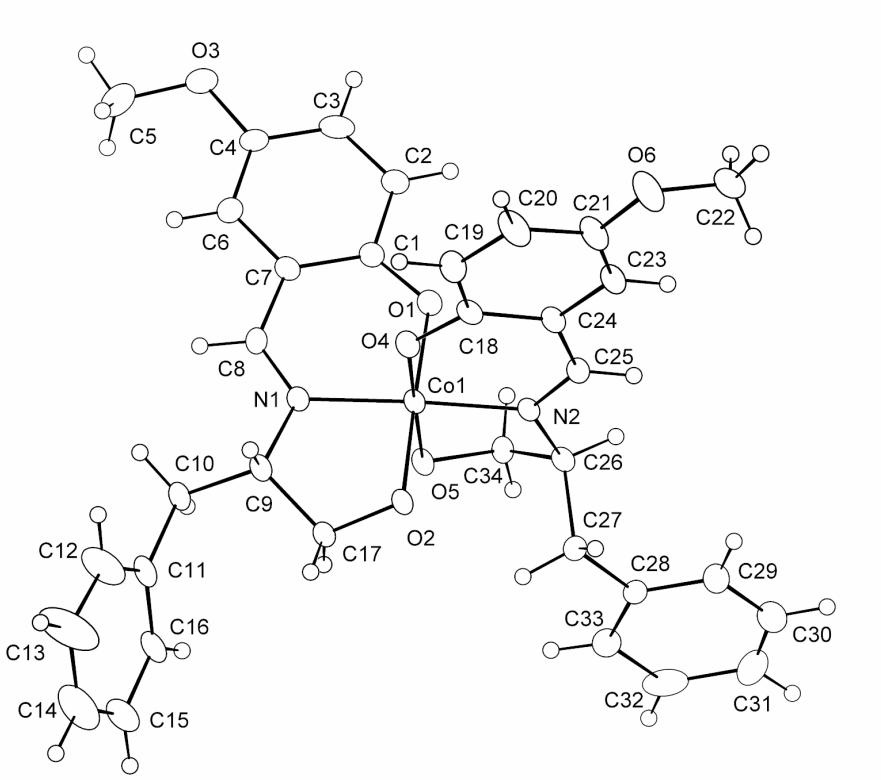

Figure 4.4. Structure of one mononuclear unit of complex **12** with atom labeling scheme. Thermal ellipsoids are represented by their 10 % probability level.

Although the respective hydrogens are not located in the difference Fourier map, it is obvious that in each mononuclear unit, one of the ligand is doubly deprotonated while the second one is singly deprotonated. In each mononuclear unit one of the Co–O_{alk} bond length is considerably longer than the other [for example Co1–O2 = 1.906(5) Å while Co1–O5 = 1.944(4) Å] probably due to the above mentioned reason. (see Table 4.6). This conclusion is also consistent with the overall charge balance of the system. Room temperature magnetic moment measurements showed that the complex is diamagnetic which indicates a low spin Co(III) complex. The average Co–O_{phe} (1.882(5) Å), Co–O_{alk} (1.932(5) Å) and Co–N_{imi} (1.902(6) Å) bond lengths are within the range reported for low spin Co(III) complexes.[15]

Table 4.6. Selected bond distances (Å) and angles (°) for complex **12**

Co(1)-N(2)	1.876(5)	Co(3)-O(13)	1.879(5)
Co(1)-O(4)	1.879(4)	Co(3)-O(16)	1.899(5)
Co(1)-O(1)	1.880(5)	Co(3)-N(5)	1.902(6)
Co(1)-O(2)	1.906(5)	Co(3)-O(17)	1.921(5)
Co(1)-N(1)	1.908(6)	Co(3)-N(6)	1.925(6)
Co(1)-O(5)	1.944(4)	Co(3)-O(14)	1.939(4)
Co(2)-O(7)	1.877(5)	Co(4)-O(22)	1.872(5)
Co(2)-O(10)	1.886(4)	Co(4)-O(19)	1.882(5)
Co(2)-N(4)	1.888(5)	Co(4)-N(7)	1.884(6)
Co(2)-N(3)	1.915(6)	Co(4)-N(8)	1.912(6)
Co(2)-O(8)	1.918(5)	Co(4)-O(20)	1.931(5)
Co(2)-O(11)	1.951(4)	Co(4)-O(23)	1.949(5)
N(2)-Co(1)-O(4)	95.4(2)	O(13)-Co(3)-N(5)	94.8(2)
O(1)-Co(1)-O(2)	178.4(2)	N(5)-Co(3)-O(14)	83.8(2)
N(2)-Co(1)-N(1)	176.8(2)	O(16)-Co(3)-O(17)	178.8(2)
O(1)-Co(1)-N(1)	95.7(2)	O(16)-Co(3)-N(6)	94.1(2)
O(2)-Co(1)-N(1)	85.9(2)	N(5)-Co(3)-N(6)	175.8(2)
N(2)-Co(1)-O(5)	83.9(2)	O(17)-Co(3)-N(6)	84.9(2)
O(4)-Co(1)-O(5)	178.9(2)	O(13)-Co(3)-O(14)	178.5(2)
O(10)-Co(2)-N(4)	95.3(2)	O(19)-Co(4)-N(7)	93.4(2)
O(7)-Co(2)-N(3)	96.4(2)	O(22)-Co(4)-N(8)	94.5(2)
N(3)-Co(2)-O(8)	85.4(2)	N(7)-Co(4)-O(8)	176.2(3)
O(10)-Co(2)-O(11)	178.5(2)	O(22)-Co(4)-O(23)	177.2(2)
N(4)-Co(2)-O(11)	84.41(19)	N(8)-Co(4)-O(23)	84.4(2)
N(4)-Co(2)-N(3)	177.8(2)	O(19)-Co(4)-O(20)	178.6(2)
O(7)-Co(2)-O(8)	178.2(2)	N(7)-Co(4)-O(20)	85.7(2)

The mononuclear complexes present in the asymmetric unit self assembles through intermolecular O–H···O interactions resulting in homochiral supramolecular helices in the crystal lattice. The four mononuclear complexes present in the asymmetric unit can be named as Co1, Co2, Co3 and Co4. The complexes Co1 and Co2 are inter connected by a strong hydrogen bond between alcoholic oxygens O2 and O8 [O2···O8 = 2.442(6) Å] and exists as a dimer. Similarly the mononuclear units Co3 and Co4 also exist as dimer by the hydrogen bonding interactions between alcoholic oxygens O14 and O23 [O14···O23 = 2.386(7) Å]. These independent dimers are further interconnected to each other through two O–H···O interactions [O5···O17 = 2.464(6) Å and O11···O20 = 2.425(6) Å] resulting in supramolecular hydrogen bonded homochiral helices in the crystal lattice.

Each mononuclear complex contains two alcoholic oxygen atoms, of which one is protonated and the other is deprotonated. The protonated alcoholic oxygen acts as the hydrogen bond donor while deprotonated alcoholic oxygen acts as the acceptor. The resulting O–H···O interactions are rather strong as evident from the O···O bond distances.

One full turn of the helix contains eight mononuclear complexes, each hydrogen bonded dimer in the asymmetric unit repeating twice. The pitch distance is 25.508 Å. The path of the helix can be traced by following the hydrogen bonds counter clockwise around the two fold screw axis of the helix. The complex is chiral and the crystal contains only one enantiomer of the complex. This local chirality translates into the formation of only left-handed helices in the supramolecular level. Figure 4.5 depicts the hydrogen bonding pattern in the asymmetric unit and the mode of propagation of helices in the crystal lattice.

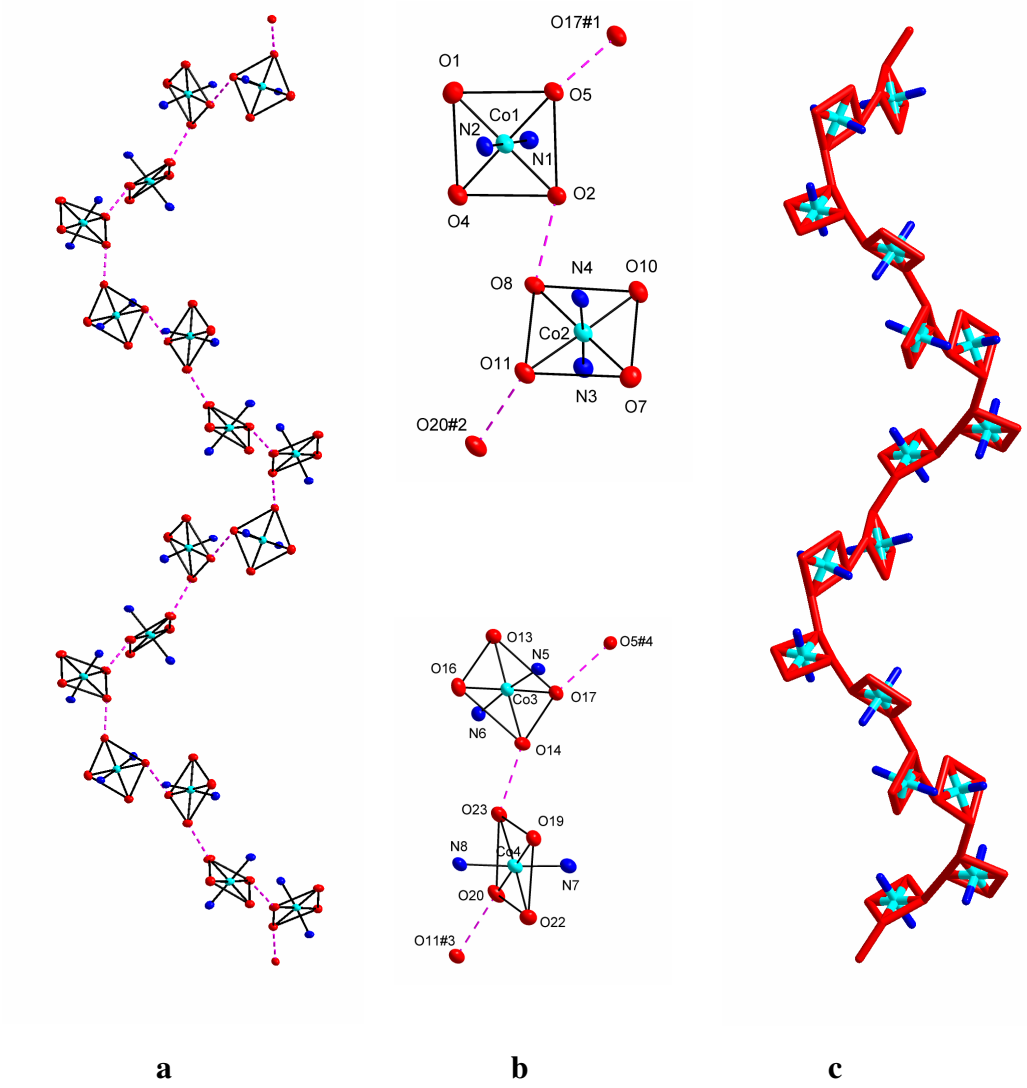

Figure 4.5. View illustrating intermolecular O–H···O hydrogen-bonding interactions between adjacent molecules that lead to the formation of hydrogen-bonded helices in complex **12**. All the carbon and hydrogen atoms are omitted for clarity. **a**: Ball and stick representation; **b**: hydrogen bonding pattern in the asymmetric unit resulting in dimers; **c**: wire-frame representation. Color code: Cyan – Cobalt, Red – Oxygen, Blue – Nitrogen. Symmetry: #1 = –1+x, y, z, #2 = 1.5–x, 1–y, 0.5+z, #3 = 1.5–x, 1–y, –0.5+z, #4 = 1+x, y, z.

4.4.4.4. Structure of complex 15

The single crystals of complex **15** suitable for X-ray analysis were grown by slow evaporation of a dimethylformamide solution. The complex crystallizes in the chiral space group tetragonal $P4_12_12$. The molecular structure and atom labeling scheme of the complex is presented in Figure 4.6.

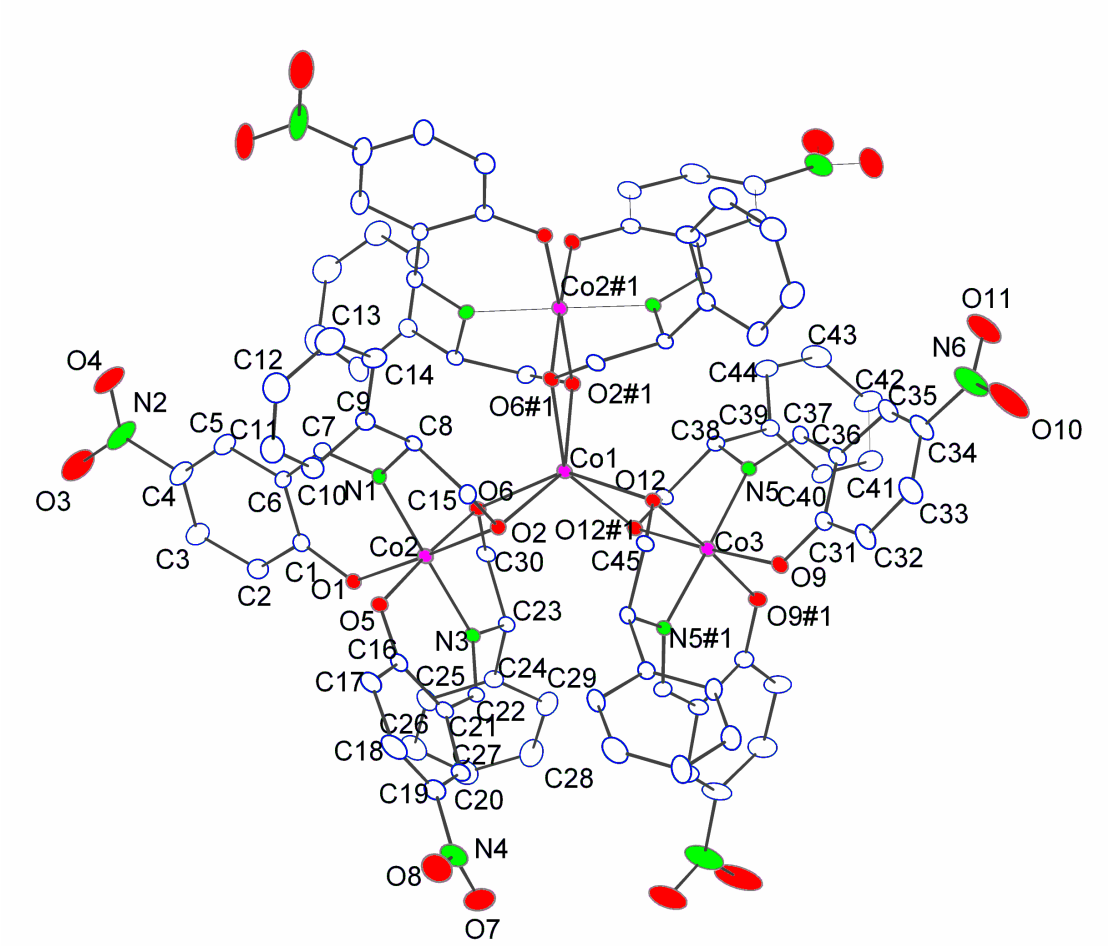

Figure 4.6. Structure of complex **15** with atom labeling scheme. Symmetry generated segments are mostly unlabelled. Hydrogen atoms and solvent molecule are omitted for clarity. Thermal ellipsoids are represented by their 5 % probability level.

The asymmetric unit contains half of the tetranuclear complex and a solvent water molecule. The crystal structure reveals an interesting tetranuclear geometry for the complex **15** in which three mononuclear cobalt complexes act as chelating units for a central cobalt ion. The terminal cobalt complexes are almost octahedral in shape with two ONO donor Schiff base ligands satisfying the coordination sites of each cobalt in a meridional manner.

The central cobalt ion is six co-ordinate. The co-ordination polyhedron exhibits, surprisingly, a distorted trigonal prismatic geometry which is rather scarce for polynuclear cobalt complexes. Four chelating alkoxide oxygens [O2, O6, O12 and O12#1] from complexes Co2 and Co3 form the square base for the trigonal prism. The oxygens O2#1 and O6#1 from the third cobalt complex Co2#1 occupy the remaining two vertices to complete the trigonal prismatic coordination sphere around the central Co1 as shown in Figure 4.6. The two trigonal faces of the trigonal prism (made up of oxygens O2, O6#1, O12 and O2#1, O12#1, O6) are not equilateral and the square base shows distortion from ideal geometry. The torsion angle involving opposing corners and the centroids of the trigonal faces are 17.39°, 17.39° and 16.50°. The distortion from the ideal trigonal prismatic geometry might be due to the severe steric overcrowding caused by the three bulky cobalt complexes which are acting as ligands for the central cobalt.

Selected bond lengths and bond angles for the complex **15** are given in the Table 4.7. The average Co–N_{imi} [1.897(5) Å for Co2, Co2#1 and 1.875(4) Å for Co3], Co–O_{phe} [1.899(4) Å for Co2, Co2#1 and 1.899 (4) Å for Co3] and Co–O_{alk} [1.885(4) Å for Co2, Co2#1 and 1.883(4) Å for Co3] distances observed for terminal cobalt complexes are comparable to the corresponding values observed in related octahedral Co(III) systems.[15] By the same argument it can be assumed that the middle cobalt is in 2+ oxidation state since the average Co–O bond distance of 2.148(3) Å is longer than that of the terminal cobalt atoms. This can be rationalized by assuming that the Shannon radius of Co^{2+} is more than that of the Co^{3+} ion.[16] The steric crowding might

have caused an additional increase in length of these bonds compared to the complexes **9** and **16**.

Table 4.7. Selected bond distances (Å) and angles (°) for complex **15**

Co(1)-O(2)	2.146(4)	Co(2)-O(6)	1.890(4)
Co(1)-O(2)#1	2.146(4)	Co(2)-N(1)	1.890(5)
Co(1)-O(12)#1	2.145(4)	Co(2)-N(3)	1.894(5)
Co(1)-O(12)	2.145(4)	Co(2)-O(5)	1.908(4)
Co(1)-O(6)	2.150(4)	Co(3)-N(5)#1	1.874(4)
Co(1)-O(6)#1	2.150(4)	Co(3)-N(5)	1.874(4)
Co(1)-Co(3)	3.1472(16)	Co(3)-O(12)	1.884(4)
Co(1)-Co(2)	3.1549(9)	Co(3)-O(12)#1	1.884(4)
Co(2)-O(1)	1.887(4)	Co(3)-O(9)	1.903(4)
Co(2)-O(2)	1.893(4)	Co(3)-O(9)#1	1.903(4)
O(2)-Co(1)-O(2)#1	145.0(2)	O(2)-Co(2)-N(3)	95.24(19)
O(2)-Co(1)-O(12)#1	118.90(14)	O(1)-Co(2)-N(3)	85.8(2)
O(2)#1-Co(1)-O(12)#1	90.28(14)	N(1)-Co(2)-N(3)	178.9(2)
O(2)-Co(1)-O(12)	90.28(14)	O(6)-Co(2)-O(5)	175.41(18)
O(2)#1-Co(1)-O(12)	118.90(14)	O(2)-Co(2)-O(5)	92.41(18)
O(12)#1-Co(1)-O(12)	71.5(2)	O(1)-Co(2)-O(5)	89.62(19)
O(2)-Co(1)-O(6)	71.63(14)	N(1)-Co(2)-O(5)	86.0(2)
O(2)#1-Co(1)-O(6)	90.36(14)	N(3)-Co(2)-O(5)	94.9(2)
O(12)#1-Co(1)-O(6)	90.86(14)	O(6)-Co(2)-Co(1)	41.71(12)
O(12)-Co(1)-O(6)	144.95(13)	O(2)-Co(2)-Co(1)	41.61(11)
O(2)-Co(1)-O(6)#1	90.36(14)	O(1)-Co(2)-Co(1)	136.37(13)
O(2)#1-Co(1)-O(6)#1	71.63(14)	N(1)-Co(2)-Co(1)	89.57(14)
O(12)#1-Co(1)-O(6)#1	144.95(13)	N(3)-Co(2)-Co(1)	89.36(14)
O(12)-Co(1)-O(6)#1	90.86(15)	O(5)-Co(2)-Co(1)	134.00(14)
O(6)-Co(1)-O(6)#1	118.2(2)	N(5)#1-Co(3)-N(5)	178.1(3)
O(2)-Co(1)-Co(3)	107.5(10)	N(5)#1-Co(3)-O(12)	84.67(19)
O(2)#1-Co(1)-Co(3)	107.5(10)	N(5)-Co(3)-O(12)	93.88(17)
O(12)#1-Co(1)-Co(3)	35.76(10)	N(5)#1-Co(3)-O(12)#1	93.88(17)
O(12)-Co(1)-Co(3)	35.76(10)	N(5)-Co(3)-O(12)#1	84.67(19)
O(6)-Co(1)-Co(3)	120.91(10)	O(12)-Co(3)-O(12)#1	83.4(2)
O(6)#1-Co(1)-Co(3)	120.91(10)	N(5)#1-Co(3)-O(9)	87.37(19)
O(2)-Co(1)-Co(2)	35.84(10)	N(5)-Co(3)-O(9)	94.0(2)
O(2)#1-Co(1)-Co(2)	120.58(11)	O(12)-Co(3)-O(9)	93.23(18)
O(12)#1-Co(1)-Co(2)	107.86(9)	O(12)#1-Co(3)-O(9)	176.27(19)
O(12)-Co(1)-Co(2)	120.53(9)	N(5)#1-Co(3)-O(9)#1	94.0(2)
O(6)-Co(1)-Co(2)	35.78(10)	N(5)-Co(3)-O(9)#1	87.37(19)
O(6)#1-Co(1)-Co(2)	107.19(10)	O(12)-Co(3)-O(9)#1	176.27(19)
Co(3)-Co(1)-Co(2)	120.13(2)	O(12)#1-Co(3)-O(9)#1	93.23 (18)
O(6)-Co(2)-O(2)	83.33(16)	O(9)-Co(3)-O(9)#1	90.2(3)
O(6)-Co(2)-O(1)	94.68(18)	N(5)#1-Co(3)-Co(1)	89.03 (15)
O(2)-Co(2)-O(1)	177.60(18)	N(5)-Co(3)-Co(1)	89.03(15)
O(6)-Co(2)-N(1)	95.21(19)	O(12)-Co(3)-Co(1)	41.70(11)
O(2)-Co(2)-N(1)	84.13(19)	O(12)#1-Co(3)-Co(1)	41.70(11)
O(1)-Co(2)-N(1)	94.7(2)	O(9)-Co(3)-Co(1)	134.91(14)
O(6)-Co(2)-N(3)	83.8(2)	O(9)#1-Co(3)-Co(1)	134.91(14)

Oxidation state assignment is supported by the magnetic moment measurements and electronic spectroscopy. The electronic spectrum of the complex is similar to the mononuclear Co(III) complexes **11** and **12**, which indicates the presence of Co(III) units in the complex. Also the complex shows a net magnetic moment of 5.1 BM at room temperature corresponding to high spin Co(II) center.

If all the tridentate ligands are doubly deprotonated, there will be an excess of one negative charge in the complex. It is assumed that this extra negative charge might have been compensated by one proton (probably due to single deprotonation of one of the ligands) at any unknown position in the complex. Similar situation is reported in the literature for a mononuclear Co(III) complex with similar ligand system.[18]

Calculations[19] using the CALC VOID option in PLATON showed a potential solvent access area of 8601.5 $Å^3$ (54.3 %) per unit cell of the complex. This fact is also supported by the relatively low ρ_{calcd} value of 0.822 gcm^{-3} observed by the X-ray analysis. This void is created as a result of intermolecular C–H···O hydrogen bonding interactions of the complex with its surrounding molecules resulting in a three dimensional hydrogen bonded network in the crystal lattice. In these interactions, the oxygens O3, O7 and O10 of the $–NO_2$ group act as the hydrogen bond acceptor while the aromatic carbons C28, C3 and C11 act as the donors. The relevant hydrogen bonding parameters are given in Table 4.8. The extension of hydrogen bonding interactions in a three dimensional manner thus results in a porous metal organic frame work with an overall solvent access area of above 50 % in the unit cell. This area is partly occupied by solvent water molecules. The solvent water oxygen O13 is involved in C–H···O hydrogen bonding interactions with the complex molecule carbons C20 and C22. The relevant hydrogen bonding parameters for these interactions are given in Table 4.8.

The present complex can be considered as a chiral porous Metal Organic Framework (MOF). Recently there has been considerable interest in such systems

because of their potential applications in the separation of enantiomers and in asymmetric catalysis.[20]

Table 4.8. Hydrogen bonding parameters (Å, °) for complex **15**

Donor–H···Acceptor	D–H	H···A	D···A	∠(DHA)	Symmetry
C28–H28···O3#1	0.93	2.72	3.575(19)	153.3	#1 2+y, -1+x, 2-z
C3–H3···O7#2	0.93	2.43	3.111(15)	130.4	#2 1.5-x, -0.5+y, 2.25-z
C11–H11···O#3	0.93	2.62	3.531(18)	166.8	#3 y, -1+x, 2-z
C20–H20···O13#4	0.93	2.34	3.23(2)	158.7	#4 x, -1+y, 1+z
C22–H22···O13#4	0.93	2.61	3.45(2)	149.5	

4.5. Conclusion

In complexes **9-16**, the ligand contains both phenolic and alcoholic OH groups. Previous works on the transition-metal chemistry of amino alcohols suggest that the introduction of the alcoholic –OH group in the ligand results in unexpected structural modifications.[21]Although both phenol and the alkoxy groups can act as bridging functionalities, in these complexes the phenolic oxygen atoms do not act as bridging group but alkoxide oxygens acts as bridging groups. This is an interesting observation and we can assume that the bridging ability of alkoxide oxygen atoms predominates in these complexes probably due to various factors like steric and overall crystal packing effects.

Due to the basicity of the coordinated alkoxide group, an octahedral metal complex functions as a bidentate chelating unit for a central metal ion in the trinuclear complexes as discussed in this chapter. These edge sharing octahedral-tbp/sp-octahedral complexes are complementary to the previous reports of edge sharing octahedral-tetrahedral-octahedral and face sharing all octahedral trinuclear complexes.[22]

In multinuclear complexes studied here, the high spin cobalt(II) adopts geometries ranging from distorted trigonal bipyramidal, distorted square pyramidal to distorted trigonal prismatic. One of the reasons for such distortions is the formation of

two/three 4-membered rings in these complexes due to alkoxide chelation. The steric effects caused by the bulky octahedral cobalt(III) complexes, acting as ligands contribute to the distortions. From the present study it is clear that alkoxide oxygen atoms are quite capable of stabilizing high spin cobalt(II) ions in a variety of geometrical arrangements.

The basic coordination sites and geometry of the ligands H_2L^1 to H_2L^8 is the same. They only differ in the substitution on salicylaldehyde part and in the length of the amino alcohol side chain. These changes have considerable influence on the overall coordination geometries of the resulting complexes although the experimental conditions are kept the same. Ligands with unsubstituted and 5-nitro and 5-bromo substituted salicylaldehyde prefer multinuclear arrangement while the methoxy substituted derivatives prefer mononuclear arrangement. The nitro-substituted derivatives gave both tri- and tetra- nuclear complexes. Here the steric effect of the lengthy side arm may be playing a crucial role in dictating the geometry. Lengthy CH_2Ph group might create more steric crowd around central cobalt in complex **16** unlike the Ph substituted derivative in complex **15**, thus preventing another octahedral complex from approaching it from top side.

High spin Co(II) has a definite preference for octahedral geometry over trigonal prismatic. The previously reported trigonal prismatic complexes of Co(II) are mostly made up of rigid multidentate ligands.[23] Here it is shown that even bulky coordination complexes can stabilize the trigonal prismatic geometry around high spin Co(II) despite its preference for octahedral geometry. Of course the role of extensive hydrogen bonding interactions, present in the crystal lattice, in dictating such a geometry cannot be completely ignored.

The crystal structures of complexes **9** and **16** belong to a limited number of structurally characterized trinuclear cobalt complexes with mixed oxidation states. There are mainly two classes of trinuclear cobalt complexes of mixed spin states reported. One includes mixed valence trinuclear complexes of the form CoIII (S = 0) –CoII (S = 3/2)–CoIII (S = 0)[1(g),13] and another, mixed-spin trinuclear complexes of

the form Co(II) (S = 1/2)–Co(II) (S = 3/2)–Co(II) (S = 1/2).[24] The present trinuclear complexes belong to the former category.

In conclusion, it has been shown that the tridentate ligands H_2L^1-H_2L^8 are very versatile in their coordination behavior towards cobalt and can readily form stable mono, tri and tetra nuclear cobalt complexes with interesting structural features.

4.6. References

1. (a) T. S. Billson, J. D. Crane, O. D. Fox and S. L. Heath, *Inorg. Chem. Commun.*, 2000, **3**, 718; (b) V.Gama, R. T. Henriques, M. Almeida, L. Veiros, M. J. Calhorda, A. Meetsma and J. L. de Boer, *Inorg. Chem.,* 1993, **32**, 3705; (c) B. Ballet, A. Bino, S. Cohen, H. Rubin and T. Zor, *Inorg. Chim. Acta,* 1991, **188**, 91; (d) J. A. Bertrand, J. A. Kelley and E. G. Vassian, *J. Am. Chem. Soc.,* 1969, **91**, 2394; (e) V. M. Novotortsev, O. G. Ellert, T. S. Kapanadze and A. Y. Buslaev, *Koord. Khim.,* 1986, **14**, 856; (f) D. A. House, V. McKee and P. J. Steel, *Inorg. Chem.*, 1986, **25**, 4884; (g) C. Fukuhara, E. Asato, T. Shimoji, K. Katsura, M. Mori, K. Matsumoto and S. Ooi, *J. Chem. Soc., Dalton Trans.,* 1987, 1305; (h) K. Okamoto, S. Aizawa, T. Konno, H. Einaga and J. Hidaka, *Bull. Chem. Soc. Jpn.,* 1986, **59**, 3859; (i) M. J. Heeg, E. L. Blinn and E. Deutsch, *Inorg. Chem.,* 1983, **24**, 1118; (j) F. A. Cotton, R. Hügel and R. Eiss, *Inorg. Chem.,* 1968, **7**, 18.
2. P. V. Bernhardt and G. A. Lawrance in *Comprehensive Coordination Chemistry II*, eds: J. A. McCleverty and T. J. Meyer, Elsevier-Pergamon, Oxford 2004, **vol 6**, p 1-145.
3. H. Sato, H. Watnabe, Y. Ohtusuka, T. Ikeno, S. Fukuzawa and T. Yamada, *Org. Lett.,* 2002, **4**, 3313; R. I. Kureshy, N. H. Khan, S. H. R. Abdi, A. K. Bhatt and P. Iyer, *J. Mol. Catal. A: Chemical*, 1997, **121**, 25; A. Nishinaga, H. Yamato, T. Abe, K. Maruyama and T. Matsuura, *Tetrahedron Lett.,* 1988, **29**, 6309; T. Fukuda and T. Katsuki, *Synlett.,* 1995, 825; E. N. Jacobsen, F.

Kakiuchi, R. G. Konsler, J. F. Larrow and M. Tokunaga, *Tetrahedron Lett.*, 1997, **38**, 773.

4. S. G. Baca, I. G. Filippova, C. Ambrus, M. Gdaniec, Y. A. Simonov, N. Gerbeleu, O. A.Gherco and S. Decurtins, *Eur. J. Inorg. Chem.*, 2005, 3118; G. S. Hanan, D. Volkmer, U. S. Schubert, J. –M. Lehn, G. Baum and D. Fenske, *Angew. Chem., Int. Ed. Engl.,* 1997, **36**, 1842.
5. Bruker, *SADABS, SMART, SAINTPLUS and SHELXTL*, Bruker AXS Inc., Madison, Wisconsin, USA, 2003.
6. G. M. Sheldrick, *Program for Crystal Structure Solution and Analysis*, University of Göttingen, Germany, 1997.
7. H. D. Flack, *Acta. Cryst.*, 1983, **A39**, 876.
8. A. C. T. North, D. C. Philips and F. S. Mathews, *Acta Crystallogr.*, 1968, **A24** 351.
9. L. J. Farrugia, *J. Appl. Crystallogr.*, 1999, **32,** 837.
10. T. Głowiak, L. Jerzykiewicz, J. M. Sobczak, J. J. Ziółkowski, *Inorg. Chim. Acta,* 2003, **356**, 387.
11. M. Tsuchimoto, R. Kasahara, K. Nakajima, M. Kojima and S. Ohba, *Polyhedron*, 1999, **18**, 3035.
12. M. S. Shongwe, S. K. M. Al-Hatmi, H. M. Marques, R. Smith, R. Nukada and M. Mikuriya, *J. Chem. Soc., Dalton Trans.*, 2002, 4064; Y. –S. Xie, X. –T. Liu, M. Zhang, K. –J. Wei and Q. –L. Liu, *Polyhedron,* 2005, **24**, 165.
13. H. Kobayashi, K. Ohki, I. Tsujikawa, K. Osaki and N. Uryû, *Bull. Chem. Soc. Jpn.,* 1976, **49**, 1210.
14. R. J. P. Williams, *J. Chem. Soc.,* 1955, 137; R. N. Mukherjee, O. A. Rajan and A. Chakravorty, *Inorg. Chem.*, 1982, **21**, 785; J. W. Pyrz, A. L. Roe, L. J. Stern and L. Que Jr., *J. Am. Chem. Soc.,* 1985, **107**, 614; A. V. Lakshmi, N. R. Sangeetha and S. Pal, *Ind. J. Chem.*, 1997, **36A**, 844; A. Choudhury, B. Geetha, N. R. Sangeetha, V. Kavita, V. Susila and S. Pal, *J. Coord. Chem.*,

1999, **48**, 87; N. R. Sangeetha, V. Kavita, S. Wocadlo, A. K. Powell and S. Pal, *J. Coord. Chem.*, 2000, **51**, 55.

15. (a) A. Böttcher, T. Takeuchi, K. I. Hardcastle, T. J. Meade, H. B. Gray, D. Cwikel, M. Kapon and Z. Dori, *Inorg. Chem.*, 1997, **36**, 2498; (b) M. Dey, C. P. Rao, P. K. Saarenketo, K. Rissanen, E. Kolehmainen and P. Guionneau, *Polyhedron*, 2003, **22**, 3515.
16. A. W. Addison, T. N. Rao, J. Reedijk, J. V. Rijn and G. C. Verschoor, *J. Chem. Soc., Dalton Trans.*, 1984, 1349.
17. R. D. Shannon, *Acta Crystallogr. Sect A,* 1976, **32**, 751.
18. R. L. De, K. Samanta, K. Maiti and E. Keller, *Inorg. Chim. Acta*, 2001, **316**, 113.
19. A. L. Spek, *PLATON, A Multipurpose Crystallographic Tool*, Utrecht University, The Netherlands, 2002.
20. B. Kesanli and W. Lin, *Coord. Chem. Rev.*, 2003, **246**, 305; X. X. Zhang, J. S. Bradshaw and R. M. Izatt, *Chem. Rev.*, 1997, **97**, 3313; E. Brunet, *Chirality*, 2002, **14**, 135; L. Pérez-García and D. B. Amabilino, *Chem. Soc. Rev.*, 2002, **31**, 342; L.-X. Dai, *Angew. Chem. Int. Ed.*, 2004, **43**, 5726; M. A. Mateos-Timoneda, M. Crego-Calama and D. N. Reinhoudt, *Chem. Soc. Rev.*, 2004, **33**, 363; R.-G. Xiong, X.-Z. You, B.F. Abrahams, Z.-L. Xue and C.-M. Che, *Angew. Chem. Int. Ed.,* 2001, **40**, 4422.
21. D. A. House, G. Hall, A. J. Matheson, W. T. Robinson, F. C. Ha, C. B. Knobler, *Inorg. Chim. Acta,* 1980, **39**, 257; J. A. Bertrand, J. A. Kelly and E. G. Vassian, *J. Am. Chem. Soc.*, 1969, **91**, 2395; R. Kuroda, S. Neidle, I. M. Ismail and P. J. Sadler, *J. Chem. Soc., Dalton Trans.*, 1983, 823; J. A. Bertrand, P. G. Kelly, E. Fujita, M. O. Lively and D. G. Van Deveer, *Inorg. Chem.*, 1979, **18**, 2419; L. Kilosci and K. Schug, *Inorg. Chem.*, 1983, **22**, 3053; J. A. Bertrand, W. J. Howard and A. R. Kalyanaraman, *J. Chem. Soc., Chem. Commun.*, 1971, 437.

22. T. C. Higgs, K. Spartalian, C. J. O'Connor, B. F. Metzanke and C. J. Carrano, *Inorg. Chem.*, 1998, **37**, 2263; U. Auerbach, C. Stockheim, T. Weyhermuller, K. Wieghardt and B. Nuber, *Angew. Chem., Int. Ed. Engl.,* 1993, **32**, 714; T. Beissel, T. Glaser, F. Kesting, K. Wieghardt and B. Nuber, *Inorg. Chem.,* 1996, **35**, 3936; T. Beissel, F. Birkelbach, E. Bill, T. Glaser, F. Kesting, C. Krebs, T. Weyhermuller, K. Wieghardt, C. Butzlaff and A. X. Trautwein, *J. Am. Chem. Soc.*, 1996, **118**, 12376.
23. P. B. Donaldson, P. A. Tasker and N. W. Alcock, *J. Chem. Soc., Dalton Trans.,* 1977, 1160; D. Funkemeier and R. Mattes, *J. Chem. Soc., Dalton Trans.*, 1993, 1313; R. L. Paul, A. J. Amoroso, P. L. Jones, S. M. Couchman, Z. R. Reeves, L. H. Rees, J. C. Jeffery, J. A. McCleverty and M. D. Ward, *J. Chem. Soc., Dalton Trans.,* 1999, 1563.
24. V. Kasempimolporn, H. Ōkawa and S. Kida, *Bull. Chem.Soc. Jpn.*, 1979, **52**, 1928.

Mono and dichlorobridged dinuclear copper(II) complexes with chiral amino alcohol based Schiff bases

5.1. Abstract

In this chapter, the characterization and properties of a series of optically active mono and dinuclear copper(II) complexes **(17-24)** derived from chiral Schiff bases H_2L^1-H_2L^8 are described. All these complexes are characterized by elemental analysis, IR, UV-Vis and EPR spectroscopic and circular dichroism studies. Four of these are characterized by single crystal X-ray analysis as well. Reaction of Schiff bases H_2L^1-H_2L^6 with $CuCl_2{\cdot}2H_2O$ in methanol at room temperature in 1:1 ratio yielded dichlorobridged dinuclear copper complexes. In these complexes, each copper shows a square pyramidal geometry with O_2NCl_2 coordination sphere having a central non planar Cu_2Cl_2 ring. Crystal structure analyses show that two penta-coordinated square-pyramidal copper complexes share a base to apex edge so that the Cl atom, situated at the vertex of one base, becomes the apex of the other square pyramid. Variable temperature magnetic study of complex **17** revealed ferromagnetic interactions between the copper centers. Complexes **17**, **18**, and **21** show C–H···Cl–Cu hydrogen bonding interactions in their respective crystal lattices, resulting in interesting supramolecular architectures like helices, one dimensional chains etc. Nitro substituted ligands (H_2L^7 and H_2L^8) gave mononuclear square planar copper(II) complexes (**23** and **24**) with ONOCl coordination sphere under the same reaction conditions. Analysis of the molecular packing of **23** revealed strong O–H···Cl–Cu intermolecular hydrogen bonding interactions resulting in the formation of supramolecular hydrogen bonded helices in the crystal.

5.2. Introduction

Dinuclear copper complexes have received much attention because of their relevance to the type 3 copper centers found in multicopper-containing proteins such as the tyrosinase, hemocyanins and copper oxidases.[1] There are several reports on modelling the active sites of these proteins using various types of ligands.[2] Since many of these proteins are believed to contain the copper ions in dissymmetric environments, modelling studies using dissymmetric ligands are expected to be more precise.[3] Chiral ligands are better choices in this respect and dinuclear copper complexes derived from chiral amino alcohol based ligands have been synthesized by Wardeska *et al* for modelling the dinuclear active sites.[4]

Dinuclear copper complexes have also been extensively used to derive magneto-structural correlations to understand the nature of spin-spin coupling phenomena in different structural arrangements. Several dihydroxo and dihalo bridged complexes are synthesized and analyzed to correlate the structure and magnetic properties. Although a good degree of success has been accomplished in the case of dihydroxo bridged dinuclear copper complexes, no unique magneto-structural correlations has been found for dihalobridged dinuclear copper complexes.[5]

At the same time, weak interactions play vital roles in highly efficient and specific biological reactions and are essential for molecular recognition and self organization of molecules in supramolecular chemistry. Systems assembled by hydrogen bonds leading to various supramolecular architectures often exhibit novel properties and are important in the crystal engineering of nonlinear optical, magnetic and conducting materials.[6] Identification of new functional groups which can act as effective hydrogen bonding functionalities is a main challenge in supramolecular chemistry. Recently much effort has been devoted to assess the hydrogen bond acceptor capabilities of the Cl atom in C–Cl and M–Cl (M = transition metal) moieties.[7] It has been shown both theoretically and experimentally that M–Cl is a much better hydrogen bond acceptor compared to C–Cl moiety.[8] Also it is found that the introduction of chirality into supramolecular systems can have considerable

influence on their structure and properties.[9] However, reports in this respect are limited probably because of the reason that the assembly of molecules through weak interactions requires careful incorporation of many factors which cannot be controlled completely.

Amino alcohol based ligands are better choices for the preparation of copper complexes to study their above mentioned properties. Although there are some reports on the copper complexes of amino alcohol based Schiff bases, their number is rather limited.[10] In this chapter, the structural, magnetic and supramolecular aspects of chiral mono- and dinuclear copper complexes **17-24,** synthesized from chiral Schiff base ligands H_2L^1-H_2L^8, are discussed.

5.3. Experimental

5.3.1. Materials

Details are given in section **2.2**

5.3.2. Physical measurements

As described in section **2.3**

5.3.3. Synthesis of Schiff base ligands H_2L^1-H_2L^8

Synthesis and characterization of chiral Schiff base ligands H_2L^1-H_2L^8 are described in section **2.4**

5.3.4. Synthesis of complexes 17-24

Synthesis and characterization of chiral copper complexes **17-24** are described in section **2.7**

5.3.5. X-ray crystallography

Single crystals of the complex **17** were grown by slow evaporation of ethanol solutions. Unit cell determination and the data collection were performed on an Enraf-Nonius Mach3 single crystal diffractometer using graphite monochromated Mo $K\alpha$ radiation (λ = 0.71073 Å). An empirical absorption correction was applied to the data based on the ψ-scans of three reflections.[11] Programs of WinGX[12] were used for data reduction and absorption correction. The structure was solved by direct methods and refined on F^2 by full-matrix least squares procedures using SHELX-97 programs.[13] Hydrogen atoms were not located in the difference Fourier maps associated with alcoholic oxygen atoms of the ligands.

X-ray data for complexes **18**, **21** and **23** were collected on a Bruker-Nonius SMART APEX CCD single crystal diffractometer using graphite monochromated Mo-Kα radiation (0.71073Å). The SMART software[14] was used for intensity data acquisition and the SAINTPLUS software[14] was used for data extraction. In each case, absorption correction was performed with the help of SADABS program.[14] The SHELX-97 was used for structure solution and least-square refinement on F^2. All the non hydrogen atoms were refined anisotropically. The hydrogen atoms were included in the structure factor calculation by using a riding model. The DIAMOND[15] software was used for molecular graphics.

For complex **18** hydrogen atoms were not located in association with alcoholic oxygen atoms of the ligands. Also the highest residual electron density of 1.99 e / Å^3 is observed near Cu3 at a distance of 1.156 Å.

The absolute configurations for all the complex molecules were successfully determined by refining the Flack parameter[16] and the values are given in the respective crystallographic data tables. The crystal and structure refinement data for complexes **17** and **18** are given in Table 5.1 and that for complexes **21** and **23** are given in Table 5.2.

Table 5.1. Crystal and structure refinement data for complexes **17** and **18**

Complex	**17**	**18**
Empirical formula	$C_{30}H_{30}N_2O_5Cu_2Cl_2$	$C_{34}H_{38}N_2O_5Cu_2Cl_2$
Formula weight	696.54	752.64
Crystal system	Orthorhombic	Triclinic
Space group	$P2_12_12_1$	$P1$
a / Å	10.21(2)	14.3436(7)
b / Å	11.574(3)	16.4026(8)
c / Å	25.364(9)	17.5196(8)
α / °		62.3290(10)
β / °		84.7990(10)
γ / °		73.1370(10)
V / Å^3	2998(6)	3488.8(3)
Z	4	4
μ / mm^{-1}	1.638	1.414
ρ_{calcd} / gcm^{-3}	1.538	1.433
Independent reflections	3856 (R_{int} = 0.02)	40729 (R_{int} = 0.0365)
Observed reflections	2882	30824
Parameters	372	1621
$R1$,[a] w$R2$[b] [($I > 2\sigma(I)$)]	0.0362 and 0.0707	0.0888 and 0.1870
Goodness-of-fit[c]	1.025	0.972
Flack parameter	0.034(19)	-0.008(15)
Largest peak and hole e / Å^3	0.37 and – 0.31	1.992 and – 0.416

[a] $R1 = \sum||F_o| - |F_c||/\sum|F_o|$. [b] $wR2 = \{\sum[(F_o^2 - F_c^2)^2]/\sum[w(F_o^2)^2]\}^{1/2}$.
[c] GOF = $\{\sum[w(F_o^2 - F_c^2)^2]/(n - p)\}^{1/2}$ where 'n' is the number of reflections and 'p' is the number of parameters refined; $w = 1/[\sigma^2(F_o^2) + (aP)^2 + bP]$ where a = 0.0336 and b = 1.0048 for complex **17**; and a = 0.1067 and b = 0 for complex **18**.

Table 5.2. Crystal and structure refinement data for complexes **21** and **23**

Complex	**21**	**23**
Empirical formula	$C_{31}H_{30}Br_2Cl_2Cu_2N_2O_5$	$C_{15}H_{13}N_2O_4CuCl$
Formula weight	868.37	384.26
Crystal system	Tetragonal	monoclinic
Space group	$P4_3$	$P2_1$
a / Å	16.0266(3)	11.3232(8)
b / Å	16.0266(3)	5.8314(4)
c / Å	13.2426(5)	12.3108(9)
β / °		112.3110(10)°
V / Å^3	3401.39(16)	752.03(9)
Z	4	2
μ / mm^{-1}	3.798	1.651
ρ_{calcd} / gcm^{-3}	1.696	1.697
Independent reflections	39729	8757
	(R_{int} = 0.0516)	(R_{int} = 0.0262)
Observed reflections	7740	3056
Parameters	407	212
$R1$,[a] w$R2$[b] [($I > 2\sigma(I)$)]	0.0427 and 0.0826	0.0338 and 0.0725
Goodness-of-fit[c]	1.007	1.046
Flack parameter	0.000(8)	0.029(13)
Largest peak and hole e / Å^3	0.578 and – 0.214	0.566 and – 0.223

[a] $R1 = \sum||F_o| - |F_c||/\sum|F_o|$. [b] w$R2 = \{\sum[(F_o^2 - F_c^2)^2]/\sum[w(F_o^2)^2]\}^{1/2}$.
[c] GOF = $\{\sum[w(F_o^2 - F_c^2)^2]/(n - p)\}^{1/2}$ where 'n' is the number of reflections and 'p' is the number of parameters refined; $w = 1/[\sigma^2(F_o^2) + (aP)^2 + bP]$ where a = 0.0403 and b = 0 for complex **21**; and a = 0.0322 and b = 0.0346 for complex **21.**

5.4. Results and discussion

5.4.1. Synthesis

Complexes **17**-**24** were synthesized in moderate yields from the reactions of 1:1 ratio of ligand to metal salt in methanol at room temperature. The reaction mixtures were green to dark green in color which on slow evaporation gave green colored solids. Elemental analysis revealed a 1:1 ligand to metal in all complexes.

5.4.2. Infrared spectral properties

The infrared spectra of the complexes were recorded in the range of 4000-400 cm^{-1}. Selected IR data are given in the experimental section. The peaks observed in the range of 2800-3000 cm^{-1} are most likely due to the aliphatic and aromatic C–H stretches. All the complexes show a strong peak in the range 1624-1643 cm^{-1} due to υ(C=N). The strong peak observed ~1540 cm^{-1} is characteristic of the phenolic C–O stretching mode acquiring partial double bond character through conjugation with the imine system in the chelate ring. The peaks observed in the range 1570-1600 cm^{-1} can be assigned to C=C stretch. Alcoholic C–O stretch appears in the range 1033-1101 cm^{-1}.

5.4.3. Electronic and circular dichroism spectra

The electronic and circular dichroism spectra of the complexes **17-24** are recorded in methanol solutions. The absorption spectra of the complexes show a weak band in the visible region around 680 nm followed by some intense absorptions in the high energy region. The origin of the weak band is assigned to d-d transition. For an octahedral complex, the expected $^2E_g \rightarrow {}^2T_{2g}$ transition is observed around 800 nm. Considerable blue shift of this band is observed as the octahedral geometry distorts to square pyramidal and square planar structures.[17] Another strong band observed around 400 nm is assigned to phenolate to copper charge transfer transition (LMCT). The sharp peaks in the 200-290 nm range of the electronic spectrum are due to

intraligand charge transfer (ILCT) transition, judging from their molar extinction coefficient values.

The optical activity of the copper complexes **17-24** is induced by the enantiopure ligands. The circular dichroism (CD) spectra of the complexes show bands corresponding to their d-d, LMCT and ILCT transitions. The d-d band is observed as a negative Cotton effect at high concentrations. Representative electronic and circular dichroism spectra are given in Figure 5.1.

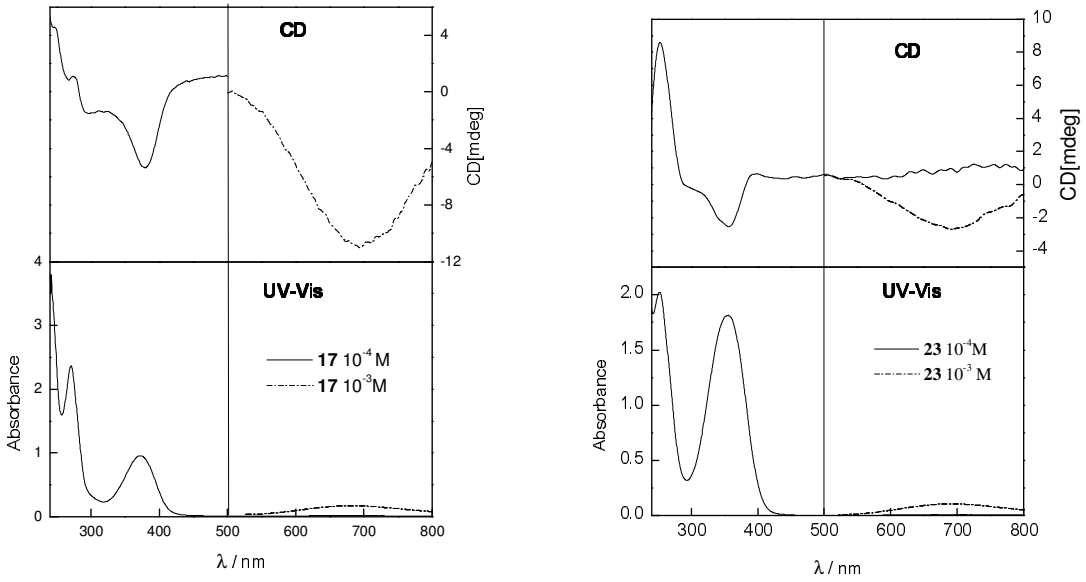

(a) **(b)**

Figure 5.1. Circular dichroism and electronic spectra for complexes **17 (a)** and **23 (b)** in methanol solutions.

5.4.4. EPR and magnetic studies

The EPR measurements of complexes **17**-**24** were performed in X-band frequency at liquid nitrogen temperature in methanol solutions. The spectra are given in Figure 5.2. The corresponding spectral parameters are given in Table 5.3.

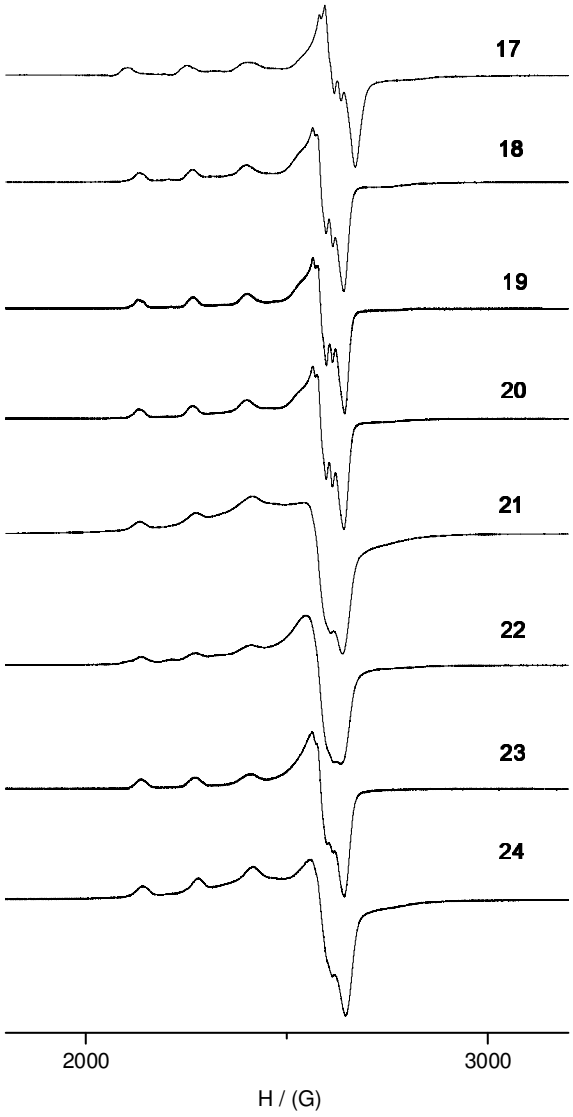

Figure 5.2. EPR spectra of complexes **17-24** in methanol solutions at liquid nitrogen temperature.

Table 5.3. EPR data and magnetic moments for complexes **17-24**

Complex	$g_{\parallel}$	$g_{\perp}$	$A_{\parallel}$	μ_{eff}/μ_B
17	2.29	2.06	169	2.51
18	2.29	2.06	160	2.63
19	2.29	2.07	165	2.70
20	2.28	2.07	167	2.83
21	2.28	2.07	168	2.90
22	2.26	2.06	166	2.84
23	2.28	2.06	164	1.80
24	2.29	2.07	163	1.77

The EPR spectra of the complexes **17-24** are similar and typical of a mononuclear square planar/square-pyramidal Cu(II) complex with a $d_{x^2-y^2}$ ground-state doublet. The data suggest that the bis(μ-halo)-bridged structures [(HL)Cu(μ-Cl)$_2$Cu(HL)] get dissociated in solution presumably due to interaction with the solvent molecules. This observation is also consistent with the fact that the chloride bridges of the complex are weak in the crystalline state in terms of Cu–Cl distances (2.8802(16) Å, 2.6872(15) Å etc.). Similar behavior has been observed for some analogous chloro-bridged dimeric copper complexes.[18] The g values ($g_{\parallel}$ = 2.26 - 2.29, $g_{\perp}$ = 2.06-2.07, $A_{\parallel}$ = 160 - 169 G) are comparable with those of other dinuclear Cu(II) complexes.[18,19] Interestingly nitrogen superhyperfine splitting is observed in the $g_{\perp}$ region for some complexes ($A_{\perp}^{N}$ = 16.5 G) as shown in Figure 5.2.

5.4.5. Magnetic susceptibility

The room temperature magnetic susceptibility data for the powdered samples of the complexes are given in Table 5.3. The magnetic moments for dinuclear complexes are in the range 2.51-2.90 μ_B which are less than the spin only values expected for two non-interacting Cu(II) centers.

Variable temperature magnetic susceptibility measurements in the temperature range 17-306 K and at constant magnetic field of 5 kG were performed with a powdered sample of complex **17**. A diamagnetic correction (-360×10^{-6} cgsu) calculated from Pascal's constant was applied to obtain the molar paramagnetic susceptibilities.[20] As shown in Figure 5.3, the μ_{eff} values increases from 2.51 at 296 K to 3.13 at 17 K indicating an overall ferromagnetic interaction between the two Cu(II) centers. The data were fitted using an expression for χ_M vs. T derived from the isotropic spin exchange Hamiltonian $H = -2JS_1 \cdot S_2$, where $S_1 = S_2 = 1/2$.[21] The best least square fit (Figure 5.3) was obtained with J = 39.13(2) cm^{-1}, g = 1.926(0.004), and TIP = 0.00012 emu/mol, where J is the ferromagnetic coupling constant, and TIP is the temperature independent paramagnetism.

A structural classification of dimers containing the $Cu(\mu\text{-}Cl)_2Cu$ core has been reported viz. coplanar bases, parallel bases and perpendicular bases, based on the relative arrangement of square pyramids around the two copper centers.[22] The complex **17** belongs to parallel bases type and in this type of complexes, either ferromagnetic or antiferromagnetic coupling can be found depending on the Cu–Cl bond lengths and Cu-Cl-Cu bond angles. Extended Hückel calculations for the ideal parallel base type of geometry show that the magnetic interaction between the copper metal centers will take place mainly through π^* type of interaction between the Cu $d_{x^2-y^2}$ and the apical p_{cl} orbitals. The theoretical studies to correlate the geometrical distortions and magnetic properties of such systems proved that even small geometric variations produce large changes in the coupling constant values.[5] The reported exchange coupling constants (J) in such complexes cover a wide range –20.8 to +12. We can assume that the geometric distortion in complex **17** — which is having a

central non-planar asymmetric Cu_2Cl_2 ring with two different Cu–Cl bond lengths and Cu-Cl-Cu bond angles — is so as to support a ferromagnetic interaction between the two Cu(II) centers.

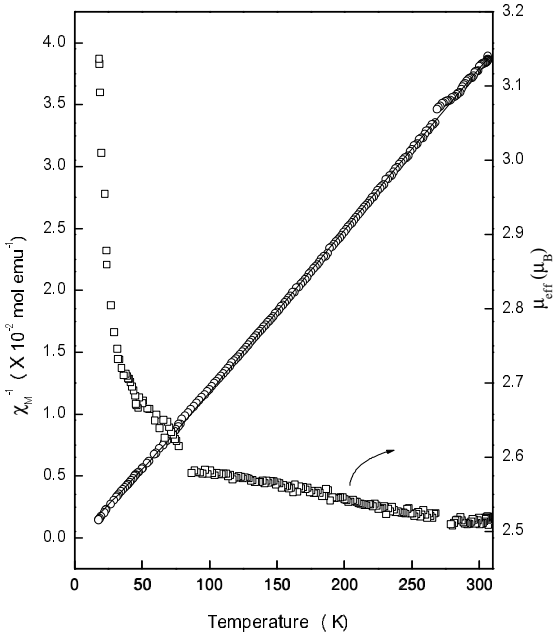

Figure 5.3. Inverse molar magnetic susceptibility (O) of **17** as a function of temperature. The solid line was generated from the best least-square fit parameters given in the text. The represents μ_{eff} values.

Variable temperature magnetic susceptibility measurements for complexes **18-24** were not performed; however room temperature magnetic susceptibility data were measured for these complexes. The data for complexes **23** and **24** corresponds to mononuclear Cu(II) complexes (Table 5.3). Although the room temperature magnetic moments for complexes **18**-**22** are comparable to that of complex **17**, one cannot expect exactly the same type of behavior for these complexes at low temperatures as that of complex **17**. Since X-ray data for complexes **18** and **21** revealed variations in respective bond lengths and angles in comparison with complex **17**, prediction of low temperature magnetic behavior based on room temperature data could be erroneous.

5.4.6. Description of molecular structures

5.4.6.1. Crystal structure of complex 17

Crystals of **17** suitable for X-ray analysis were obtained by re-crystallization from ethanol. The relevant crystallographic parameters are given in Table 5.1 and the thermal ellipsoid plot for the molecular structure of complex **17** is presented in Figure 5.4.

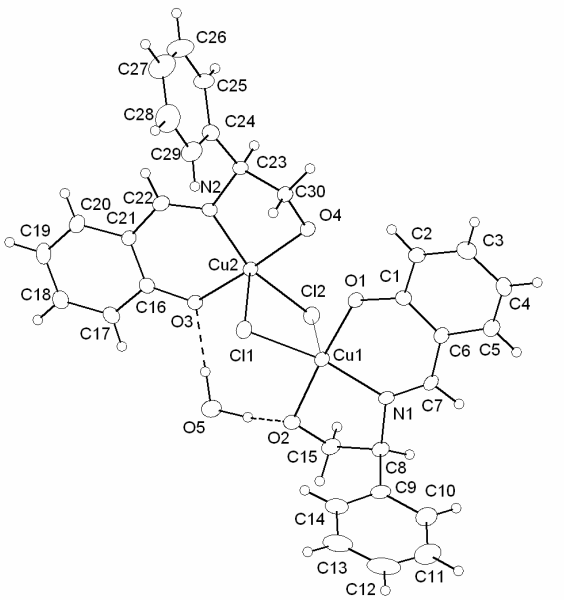

Figure 5.4. Thermal ellipsoid plot (20 % probability) and atom labeling scheme for complex **17**. The hydrogen bonding parameters for the solvent water are O5–H151···O3 0.99 1.84 2.783(5) 158.3, O5–H252···O2 1.00 1.76 2.641(7) 143.4.

The complex **17** crystallizes in the orthorhombic chiral space group $P2_12_12_1$ with four molecules per unit cell. The unit cell also contains four water molecules. Each complex is hydrogen bonded to one water molecule. The structure consists of dimeric $Cu_2Cl_2(HL)_2$ units with a central non-planar Cu_2Cl_2 ring. The dihedral angle between the planes defined by Cu1, Cl1, Cl2 and Cu2, Cl1, Cl2 is 25.8°. Each Cu is penta-coordinated with a distorted square pyramidal geometry. Generally, the dichloro-bridged penta-coordinated copper complexes with square pyramid geometry

exhibit three different geometries with regard to the relative arrangement of square pyramids viz. perpendicular bases (type I), parallel bases (type II) and coplanar bases (type III)[22] as shown in Scheme 5.1.

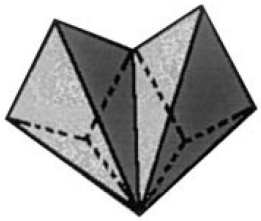

Type I

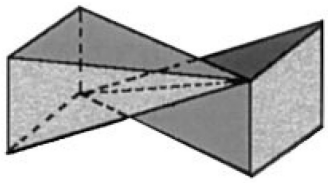

Type II

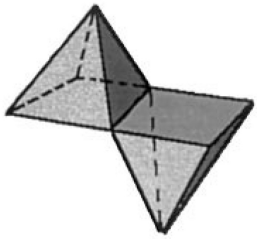

Type III

Scheme 5.1. Polygon arrangements found for dinuclear copper complexes with square-pyramidal geometry.

The asymmetric arrangement of the Cu_2Cl_2 moiety in complex **17** belongs to type II. In this geometry, two penta-coordinated copper complexes with a square pyramidal geometry share a base to apex edge so that the Cl atom, situated at the vertex of one base, becomes the apex of the other square pyramid and the just opposite happens for the other Cl bridging ligand. Table 5.4 presents the selected bond distances and angles. Analysis of the shape-determining angles using the approach of Reedijk *et al*,[23] yields a τ value of 0.1528 for Cu1 and 0.2878 for Cu2, indicating that the distortion is more towards square pyramidal than trigonal

bipyramidal (τ = 0 for square pyramidal and τ = 1 for trigonal bipyramidal geometry). There are evidences for the involvement of imidazole and phenoxide ligands around copper centers in oxyhemocyanins in a square-pyramidal geometry. Within the asymmetric Cu(μ-Cl)$_2$Cu core, the Cu···Cu distance is 3.3809(9) Å; the two shorter (equatorial) Cu1–Cl1 and Cu2–Cl2 distances are 2.245(4) and 2.267(2) Å; the two longer (apical) Cu1–Cl2 and Cu2–Cl2 distances are 2.8802(17) and 2.6874(15) Å; the Cu1-Cl1-Cu2 and Cu1-Cl2-Cu2 angles are 86.03(5) and 81.16(6)°, respectively.

Table 5.4. Selected bond distances (Å) and angles (°) for complex **17**

Cu(1)-O(1)	1.901(4)	Cu(2)-O(3)	1.895(4)
Cu(1)-N(1)	1.949(5)	Cu(2)-N(2)	1.933(4)
Cu(1)-O(2)	1.996(3)	Cu(2)-O(4)	2.037(4)
Cu(1)-Cl(1)	2.245(4)	Cu(2)-Cl(2)	2.267(2)
Cu(1)-Cl(2)	2.8802(17)	Cu(2)-Cl(1)	2.6874(15)
N(1)-C(7)	1.281(7)	N(2)-C(22)	1.291(6)
Cu(1)-Cu(2)	3.3809(9)		
O(1)-Cu(1)-N(1)	93.19(19)	O(3)-Cu(2)-N(2)	94.74(19)
O(1)-Cu(1)-O(2)	174.81(16)	O(3)-Cu(2)-O(4)	176.70(15)
N(1)-Cu(1)-O(2)	82.94(18)	N(2)-Cu(2)-O(4)	82.64(18)
O(1)-Cu(1)-Cl(1)	92.29(15)	O(3)-Cu(2)-Cl(2)	93.65(16)
N(1)-Cu(1)-Cl(1)	165.64(12)	N(2)-Cu(2)-Cl(2)	159.43(12)
O(2)-Cu(1)-Cl(1)	92.28(14)	O(4)-Cu(2)-Cl(2)	88.18(15)
Cl(2)-Cu(2)-Cl(1)	96.10(5)	O(3)-Cu(2)-Cl(1)	93.80(12)
Cu(1)-Cl(1)-Cu(2)	86.03(5)	N(2)-Cu(2)-Cl(1)	102.03(12)
Cu(2)-Cl(2)-Cu(1)	81.16(6)	O(4)-Cu(2)-Cl(1)	88.73(11)

In the molecular structure, the alcoholic oxygen O4 and phenolic oxygen O1 are interconnected through O–H···O intramolecular hydrogen bonding interaction. The relevant distance is O4···O1 2.603(5) Å. It is assumed that this interaction plays some role in determining the 'bent' geometry of the complex with a central non planar Cu_2Cl_2 ring.

Detailed analysis of the crystal structure revealed some weak intermolecular C–H···Cl hydrogen bonding interactions among the molecules. Both the metal bound chloride ligands Cl1 and Cl2 involve in these interactions as acceptors while the aromatic carbons C25, C12 and aliphatic chiral carbon C23 act as hydrogen bond

donors. The hydrogen bonding pattern of a single molecule of complex **17** is shown in Figure 5.5. These interactions propagate through the crystal lattice in a three dimensional manner resulting in a complicated hydrogen bonded network as shown in Figure 5.6(a). Among these, one particular interaction can be traced in a helical fashion as shown in Figure 5.6(b). The relevant hydrogen bonding parameters are given in Table 5.5.

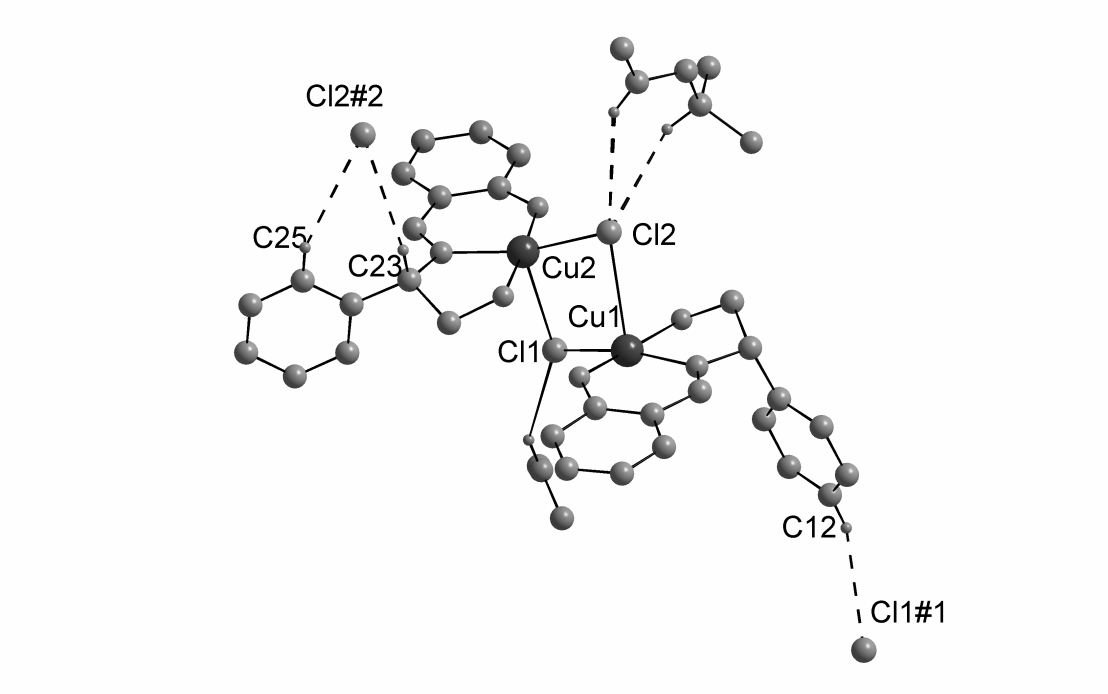

Figure 5.5. C–H···Cl hydrogen bonding pattern of a single molecule of complex **17**.

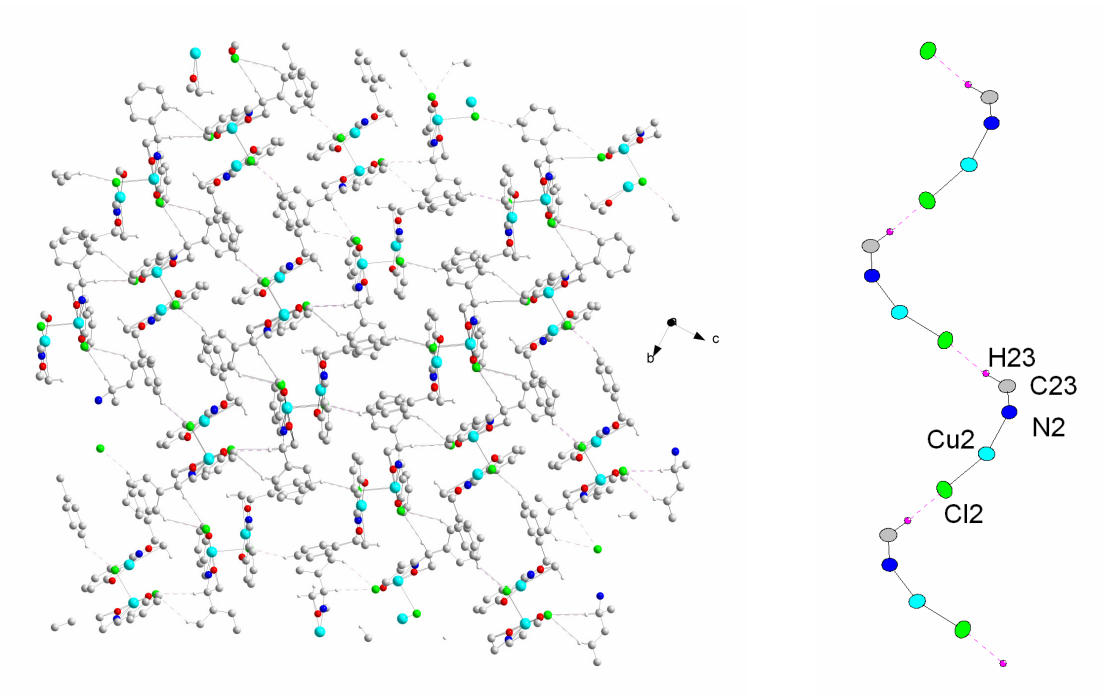

a **b**

Figure 5.6. (a) Intricate hydrogen bonded network in the crystal lattice of complex **17 (b)** one particular C–H···Cl interaction in a helical manner.

Table 5.5. Hydrogen bonding parameters (Å, °) for complex **17**

Donor–H···Acceptor	D–H	H···A	D···A	∠D–H···A	Symmetry
C23–H23···Cl2 #2	0.98	2.89	3.725(5)	143.7	-x, 0.5+y, 1.5-z
C25–H25···Cl2#2	0.93	3.00	3.806(7)	146.4	-x, 0.5+y, 1.5-z
C12–H12···Cl1#1	0.93	2.90	3.728(8)	148.9	0.5+x, 1.5-y, 2-z

5.4.6.2. Crystal structure of complex 18

Single crystals of complex **18** suitable for X-ray analysis were grown from a solution of ethanol. Crystal and structure refinement data are presented in Table 5.1.

The complex crystallizes in the non-centrosymmetric space group triclinic *P*1. The asymmetric unit contains four dinuclear dichlorobridged copper(II) complexes and four solvent ethanol molecules. In each of the four dimeric copper complexes, the copper ions are in distorted square pyramidal geometry, with the planar Schiff base ligand coordinating to the metal ion via the phenolate oxygen, alcohol oxygen and imine nitrogen atoms. The fourth and fifth positions are occupied by bridging chloro ligands. The thermal ellipsoid plot for a representative dinuclear unit from the asymmetric unit is given in Figure 5.7.

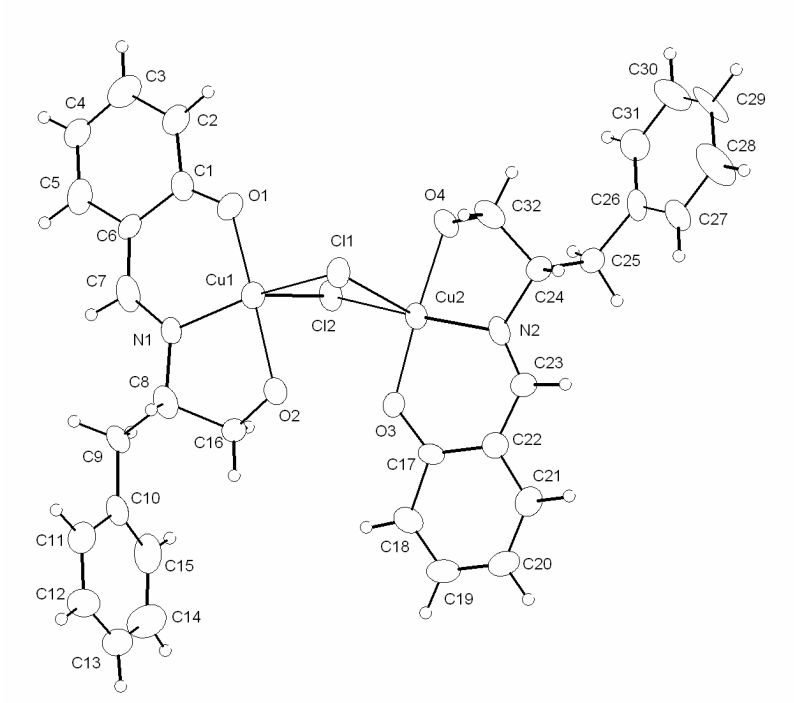

Figure 5.7. Thermal ellipsoid plot (20 % probability level) and atom labeling scheme for a representative dinuclear unit of complex **18.**

The four dinuclear units present in the asymmetric unit show variations in their respective bond lengths and angles. In each dinuclear unit, bridging through chloro ligands leads to the formation of a central non-planar Cu_2Cl_2 ring. The dihedral angle between the planes defined by Cu1, Cl1, Cl2 and Cu2, Cl1, Cl2 for the dinuclear unit given in Figure 5.7 is 28.69°. Similar dihedral angles for other dimeric units are 23.11° (Cu3-Cu4), 23.46° (Cu5-Cu6) and 22.57° (Cu7-Cu8). Selected bond lengths and angles for one representative dinuclear unit are given in Table 5.6.

Table 5.6. Selected bond distances (Å) and angles (°) for one representative dimeric unit of complex **18**

Cu(1)-O(1)	1.895(8)	Cu(2)-O(3)	1.883(9)
Cu(1)-O(2)	2.033(8)	Cu(2)-O(4)	1.988(8)
Cu(1)-N(1)	1.944(9)	Cu(2)-N(2)	1.959(10)
Cu(1)- Cl(1)	2.256(3)	Cu(2)- Cl(1)	2.901(3)
Cu(1)-Cl(2)	2.748(3)	Cu(2)-Cl(2)	2.252(3)
Cu(1)-Cu(2)	3.492(2)		
O(1)-Cu(1)-N(1)	95.2(4)	O(3)-Cu(2)-N(2)	91.2(4)
O(1)-Cu(1)-O(2)	177.6(3)	O(3)-Cu(2)-O(4)	174.4(4)
N(1)-Cu(1)-O(2)	82.7(4)	N(2)-Cu(2)-O(4)	83.4(4)
O(1)-Cu(1)-Cl(1)	94.8(3)	O(3)-Cu(2)-Cl(2)	92.1(3)
N(1)-Cu(1)-Cl(1)	162.2(3)	N(2)-Cu(2)-Cl(2)	171.4(3)
O(2)-Cu(1)-Cl(1)	87.5(2)	O(4)-Cu(2)-Cl(2)	93.4(3)
O(1)-Cu(1)-Cl(2)	91.5(3)	O(3)-Cu(2)-Cl(1)	95.7(3)
N(1)-Cu(1)-Cl(2)	102.1(3)	N(2)-Cu(2)-Cl(1)	99.1(3)
O(2)-Cu(1)-Cl(2)	87.8(3)	O(4)-Cu(2)-Cl(1)	83.4(3)
Cl(1)-Cu(1)-Cl(2)	92.37(11)	Cl(2)-Cu(2)-Cl(1)	88.54(10)
O(1)-Cu(1)-Cu(2)	108.4(3)	O(3)-Cu(2)-Cu(1)	82.1(2)
N(1)-Cu(1)-Cu(2)	133.5(3)	N(2)-Cu(2)-Cu(1)	136.6(3)
O(2)-Cu(1)-Cu(2)	72.4(2)	O(4)-Cu(2)-Cu(1)	100.5(2)
Cl(1)-Cu(1)-Cu(2)	55.75(9)	Cl(2)-Cu(2)-Cu(1)	51.85(8)
Cl(2)-Cu(1)-Cu(2)	40.12(6)	Cl(1)-Cu(2)-Cu(1)	40.01(6)
Cu(1)-Cl(1)-Cu(2)	84.25(10)	Cu(2)-Cl(2)-Cu(1)	88.03(10)

As expected the $Cu–Cl_{equatorial}$ bond lengths are found to be shorter than the $Cu–Cl_{apical}$ distances for each copper center [average $Cu–Cl_{equatorial}$ = 2.257(4) Å, average $Cu–Cl_{apical}$ = 2.808(4) Å]. The average Cu-Cl-Cu bond angle and Cu···Cu distance for the four dinuclear units present in the asymmetric unit are 86.10(10)° and 3.605(2) Å respectively.

The arrangement of the Cu_2Cl_2 moieties in all the four dinuclear complexes present in the asymmetric unit belongs to Type II as explained in Scheme 5.1. Analysis of the shape-determining angles using the approach of Reedijk *et al*[23] yielded values in the range 0.05-0.38. The variation in τ values reflects the distortions in geometry from complex to complex. But in all cases the distortion is found to be more towards square pyramidal rather than trigonal bipyramidal.

Crystal packing analysis of the complex **18** revealed the presence of intermolecular C–H···Cl hydrogen bonding interactions among the dinuclear units present in the asymmetric unit. The four dinuclear units present in the asymmetric unit can be identified as CuA (containing Cu1 and Cu2), CuB (containing Cu3 and Cu4), CuC (containing Cu5 and Cu6) and CuD (containing Cu7 and Cu8). In the crystal lattice the copper dimers CuA and CuB are interconnected through two intermolecular C–H···Cl interactions [C23–H23···Cl4 and C55–H55···Cl2] resulting in the formation of an infinite one dimensional chain type arrangement as shown in Figure 5.8(a). At the same time the dinuclear complexes CuC and CuD are interconnected through another C–H···Cl interaction [C119–H119···Cl5] resulting in the formation of a discrete hydrogen bonded dimer (Figure 5.8(b)). Interestingly these discrete dimers are 'hooked' to the above mentioned one dimensional chain through yet another C–H···Cl interaction [C69–H69···Cl2]. The resulting structure appears as if the discrete hydrogen bonded dimers are 'hanging' from the infinite one dimensional chain formed by CuA and CuB as shown in Figure 5.8(c). The relevant hydrogen bonding parameters are given in the upper portion of Table 5.7 which are comparable to the previously reported similar systems.[7(a)]

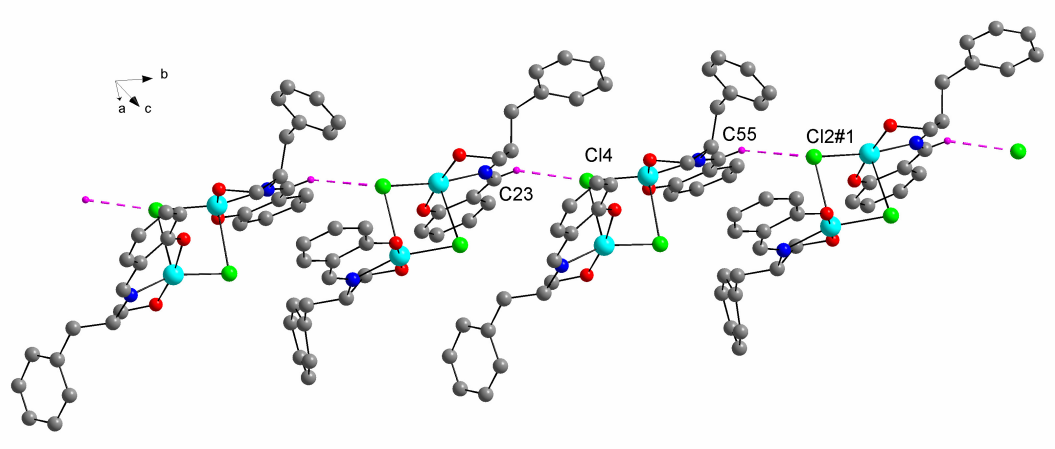

Figure 5.8(a). Infinite one dimensional chain found in the crystal lattice of complex **18**.

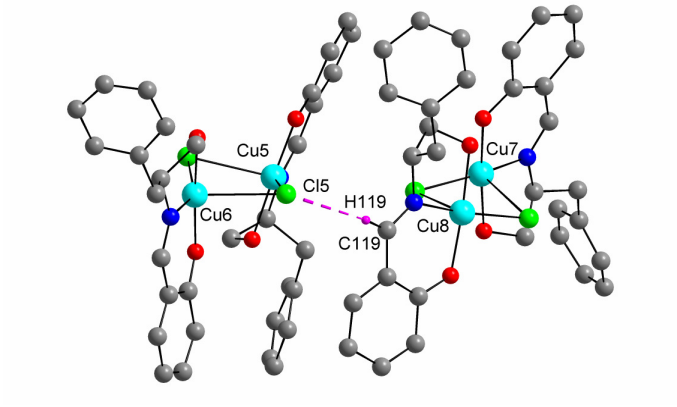

Figure 5.8(b). Discrete dimer formed by two dinuclear units of complex **18.**

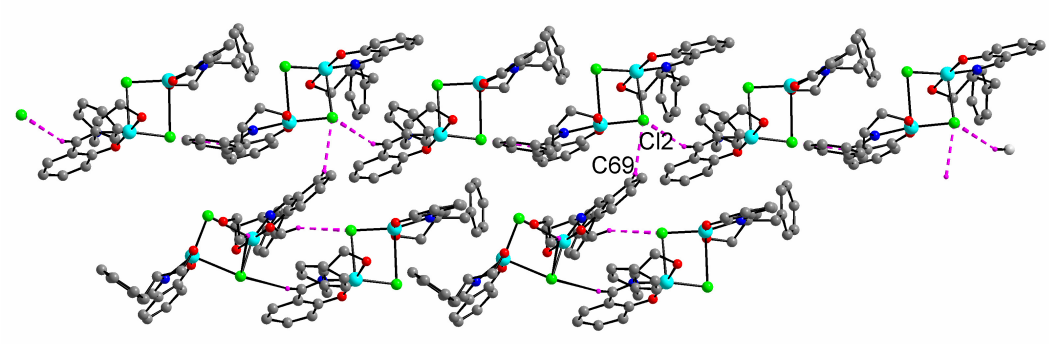

Figure 5.8(c). Dimers 'hanging' from the one dimensional chain.

In addition to the above mentioned C–H···Cl interactions, there is an intra-molecular O–H···O hydrogen bonding interaction between a pair of metal bound alcoholic and a phenolic oxygen atoms in each dinuclear units. Although the relevant hydrogen atoms are not located, it appears that in these interactions, the protonated alcoholic oxygens acts as donors while the deprotonated phenolic oxygens act as acceptors. The relevant parameters are O2···O3 2.638(12) Å (CuA), O8···O5 2.588(13) Å (CuB), O10···O11 2.612(11) Å (CuC) and O16···O13 2.688(12) Å. As in the case of complex **17,** these interactions play some role in determining the 'bent' geometry of these complexes having a central non-planar Cu_2Cl_2 ring.

The other pair of alcoholic and phenolic oxygens present in the dinuclear units CuA, CuB and CuD are hydrogen bonded to one solvent ethanol molecule each through inter molecular O–H···O interactions. In these interactions the ethanol oxygen atom acts as both hydrogen bond donor as well as acceptor. The parameters are O19···O1 2.887(14) Å and O19···O4 2.552(14) Å for CuA, O6···O17 2.576(12) Å and O17···O7 2.866(12) Å for CuB and O14···O20 2.601(12) Å and O20···O15 2.794(12) Å for CuD.

Interestingly in the dinuclear unit CuC, the solvent ethanol molecule is hydrogen bonded to the alcoholic and phenolic oxygens through C–H···O interactions instead of O–H···O interactions. The relevant hydrogen bonding parameters are presented in the lower portion of the Table 5.7.

Table 5.7. The hydrogen bonding parameters (Å, °) for the complex **18**

Donor–H···Acceptor	D–H	H···A	D···A	∠D–H···A	Symmetry
C69–H69···Cl2	0.93	2.88	3.578(14)	132.5	
C55–H55···Cl2#1	0.93	2.84	3.687(12)	152.1	x, 1+y, z
C23–H23···Cl4	0.93	2.75	3.598(12)	152.1	
C119–H119···Cl5#1	0.93	2.81	3.711(14)	164.2	x, 1+y, z
C132–H13A···O9#2	0.96	1.87	2.815(15)	168	1+x, y, z
C132–H13B···O12#2	0.96	1.72	2.631(15)	158	1+x, y, z

5.4.6.3. Crystal structure of complex 21

Single crystals of complex **21** suitable for X-ray analysis were grown from methanol solution by slow evaporation method. Table 5.2 displays the details of the data collection parameters and refinement. Thermal ellipsoid plot of complex **21** with atom labeling scheme is given in Figure 5.9.

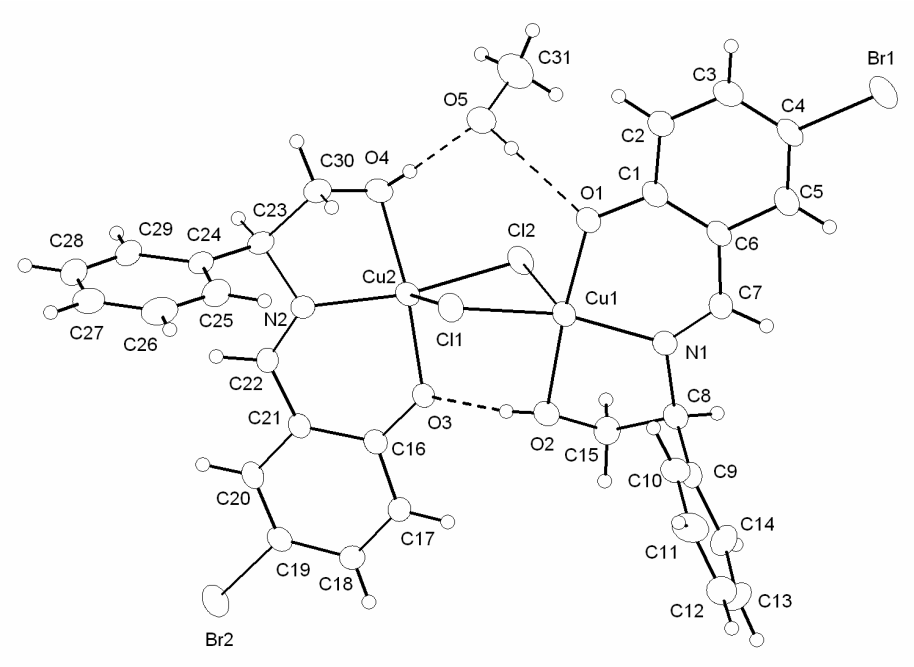

Figure 5.9. Thermal ellipsoidal plot (20 % probability level) for complex **21** with atom labeling scheme.

The complex crystallizes in chiral space group tetragonal $P4_3$. The asymmetric unit of **21** contains one molecule of the complex and one solvent methanol molecule. As in the case of complexes **17** and **18**, the structure of **21** contains two penta-coordinate copper(II) ions which are bridged by two chloro ligands. The other three coordination sites of each copper are occupied by phenolate O, alcohol O and imine N atoms of the chiral Schiff base ligand. The central Cu_2Cl_2 ring is non planar with a dihedral angle of 25.59^o between the planes defined by Cu1, Cl1, Cl2 and Cu2, Cl1, Cl2.

Each Cu has a distorted square pyramidal type geometry as ascertained by Reedijk's τ factor of 0.1588 for Cu2 and 0.255 for Cu1. As expected the $Cu–Cl_{equatorial}$ bond lengths [average $Cu–Cl_{equatorial}$ = 2.2677(14) Å] are found to be shorter than the $Cu–Cl_{apical}$ distances [average $Cu–Cl_{apical}$ = 2.7295(15) Å]. The average Cu-Cl-Cu bond angle is 84.44(5)^o and the Cu···Cu separation is 3.3752(8) Å. The selected bond lengths and angles for the complex **21** are given in Table 5.8.

Table 5.8. Selected bond distances (Å) and angles (^{o}) for complex **21**

Cu(1)-O(1)	1.906(3)	Cu(2)-O(3)	1.912(3)
Cu(1)-O(2)	2.028(3)	Cu(2)-O(4)	1.996(4)
Cu(1)-N(1)	1.937(4)	Cu(2)-N(2)	1.937(4)
Cu(1)-Cl(1)	2.2600(14)	Cu(2)-Cl(2)	2.2753(14)
Cu(1)-Cl(2)	2.7327(15)	Cu(2)-Cl(1)	2.7263(15)
O(1)-C(1)	1.321(5)	O(3)-C(16)	1.331(5)
N(2)-C(21)	1.282(6)	C(7)-N(1)	1.280(6)
Cu(2)-Cu(1)	3.3752(8)		
O(1)-Cu(1)-N(1)	94.35(16)	O(3)-Cu(2)-N(2)	92.43(14)
O(1)-Cu(1)-O(2)	175.28(16)	O(3)-Cu(2)-O(4)	173.25(16)
N(1)-Cu(1)-O(2)	81.24(16)	N(2)-Cu(2)-O(4)	80.97(16)
O(1)-Cu(1)-Cl(1)	91.64(11)	O(3)-Cu(2)-Cl(2)	94.44(10)
N(1)-Cu(1)-Cl(1)	159.97(13)	N(2)-Cu(2)-Cl(2)	163.72(12)
O(2)-Cu(1)-Cl(1)	93.07(12)	O(4)-Cu(2)-Cl(2)	92.30(13)
O(1)-Cu(1)-Cl(2)	93.93(12)	O(3)-Cu(2)-Cl(1)	90.78(11)
N(1)-Cu(1)-Cl(2)	105.59(13)	N(2)-Cu(2)-Cl(1)	101.81(12)
O(2)-Cu(1)-Cl(2)	85.68(11)	O(4)-Cu(2)-Cl(1)	89.18(14)
Cl(1)-Cu(1)-Cl(2)	93.02(5)	Cl(2)-Cu(2)-Cl(1)	92.85(5)
O(1)-Cu(1)-Cu(2)	106.78(10)	O(3)-Cu(2)-Cu(1)	80.97(9)
N(1)-Cu(1)-Cu(2)	141.05(12)	N(2)-Cu(2)-Cu(1)	142.29(12)
O(2)-Cu(1)-Cu(2)	76.02(10)	O(4)-Cu(2)-Cu(1)	103.36(13)
Cl(1)-Cu(1)-Cu(2)	53.54(4)	Cl(2)-Cu(2)-Cu(1)	53.66(4)
Cl(2)-Cu(1)-Cu(2)	42.12(3)	Cl(1)-Cu(2)-Cu(1)	41.81(3)
Cu(1)-Cl(1)-Cu(2)	84.65(5)	Cu(2)-Cl(2)-Cu(1)	84.22(5)

The arrangement of two copper square pyramids in this complex also belongs to Type II as explained in Scheme 5.1.

The solvent methanol molecule present in the asymmetric unit is hydrogen bonded to the complex through two intermolecular O–H···O interactions. In the first case, the methanolic oxygen O5 acts as hydrogen bond donor to metal coordinated phenolate oxygen O1. In the second interaction, the methanol oxygen O5 acts as

hydrogen bond acceptor while the metal coordinated alcoholic oxygen atom O4 acts as hydrogen bond donor. As in the case of complexes **17** and **18**, an intramolecular O–H···O hydrogen bond also exists in the complex molecule in which the metal coordinated alcoholic oxygen O2 acts as the hydrogen bond donor while the metal coordinated phenolate oxygen O3 acts as the hydrogen bond acceptor. The details of the hydrogen bonding parameters are summarized in Table 5.9.

Table 5.9. Hydrogen bonding parameters for complex **21**

Donor–H···Acceptor	D–H	H···A	D···A	D–H···A
O2–H2A···O3	0.87(6)	1.73(6)	2.588(4)	170(6)
O4–H4A···O5	0.79(6)	1.83(7)	2.617(6)	173(9)
O5–H5A···O1	0.82	1.98	2.792(6)	171
C29–H29···Cl1#1	0.93	2.76	3.657(6)	161

#1 = 1-x, y, 0.25+z

The molecule also exhibits infinite one dimensional helical self assembly via intermolecular C–H···Cl interactions in its crystal lattice. Here the metal coordinated chlorine Cl1 acts as the hydrogen bond acceptor while the C–H moiety of the benzene ring on the ligand (C29) acts as the hydrogen bond donor. The C–H···Cl bond parameters are quite comparable to those of the reported C–H···Cl systems.[7] (Table 5.9). In D–H···Cl–M interaction, the intermolecular contacts are categorized as 'short' (2.52), 'intermediate' (2.52-2.95) and 'long' (2.95-3.15 Å) based on the H···Cl distance.[24] The present case belongs to 'intermediate' category according to this classification.

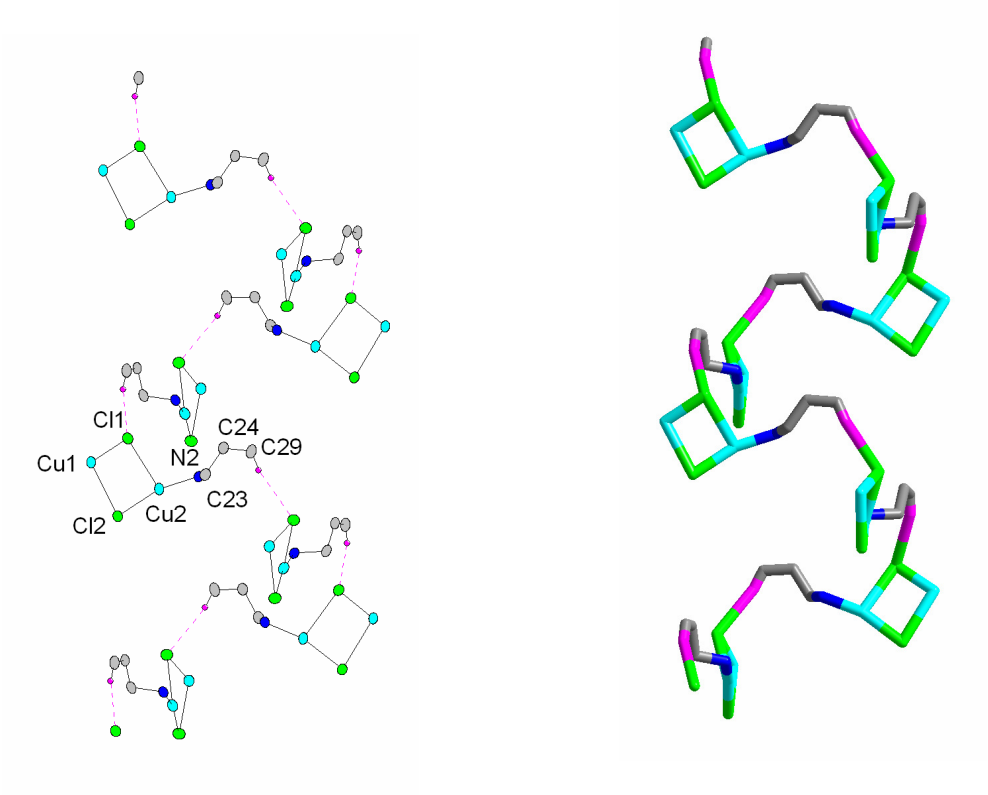

a **b**

Figure 5.10. Intermolecular C–H···Cl–Cu hydrogen bonding interactions between adjacent molecules that lead to the formation of homochiral helices. **a**: helical backbone ball-and-stick, **b**: wire-frame representation. Colour code: Cu, cyan; Cl, green; N, blue; C, grey; H, purple.

The helix propagates through *c* axis. One turn of the helix contains four molecules of the dinuclear copper complex with a pitch distance of 13.24 Å. The path of the helix can be traced by following the hydrogen bonds counter-clockwise around the 4-fold screw axis of the helix. Since the ligand H_2L^5 used is enantiopure, the crystal contains a single enantiomer of the complex **21**. This local chirality translates throughout the crystal into the formation of only left handed helices at the supramolecular level (Figure 5.10).

It has been shown recently that halogens act as strong hydrogen bond acceptors when bound to transition metals, in contrast to their limited ability to serve as weak hydrogen-bond acceptors when bound to carbon.[7,8] The present complex belongs to the rather limited number of chiral supramolecular systems containing M–Cl group as the hydrogen bond acceptor.

5.4.6.4. Crystal structure of complex 23

Single crystals of complex **23** were grown from mother liquor by slow evaporation method. The details of data collection and refinement are given in Table 5.2. The thermal ellipsoidal plot of **23** with atom labelling scheme is given in Figure 5.11.

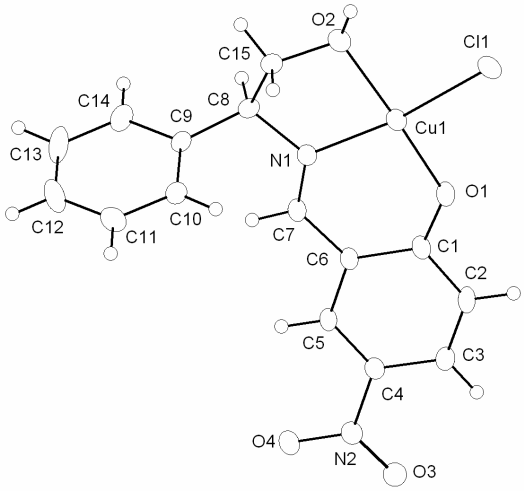

Figure 5.11. Thermal ellipsoid plot (20 %) of **23**. Relevant bond lengths (Å) and angles (°): Cu1–O1 1.880(2), Cu1–O2 1.968(2), Cu1–N1 1.954(2), Cu1–Cl1 2.2482(8), O1–C1 1.289(3), N1–C7 1.265(4); O1–Cu1–N1 94.04(9), O1–Cu1–O2 172.12(11), N1–Cu1–O2 81.37(10), O1–Cu1–Cl1 94.99(6), N1–Cu1–Cl1 170.74(7), O2–Cu1–Cl1 89.88(8).

The structure consists of a neutral mononuclear four coordinated copper(II) complex with the chiral tridentate Schiff base ligand providing the ONO donor atom set. The fourth position is occupied by a chloride ion. The overall coordination geometry of the compound is distorted square planar with the copper ion lying at *ca.* center of the plane consisting of ligand donor atoms Cl1, O1, N1 and O2.

The molecular packing in the crystal structure of **23** reveals strong O–H···Cl–Cu intermolecular hydrogen bonding interactions involving the hydrogen atom on O2 and the Cl1 anion coordinated to the copper center (Figures **5.11** and **5.12**). This results in the formation of supramolecular hydrogen bonded helices that extend indefinitely through out the crystal lattice (Figure **5.12**). (Relevant hydrogen bonding parameters: *d*(H–O) = 0.80(4) Å, *d*(H···Cl) = 2.26(4) Å, *d*(O···Cl) = 3.024(3) Å, and ∠(OHCl) 159(4)^{o}).

The O–H···Cl distance observed in this study (2.26(4) Å) is appreciably shorter than the sum of the van der Waals radii for the H and the neutral Cl atoms (2.95 Å). This can be classified as 'short' interaction (< 2.52 Å are termed 'short').[24] Similar strong M–X···H–O bonds are known in literature but that do not result in helical structures. Representative examples include Cu–Cl···H–O hydrogen bond (*d*(H–O) = 0.84 Å, *d*(H···Cl) = 2.25 Å, *d*(O···Cl) = 3.08 Å, and ∠(OHCl) 173.3^{o}) in the crystal structure of $CuCl(C_{19}H_{19}N_3O)$[25] and Cu–Cl···H–O hydrogen bond (*d*(H–O) = 0.98 Å, *d*(H···Cl) = 2.26 Å, *d*(O···Cl) = 3.228 Å, and ∠(OHCl) 171^{o}) in the compound $[CuCl(C_5H_9N_3)(C_{12}H_8N_2)]Cl{\cdot}H_2O$.[26] The strength of the interaction can be attributed to the strong hydrogen bond donor ability of the O–H group due to its greater acidity and to the strong H-bonding acceptor property of the metal bound chloride.

The path of the helix can easily be traced by following the hydrogen bonds clockwise around the two fold screw axis of the helix. Three copper complex fragments form one helix turn in **23** with a pitch of 5.831 Å (Figure 5.12). We believe that the required turn to generate a perfect periodic self-assembly of [Cu(HL^7)Cl] **23** in a helical fashion, is induced by the chirality of the building block coupled with the strong O–H···Cl–Cu hydrogen bonding interactions. Also the rigidity of the Schiff-base ligand, which occupies three binding sites of the Cu atom, may have some role in dictating such helical arrangement in this self-assembly process.

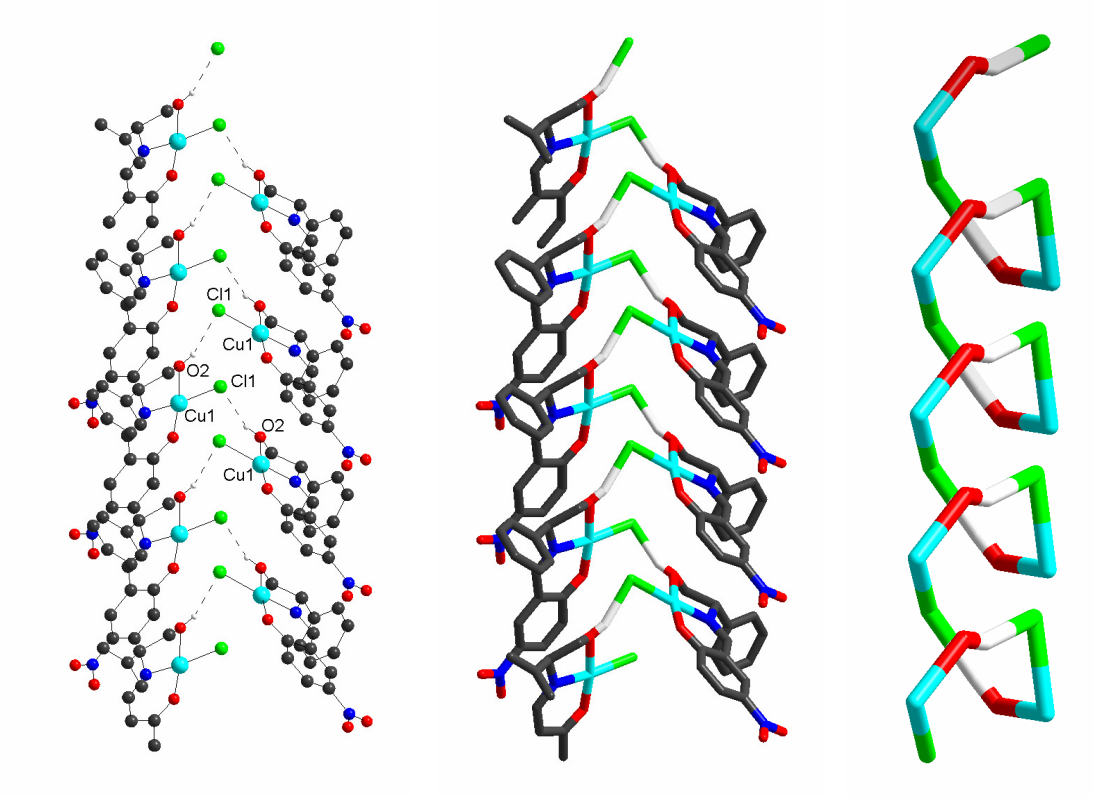

Figure 5.12. Intermolecular O–H···Cl–Cu hydrogen bonding interactions between adjacent molecules that lead to the formation of homochiral helices. **a**: Ball-and-stick, **b**: wire-frame representations and **c**: helical backbone (wire-frame representation). Colour code: Cu, cyan; Cl, green; O, red; N, blue; C, dark gray; H, white spheres.

5.5. Conclusion

A series of chiral copper complexes have been synthesized and structurally characterized starting from chiral amino alcohol bases Schiff bases. The chirality of the complexes is supported by circular dichroism studies. In all these complexes the chiral ONO donor ligands satisfy the three coordination sites of each copper. In dinuclear complexes, each copper center is in distorted square pyramidal geometry with two chloride ligands bridging the copper centers in equatorial-apical fashion. The amount of distortion from ideal square pyramidal geometry is different for different complexes probably due to various factors like the differences in the steric and electronic properties of the ligands, hydrogen bonding possibilities, crystal packing effects etc. One apical Cu–Cl bond length in dinuclear complexes is very large compared to the axial Cu–Cl distance. As a result, the complexes behave as mononuclear units in solutions as evidenced by EPR spectral studies. In mononuclear complexes, the apical bridging chlorine is missing. It can be concluded that hydrogen bonding interactions and the overall crystal packing effects play important roles in determining the overall nuclearity of these complexes.

Copper containing proteins are known to contain the copper ions in dissymmetric ligand arrangements. For the first time, a series of chiral dichlorobridged dimeric copper(II) complexes are described. Both copper centers in these complexes adopt square–pyramidal geometry, which is also found in copper containing oxyhemocyanins. These complexes exhibit hydrogen bonding interactions of the type C–H···Cl–M and O–H···Cl–M in their crystal lattices resulting in intetesting supramolecular architectures. M–Cl moiety has been recognized as an important hydrogen bond acceptor in inorganic supramolecular chemistry. The present complexes are good examples in which M–Cl acts as hydrogen bond acceptor and they belong to the rather limited number of chiral supramolecular systems containing M–Cl group as the hydrogen bond acceptors.

5.6. References

1. E. I. Ochiai, *Bioinorganic Chemistry, An Introduction,* Allyn and Bacon, Boston MA, 1977, Chapter 9.
2. T. N. Sorrell, *Tetrahedron,* 1989, **45,** 3
3. S. G. Telfer, T. Sato, T. Harada, R. Kuroda, J. Lefebvre and D. B. Leznoff, *Inorg. Chem.,* 2004, **43**, 6168; P. Deschamps, P. P. Kulkarni and B. Sarkar, *Inorg. Chem.,* 2003, **42,** 7366; J. M. Rowland, M. M. Olmstead and P. Mascharak, *Inorg. Chem.,* 2002, **41,** 1545; M. A. Masood, E. J. Enemark and T. D. P. Stack, *Angew. Chem., Int. Ed.,* 1998, **37**, 928; H. Adams, D. E. Fenton, P. E. McHugh and T. J. Potter, *Inorg. Chim. Acta*, 2002, **331**, 117; P. Amudha, P. Akilan and M. Kandaswamy, *Polyhedron*, 2000, **19**, 1769.
4. J. C. Brown and J. G. Wardeska, *Inorg. Chem.,* 1982, **21**, 1530.
5. M. Rodríguez, A. Llobet and M. Corbella, *Polyhedron*, 2000, **19**, 2483.
6. (a) J. -M. Lehn, *Supramolecular Chemistry-Concepts and Perspectives*, VCH, Weinheim, 1995; (b) E. C. Constable in *Comprehensive Supramolecular Chemistry*, eds. J. P. Sauvage and M. W. Hosseini, **vol. 9**, Pergamon Press, Oxford, 1996, p213-252; (c) E. C. Constable, C. E. Housecroft, M. Neuburger, D. Phillips, P. R. Raithby, E. Schofield, E. Sparr, D. A. Tocher, M. Zehnder and Y. Zimmermann, *J. Chem.Soc*., *Dalton Trans*., 2000, 2219; (d) C. Piguet and J.-C. G. Bünzli, *Chem. Soc. Rev*., 1999, **28**, 347; (e) M. Albrecht, *Chem. Rev*., 2001, **101**, 3457; (f) M. J. Hannon, V. Moreno, M. J. Prieto, E. Moldrheim, E. Sletten, I. Meistermann, C. J. Isaac, K. J. Sanders and A. Rodger, *Angew. Chem*., *Int. Ed*., 2001, **40**, 879.
7. (a) V. Balamurugan, M. S. Hundal and R. Mukherjee, *Chem. Eur. J*., 2004, **10**, 1683; (b) R. Banerjee, G. R. Desiraju, R. Mondal and J. A. K. Howard, *Chem. Eur. J*., 2004, **10**, 3373; (c) T. M. Kooistra, K. F. W. Hekking, Q. Knijnenburg, B. de Bruin, P. H. M. Budzelaar, R. de Gelder, J. M. M. Smits and A. W. Gal, *Eur. J. Inorg. Chem.*, 2003, 648.

8. L. Brammer, *Chem. Soc. Rev*., 2004, **33,** 476; L. Brammer, E. A. Bruton and P. Sherwood, *Cryst. Growth Des*., 2001, **1**, 277.
9. (a) S. G. Telfer and R. Kuroda, *Coord. Chem. Rev.*, 2003, **242**, 33; (b) *Supramolecular Chemistry*, eds. V. Balzani and L. De Cola, NATO ASI Series, Kluwer Academic Publishers, Dordrecht, 1992; (c) U. Knof and A. Von Zelewsky, *Angew. Chem*., *Int. Ed*., 1999, **38**, 302; (d) C. Piguet, G. Bernardinelli and G. Hopfgartner, *Chem. Rev*., 1997, **97**, 2005; (e) M. Prabhakar, P. S. Zacharias and S. K. Das, *Inorg. Chem*., 2005, **44**, 2585; (f) G. Baum, E. C. Constable, D. Fenske, C. E. Housecroft and T. Kulke, *Chem. Eur. J*., 1995, **5**, 1862 and references cited therein.
10. (a) K. Yanagi and M. Minobe, *Acta Cryst.,* 1987, **C43**, 2060; (b) K. Yanagi and M. Minobe, *Acta Cryst.,* 1987, **C43**, 1045; (c) Y. Yuan, J. Yao, J. Lu, Y. Zhang and R. Gu, *Inorg. Chem. Commun.,* 2005, **8**, 1014; (d) N. Oi, H. Kitahara, R. Kira and F. Aoki, *Anal. Sci*., 1991, **7**, 151; (e) F. Nepveu, F. –J. Bormuth and L. Walz, J. Chem. Soc., Dalton Trans., 1986, 1213.
11. A. C. T. North, D. C. Philips and F. S. Mathews, *Acta Crystallogr*., 1968, **A24** 351.
12. L. J. Farrugia, *J. Appl. Crystallogr*., 1999, **32,** 837.
13. G. M. Sheldrick, *Programs for Crystal Structure Solution and Analysis*, University of Göttingen, Germany, 1997.
14. Bruker, *SADABS, SMART, SAINTPLUS and SHELXTL*, Bruker AXS Inc., Madison, Wisconsin, USA, 2003.
15. K. Brandenburg, *DIAMOND Version 2.1e*, Crystal Impact GbR, Bonn, Germany, 2001.
16. H. D. Flack, *Acta. Cryst*., 1983, **A39**, 876.
17. (a) T. M. Dunn in *Modern Coordination Chemistry*, eds. J. Lewis and R. G. Wilkins, Interscience, New York, 1960; (b) L. Sacconi and M. Ciampolini, *J. Chem. Soc.,* 1964, 276; (c) A. B. P. Lever, *Inorganic Electronic Spectroscopy*, Elsevier, New York, 1968.

18. S. J. Brown, X. Tao, T. A. Wark, D. W. Stephan and P. K. Mascharak, *Inorg. Chem.*, 1988, **27,** 1581.
19. S. J. Brown, X. Tao, D. W. Stephan and P. K. Mascharak, *Inorg. Chem.*, 1986, **25,** 3377.
20. W. E. Hatfield in *Theory and Applications of Molecular Paramagnetism*, eds. E. A. Boudreaux and L. N. Mulay, Wiley, New York, 1976.
21. C. J. O'Connor, *Prog. Inorg. Chem.*, 1982, **29**, 203.
22. M. Rodríguez, A. Llobet, M. Corbella, A. E. Martell and J. Reibenspies, *Inorg. Chem.*, 1999, **38,** 2328.
23. A. W. Addison, T. N. Rao, J. Reedijk, J. V. Rijn and G. C. Verschoor, *J. Chem. Soc., Dalton Trans.*, 1984, 1349.
24. G. Aullón, D. Bellamy, L. Brammer, E. A. Bruton and A. G. Orpen, *Chem. Commun.*, 1998, 653.
25. M. M. Olmstead, T. E. Patten and C. Troeltzsch, *Inorg. Chim. Acta,* 2004, **357**, 619.
26. E. Y. Bivián-Castro, S. Bernès, J. Escalante and G. Mendoza-Díaz, *Acta Cryst.,* 2004, **C60**, m205.

Chapter 6

Summary and scope of further work

This chapter presents the summary of the results of the current investigation. Also presented in this chapter is the scope of the future work.

6.1. Summary

Chiral metal complexes have found applications in various fields ranging from bioinorganic chemistry, materials chemistry, asymmetric catalysis to supramolecular chemistry. Amino alcohol based systems are emerging as ideal precursors for the synthesis of chiral coordination compounds with desired properties. Schiff base systems are more appropriate since their steric and electronic properties can be tailored by selecting appropriate amine and aldehyde precursors. Chapter one overviews the reported works on chiral amino alcohol based systems which gives an idea about the potential areas to be explored.

Some simple Schiff base ligand systems with different steric and electronic properties were designed to study the structure, coordination chemistry, catalytic properties and supramolecular chemistry of the metals Mn, Co and Cu. These metals are selected because of their importance with respect to areas like catalysis, bioinorganic modeling, materials chemistry etc. Moreover, the chemistry of these metals with chiral amino alcohol based systems is not explored much. The synthetic procedures and characterization details of the Schiff bases and their complexes form the content of the second chapter.

Manganese in its various oxidation states are well studied in coordination chemistry. Among the various oxidation states of manganese, Mn(IV) is rather rare

but is most important with respect to bioinorganic chemistry and asymmetric catalysis. Photosystems II, a vital enzyme of living beings is believed to contain a mononuclear Mn(IV) center. With respect to asymmetric catalysis, the most effective catalytic system for the asymmetric epoxidation of olefins is salen-manganese system. This system is believed to produce some Mn(IV) species during the course of the reaction which controls the final outcome of the reaction. Over the last two decades there are reports on the structures of Mn(IV) complexes. But there is no report on chiral mononuclear Mn(IV) systems. Chiral systems are more suitable for bioinorganic modeling studies since the metalloenzymes are believed to contain the metal centers in dissymmetric ligand environment. The chapter three of this thesis describes the structure and properties of a series of chiral mononuclear Mn(IV) complexes for the first time. The spectral properties including UV-VIS, CD and EPR for all the complexes along with CV and magnetic studies are described which confirm the Mn(IV) oxidation state. The X-ray structure analysis revealed interesting supramolecular interactions in these complexes resulting in chains, channels etc. in the crystal lattice. These complexes are found to be catalytically active towards epoxidation of olefins although enantioselectivity is absent. This may be probably due to the octahedral structure of Mn which demands the dissociation of catalyst during catalysis thus compromising on enantioselectivity.

Over the past two decades, interest in the biological chemistry of cobalt has increased rapidly because of the discovery of at least eight distinctly different cobalt dependant proteins during this period. Also the spectroscopic properties of cobalt have gained attention because the substitution of Co for spectroscopically silent ions in metalloproteins has been found to be an invaluable tool in the determination of active site structures and reaction mechanisms. Here also the complexes with chiral ligands will be advantageous. Our study on the cobalt chemistry of chiral amino alcohol based systems, which form the subject of fourth chapter is of relevance. A variety of complexes which include octhahedral mono nuclear Co(III), mixed valent octahedral-tbp/sp-octahedral trinuclear complexes and trigonal prismatic tetranuclear

structures are described. The tri- and tetranuclear complexes are found to be mixed valent, in which terminal octahedral cobalt(III) complexes act as chelating ligands for the central cobalt(II). Depending on the steric constraints, the central cobalt adopts different geometries such as distorted trigonal bipyramidal, distorted square pyramidal and distorted trigonal prismatic. In mononuclear cobalt complexes, O–H···O supramolecular interactions among the molecules lead to helical arrangement in the crystal lattice. These complexes belong to the rather limited examples of such uncommon geometries reported in the literature. One of the complexes is found to contain large voids in its lattice which may be of relevance with respect to the study of porous metal organic frameworks.

Study on the chiral copper complexes prepared from the Schiff bases of chiral amino alcohols forms the subject of fifth chapter. Copper is an essential element present in living organisms. Systematic development of coordination chemistry of copper using various chelating ligands is of importance in areas like bioinorganic modeling, catalysis, magnetic chemistry etc. Chiral copper complexes from chiral ligands are of special importance in this regard. The previous studies on copper complexes of chiral amino alcohol based ligands have concentrated mainly on their catalytic properties. The present study highlights their structural and supramolecular chemistry in addition to their spectroscopic properties. Through our studies we have shown that these simple copper complexes can act as wonderful inorganic synthons giving interesting supramolecular architectures. The ability of M–Cl moiety to act as hydrogen bond acceptors has been the subject of some current research in inorganic supramolecular chemistry. It is shown that copper complexes derived from amino alcohol based systems are ideal choices for building inorganic supramolecular architectures. The advantage of these systems is that they contain both hydrogen bond donor as well as acceptor groups and are effective in connecting among themselves so that involvement of solvents and counter ions are minimized. The involvement of solvents and counter ions are undesirable in a supramolecular architecture since they are shown to have adverse effect on the expected supramolecular assembly. Apart

from their relevance in inorganic supramolecular chemistry, these complexes are also relevant with respect to magneto chemistry and bioinorganic chemistry. Magnetic study of one of the complex revealed ferromagnetic interaction between metal centers. The dinuclear copper complexes explained in this chapter contain square pyramidal copper ions in chiral environment. This may be of biological relevance since similar copper geometry has been found in some copper containing oxyhemocyanins.

6.2. General conclusions

The chiral amino alcohol based ligands are found to be versatile ligands which can lead to a variety of structural arrangements. Depending on the changes in substitution on the salicylaldehyde and β position of the amino alcohol part of the ligands as well as on the stereo-electronic preferences of the metal ions, the nuclearity of the resulting complexes changed. The various hydrogen bonding groups present on the ligands also plays an important role in determining the final structure. Thus we can conclude that in these complexes, the stereo-electronic preferences of the metal, steric and electronic effects of the ligands and the possibility of various hydrogen bonds determine the final outcome of the complexation reaction.

The Schiff base ligands studied here contain phenol and alcoholic groups. In all the complexes, the phenolic group is found to be deprotonated and is not acting as bridging groups. In cobalt complexes the alcoholic group acts as the bridging groups. This is in contrast with the well known bridging ability of phenolic groups to bridge two metal centers. The deprotonation and bridging behavior of alcoholic group was found to depend on the nature of the metal ions. Some of these complexes might be useful in biomodeling studies due to their chirality and to the presence of $-H_2C-$, $-HC=N-$, phenolic and alcoholic groups in them.

Most of these complexes exhibited interesting supramolecular interactions in their crystal structures as a manifestation of O–H···O, C–H···O, C–H···Cl, O–H···Cl etc interactions and some of these led to the formation homochiral helices in the crystal lattice. In some other cases these interactions led to the formation of channels

and voids in the crystal lattice. The chirality of the ligand system is supposed to have some role in dictating the final outcome of the self assembly process. Thus the metal complexes derived from chiral amino alcohol based ligands are promising new materials in inorganic supramolecular chemistry, a topic not explored much.

These results provide further insight into the various structure directing factors of metal complexes such as metal coordination preferences, the disposition of the bridging groups, the conformational flexibility, the hydrogen bonds and the steric effect of the ligands. The results in this work may be valuable in designing new complexes of similar ligand systems suitable for applications in catalysis, supramolecular chemistry, materials chemistry etc. These results also provide some insights into the reasons for the dramatic changes in the catalytic ability of similar systems on introducing small changes in the ligand back bone or with change of metal ions.

6.3. Scope of further work

The present study revealed that the Schiff bases prepared from chiral amino alcohols and substituted salicylaldehydes can act as versatile ligands capable of producing variety of coordination geometries with different metal ions. One can explore this area further by complexing these ligands with other metal ions having different stereoelectronic preferences. Also one can change the position and nature of the substituents both on the amino alcohol as well as on the slicylaldehyde portions of the ligands and study their effect on the properties of the resulting complexes. Reduction of the C=N moiety will produce a new class of ligands probably with different complexing abilities.

In addition to this work on amino alcohol based systems with salicylaldehyde derivatives, some preliminary studies on symmetric and asymmetric compartmental ligands containing amino acid side arms have been carried out (See appendix). Compartmental ligands are of current interest because of their relevance in structural, biomimetic, magnetic and supramolecular studies. One can combine the chemistry of

amino alcohols with that of compartmental type ligands, an area not explored much. By doing so a new series of Schiff bases and their complexes relevant to structural studies, biomimetic chemistry, catalysis, magnetism and supramolecular chemistry may be prepared. Some mono and dialdehydes which can be used as starting materials for such studies are given in Scheme 6.1

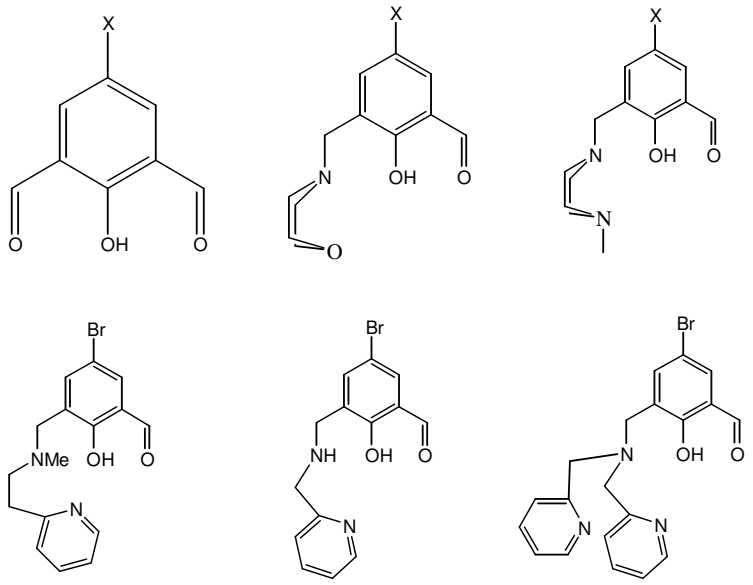

Scheme 6.1.

Another series of ligands can be synthesized by reducing the C=N moiety of the resulting Schiff bases. The reduction of the C=N moiety will bring about more flexibility to the system and one can expect a new series of complexes with entirely different structure and properties.

Appendix 1

Synthesis and structural characterization of two tetranuclear copper complexes derived from symmetric and asymmetric compartmental ligands containing amino acid side arms

A.1. Abstract

Synthesis, structural characterization and properties of two carboxylate bridged tetranuclear copper complexes $[Cu_4(C_{54}H_{46}N_4O_{14})(OH)_2]\cdot 10H_2O$ (**25**) and $[Cu_4(C_{40}H_{56}N_6O_{14}Br_2)]\cdot 2CH_3CN\cdot 2H_2O$ **(26)** derived from symmetric and asymmetric compartmental ligands respectively are reported. The crystal structure of complex **25** revealed an interesting self-assembly of crystal water molecules into acyclic water nonamer in the crystal lattice.

A.2. Introduction

Compartmental ligands are capable of accommodating two metal ions in close proximity and can communicate to each other through suitable bridging groups. Such systems are receiving renewed interest owing to their ability to give complexes relevant to fields as diverse as magneto chemistry, catalysis, bioinorganic and molecular recognition studies. Schiff bases prepared by the 1:2 condensation of 2,6-diformyl-4-substituted phenols and suitable amines are good examples for symmetric compartmental ligands which contain two identical metal recognition sites in close proximity. The cyclic and acyclic varieties of these ligands are widely used for the synthesis of homodinuclear complexes.[1] On the other hand asymmetric compartmental ligands contain two different metal recognizing chambers. They provide entirely different coordination environments for two metal ions while keeping them in close proximity. Because of this property such systems are widely employed for bioinorganic modeling studies.[2,3]

The number of multinuclear complexes with compartmental ligands is less in the literature compared to their dinuclear complexes. Introduction of suitable bridging groups into the ligand back bone might result in interesting multinuclear systems. Carboxylate group is well known for its ability to bridge two metal centers and a large number of carboxylate bridged systems are known in the literature.[4]

Here we report the syntheses and crystal structures of two tetranuclear copper complexes **25** and **26** derived from symmetric and asymmetric compartmental ligands **A** and **B** respectively (Scheme A.1.) containing amino acid side arms.

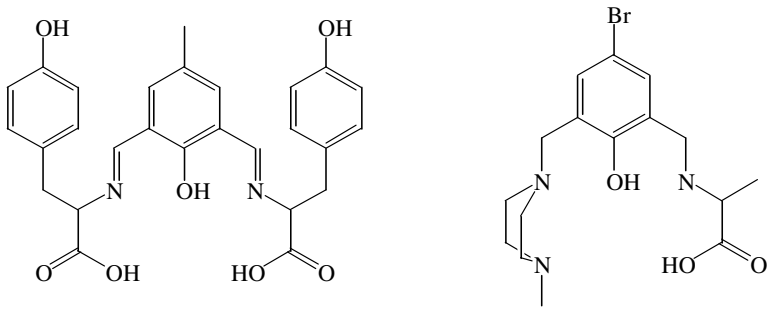

A B

Scheme A. 1. Symmetric and asymmetric compartmental ligands.

A.3. Experimental

2,6-Diformyl-4-methylphenol[5] and 5-bromo-2-hydroxy-3-(4-methyl-piperazin-1-ylmethyl)-benzaldehyde[3] were prepared according to the reported procedures. The amino acids L-tyrosine and L-alanine were procured from Acros India and used as received. Sodium borohydride used for the reduction of Schiff base was purchased from Lancaster India. All other chemicals and solvents used were of Lab Reagent grade and used without further purifications. The physical measurement methods are as explained in Section **2.3.**

A.3.1. Synthesis of $[Cu_4(C_{54}H_{46}N_4O_{14})(OH)_2]\cdot 10\ H_2O$ (25)

To a solution of L-tyrosine (0.18 g, 1 mmol) in ethanol-water mixture (3:1, 40 mL) was added NaOH (0.04 g, 1 mmol) and 2,6-diformyl-4-methylphenol (0.082 g, 0.5 mmol). The reaction mixture was stirred for 1h at room temperature. To the resulting Schiff-base, formed *in situ*, was added $CuSO_4\cdot 5H_2O$ (0.25 g, 1 mmol), and stirred again for another 12 h at room temperature. The resulting dark green solution was filtered and the filtrate on slow evaporation yielded green crystals of **25**. The crystals lose water molecules on exposure to atmosphere (taken out from mother liquor) at room temperature (as is evidenced from TGA studies and loss of single-

crystallinity). Yield after water loss 55 %. IR (KBr, cm^{-1}): 3391, 1641, 1552, 1516, 1452, 1367, 1321, 1242, 1084, 1045, 885, 858, 810, 765, 542. Anal. calcd for $C_{54}H_{48}N_4O_{16}Cu_4$ (after water loss): C 51.35, H 3.83, N 4.44 %. Found: C 50.98, H 3.95, N 4.18 %. UV-Vis (N, N-dimethylformamide); λ_{max}/nm ($\varepsilon/M^{-1}cm^{-1}$): 652 (348), 378 (14951).

A.3.2. Synthesis of complex 26

5-Bromo-2-hydroxy-3-(4-methyl-piperazin-1-ylmethyl)-benzaldehyde (0.33 g, 1 mmol) was stirred with L-alanine (0.09 g, 1 mmol) for 3 hrs in presence of NaOH (0.04 g, 1 mmol) in methanol at room temperature. To the resulting yellow solution containing the corresponding Schiff base was added sodium borohydride (0.075 g, 2 mmol) to get a colorless solution. This solution was evaporated completely using rotavapor and vacuum pump followed by extraction with dichloromethane (DCM). The DCM solution on evaporation gave a white solid which was dissolved in ethanol, added $(CH_3COO)_2Cu{\cdot}H_2O$ (0.4 g, 2 mmol) and stirred at room temperature overnight. The resulting green colored solution on slow evaporation yielded the green complex of **26** which was recrystallized from acetonitrile solutions. Yield after solvent loss: 63 %. IR (KBr, cm^{-1}): 3418, 3217, 2974, 2924, 2874, 1641, 1602, 1444, 1398, 1336, 1278, 1238, 1149, 1086, 1022, 893, 808, 771, 659, 619, 530, 451. Anal. Calcd for $C_{54}H_{48}N_4O_{16}Cu_4$ (after solvent loss): C 38.16, H 4.48, N 6.68 %. Found: C 38.31, H 4.57, N 6.39 %. UV-Vis (MeOH); λ_{max}/nm ($\varepsilon/M^{-1}cm^{-1}$): 650 (740), 380sh (3350), 335 (7100), 290 (22861).

A.3.3. X-ray crystallography

Since the crystals of compounds $[Cu_4(C_{54}H_{46}N_4O_{14})(OH)_2]\cdot 10\ H_2O$ (**25**) and $[Cu_4(C_{40}H_{56}N_6O_{14}Br_2)]\cdot 2CH_3CN\cdot 2H_2O$ **(26)** start losing solvent molecules on exposure to atmosphere, they are taken out from mother liquor at ambient conditions and immediately cooled to 100(2) K. The data were collected on a Bruker SMART APEX CCD area detector system [λ(Mo-Kα) = 0.71073 Å], graphite monochromator, 2400 frames were recorded with an ω scan width of 0.3°, each for 20 s (complex **25**) [10 s for complex **26**], crystal-detector distance 60 mm, collimator 0.5 mm. The data were reduced using SAINTPLUS[6] and a multi-scan absorption correction using SADABS[6] was performed. Structure solution and refinement were done using programs of SHELX-97.[7]

In the case of complex **25**, all non-hydrogen atoms were refined anisotropically. Water hydrogen atoms were located in the differential Fourier maps and their positions were refined using isotropic thermal parameters. One of the water molecules (O11) shows disorder over two positions with equal occupancy.

For complex **26**, the methyl group of the amino acid shows disorder over two positions with almost equal occupancies (0.51 and 0.49). The solvent water molecule also shows disorder over two positions with occupancies 0.54 and 0.46. Hydrogen atoms are not located for the disordered water molecule. The largest residual electron density (1.85 e / Å^3) is found near the nitrogen of solvent acetonitrile molecule at a distance of 1.036 Å. Crystallographic data for the complexes **25** and **26** are presented in Table A.1.

Table A.1. Crystallographic data for the complexes **25** and **26**

Complex	**25**	**26**
Empirical formula	$C_{54}H_{68}Cu_4N_4O_{26}$	$C_{44}H_{66}Br_2Cu_4N_8O_{16}$
Formula weight	1443.28	1377.03
Crystal system	Triclinic	Monoclinic
Space group	$P\bar{1}$	$P2_1/c$
a / Å	10.7136(8)	10.8233(7)
b / Å	10.7365(8)	15.9198(11)
c / Å	13.7677(10)	16.3139(11)
α / °	67.6070(10)	
β / °	87.3940(10)	97.6880(10)
γ / °	82.0860(10)	
V / Å 3	1450.24(19)	2785.7(3)
Z	1	2
μ / mm-1	1.538	3.011
ρ_{calcd} / gcm^{-3}	1.653	1.642
Independent reflections	16998 (R_{int} = 0.0275)	31886 (R_{int} = 0.0255)
Observed reflections	6813	6613
Parameters	436	359
*R*1,[a] w*R*2[b] [($I > 2\sigma(I)$)]	R1 = 0.0396, wR2 = 0.1030	R1 = 0.0359, wR2 = 0.0901
Goodness-of-fit[c]	0.983	1.087
Largest peak and hole e/ Å3	+0.774 and – 0.363	+1.847 and – 0.787

[a] $R1 = \sum||F_o| - |F_c||/\sum|F_o|$. [b] $wR2 = \{\sum[(F_o^2 - F_c^2)^2]/\sum[w(F_o^2)^2]\}^{1/2}$.
[c] GOF = $\{\sum[w(F_o^2 - F_c^2)^2]/(n - p)\}^{1/2}$ where 'n' is the number of reflections and 'p' is the number of parameters refined; $w = 1/[\sigma^2(F_o^2) + (aP)^2 + bP]$ where a = xxx and b = 0 for xx

A.4. Structure and properties of complex 25

A.4.1. Synthesis and properties

The complex **25** is obtained as green diamond shaped crystals, which loses solvent molecules on exposure to atmosphere. The elemental analytical data of the dried sample matched with the expected structure. The IR spectrum of the complex shows band corresponding to the υ(C=N) at 1641 cm^{-1}. The electronic spectrum (Figure A.1) consists of a low-intense broad band with a maximum at around 650 nm, which can be assigned to d-d transition for a Cu^{2+} (d^9) system. The peak around 400 nm is due to charge transfer transition.

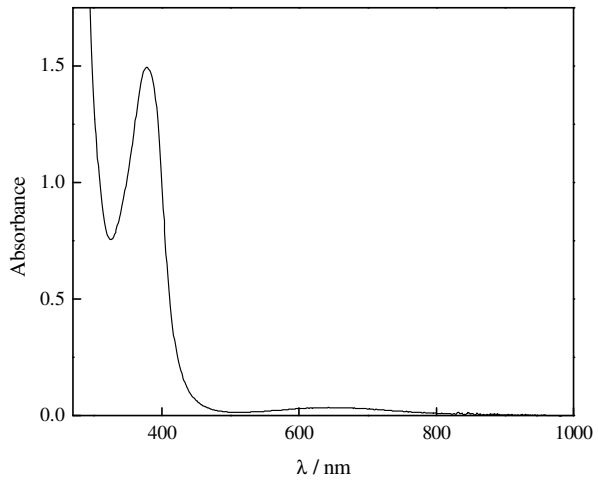

Figure A.1. Electronic spectrum of **25** (10^{-4}M in DMF).

A.4.2. Crystal structure

Crystals suitable for X-ray analysis were grown by the slow evaporation of the mother liquor. The relevant crystallographic data are given in Table A.1. The crystal structure of $[Cu_4(C_{54}H_{46}N_4O_{14})(OH)_2]$ in complex **25** with the atom numbering scheme is shown in Figure A.2.

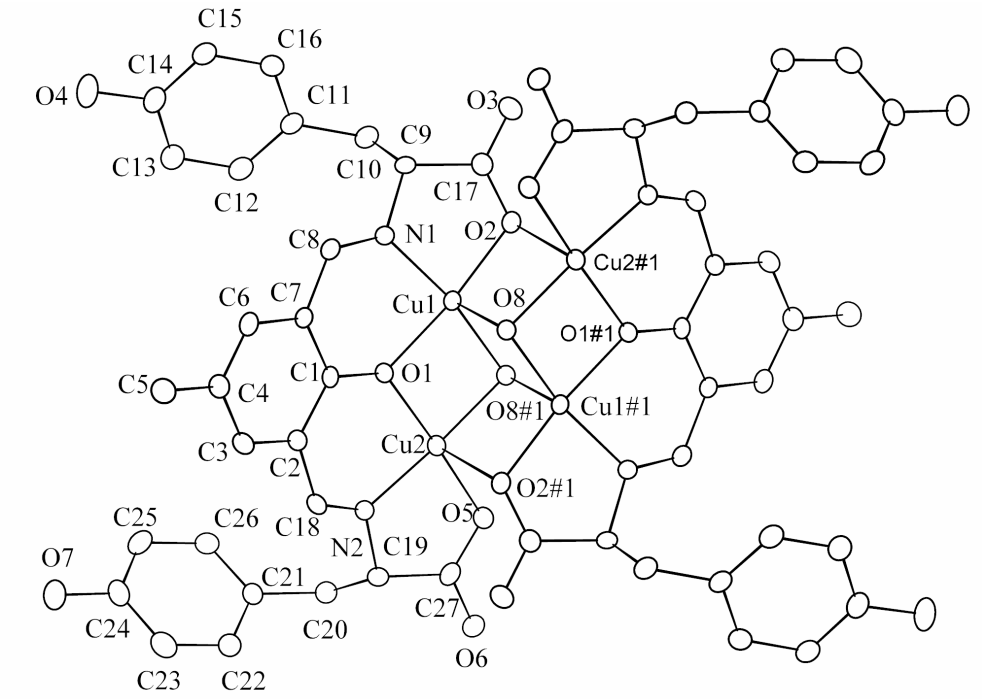

Figure A.2. Thermal ellipsoidal plot (20 % probability) of $[Cu_4(C_{54}H_{46}N_4O_{14})(OH)_2]$ in $[Cu_4(C_{54}H_{46}N_4O_{14})(OH)_2]\cdot 10\ H_2O$. Hydrogen atoms and solvent molecules are omitted for clarity. Symmetry operations: #1 2–x, 1–y, 1–z.

Two binuclear units related by the center of symmetry are bridged by two hydroxide oxygen atoms O8 and O8#1 (#1 = –x+2, –y+1, –z+1) and as a result form a tetranuclear structure. In the binuclear unit, the two copper atoms are also bridged endogenously by phenolic oxygen. The coordination geometries of Cu1 and Cu2 in the crystallographically unique unit are slightly different. That of Cu2 is best described as distorted square pyramid with the oxygen atom (O2#1) of the carboxylate group of the adjacent binuclear unit approaching Cu2 with a long axial distance of Cu2–O2#1 2.711(2) Å. The coordination geometry of Cu1 is square

pyramidal with the equatorial co-ordination plane provided by O1, O2 and N1 of the same binuclear unit and O8#1 from the adjacent binuclear unit. The axial co-ordination site is occupied by hydroxide oxygen O8 [Cu1–O8 2.3484(19) Å]. Atom Cu1 deviates by 0.1074(10) Å toward the axial ligand O8 from the equatorial co-ordination plane. Due to the small difference in co-ordination geometries around Cu1 and Cu2, the bond distances of Cu2 are shorter than the corresponding ones of Cu1. For example, Cu2–O1 [1.9216(17) Å] is shorter than Cu1–O1 [1.9442(17) Å]. Selected bond distances and angles for complex **25** are given in Table A.2.

Table A.2. Selected bond distances (Å) and angles (°) for the complex **25**

Cu(1)-N(1)	1.923(2)	Cu(2)-O(1)	1.9216(17)
Cu(1)-O(2)	1.9358(19)	Cu(2)-O(5)	1.9002(18)
Cu(1)-O(8)	2.3484(19)	Cu(2)-N(2)	1.916(2)
Cu(1)-O(8)#1	1.9329(18)	Cu(2)-O(8)#1	1.9321(18)
Cu(1)-O(1)	1.9442(17)	O(8)-Cu(2)#1	1.9321(18)
Cu(1)-Cu(2)	2.9488(5)	O(8)-Cu(1)#1	1.9329(18)
N(1)-Cu(1)-O(2)	85.50(8)	O(5)-Cu(2)-O(1)	175.90(8)
N(1)-Cu(1)-O(8)#1	169.33(8)	O(5)-Cu(2)-N(2)	86.13(8)
O(8)#1-Cu(1)-O(2)	103.37(8)	N(2)-Cu(2)-O(1)	92.01(8)
N(1)-Cu(1)-O(1)	90.24(8)	O(5)-Cu(2)-(8)#1	101.52(8)
O(8)#1-Cu(1)-O(1)	80.20(7)	N(2)-Cu(2)-O(8)#1	169.69(9)
O92)-Cu(1)-O(1)	171.63(8)	O(1)-Cu(2)-O(8)#1	80.79(7)
N(1)-Cu(1)-O(8)	102.47(8)	O(5)-Cu(2)-Cu(1)	141.45(6)
O(2)-Cu(1)-O(8)	91.72(7)	Cu(2)#1-O(8)-Cu(1)#1	99.45(8)
O(1)-Cu(1)-O(8)	96.24(7)	O(1)-Cu(2)-Cu(1)	40.57(5)
N(1)-Cu(1)-Cu(2)	129.83(6)	Cu(1)#1-O(8)-Cu(1)	96.58(8)
O(8)#1-Cu(1)-Cu(2)	40.26(5)	Cu(2)-O(1)-Cu(1)	99.42(8)
O(2)-Cu(1)-Cu(2)	142.62(6)	Cu(2)#1-O(8)-Cu(1)	99.02(8)
O(1)-Cu(1)-Cu(2)	40.00(5)		
O(8)-Cu(1)-Cu(2)	91.58(4)		

Although a chiral amino acid L-tyrosine was used as starting material, it has undergone racemization under the reaction conditions. As a result, both the chiral carbons present in a particular dimer has opposite absolute configurations and the compound crystallizes in an achiral space group $P\bar{1}$ (C9 andC19#1-(S) and C19 and C9#1-(R)). Similar racemization phenomena have been reported previously.[8]

The geometry of the centrosymmetric Cu_4O_4 central core of the molecule can be described as a 'double-open' face shared dicubane with two missing vertices (Figure A. 3). One of the two cubanes may be outlined by three 4-membered rings: (a) O1-Cu1-O8#1-Cu2, (b) Cu2-O8#1-Cu1#1-O2#1 and (c) Cu1-O8#1-Cu1#1-O8 (#1 = –x+2, –y+1, –z+1). The two open cubanes are related by a crystallographic center of symmetry located at the centroid of the face (c). A Cu_4N_6 defective dicubane-type motif with two missing vertices has been reported in the case of azido bridged 1D molecular railroad copper complex.[9]

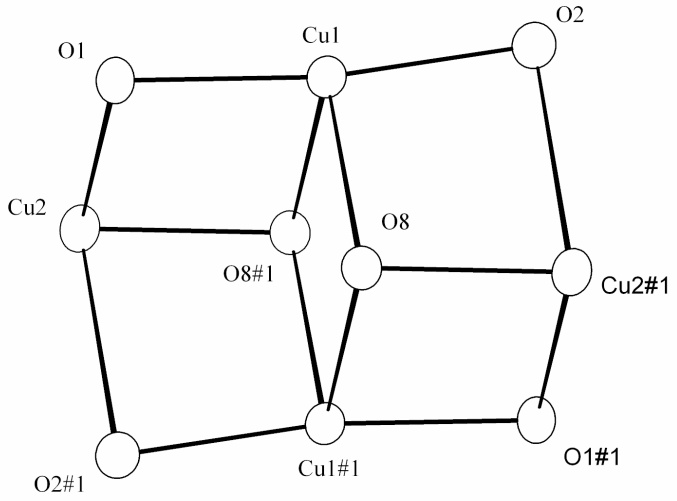

Figure A.3. The central double open face shared dicubane motif present in the complex **25**.

A.4.2.1. Water nonamer $(H_2O)_9$ in the crystal lattice of complex 25

An interesting aspect of the crystal structure of complex **25** is the formation of an acyclic water nonamer in the crystal lattice. Water nonamer is formed from the water molecules O9-O13 located in the asymmetric unit as shown in Figure A.4. This water nonamer can be described as an "S"- shaped water hexamer that connects a near linear water trimer. The O11 water molecule is disordered over two symmetry related positions (O11 and O11#8). Interestingly, the water nonamer features an inbuilt "cyclic" water dimer. This dimer is formed by two O9 water molecules which are related by a symmetry operation. The hydrogen bonding parameters for this water nonamer are presented in Table A.3.

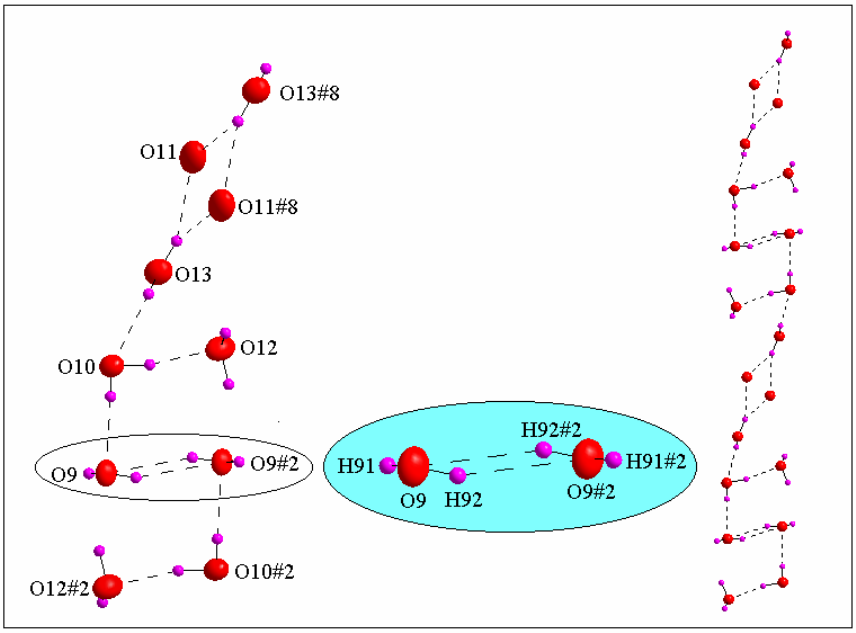

Figure A.4. Left: "S" shaped water nonamer present in the crystal lattice of complex **25** incorporating a cyclic water dimer. O11 water is disordered over two positions. Middle: cyclic water dimer is highlighted separately. Right: water nonamer self-assembles to a chainlike structure. Color code: O, red; H, purple. Symmetry operations: #2 –x, 2–y, 2–z; #8 –x, 2–y, 1–z.

Table A.3. Geometrical parameters of hydrogen-bonds (Å, °) for complex **25**

D─H···A	*d*(D···H)	*d*(H···A)	*d*(D···A)	∠(DHA)
O10–H101···O12	0.94(5)	1.74(4)	2.669(4)	167(3)
O10–H102···O9	0.82(4)	2.03(4)	2.848(3)	178(5)
O13–H132···O10	0.84(4)	2.10(5)	2.901(4)	158(9)
O13–H131···O11	0.89(4)	2.01(6)	2.822(6)	150(9)
O13–H131···O11#8	0.89(4)	2.16(7)	2.931(7)	144(9)
O9–H92···O9#2	0.70(3)	2.08(3)	2.747(5)	160(4)
O7–H7···O10	0.82	1.86	2.658(3)	165.2
O4–H4···O9#3	0.82	1.95	2.758(3)	166.4
O8–H1···O13#4	0.90(3)	1.90(4)	2.794(3)	173(3)
O12–H121···O3#5	0.87(4)	1.86(4)	2.708(3)	166(5)
O12–H122···O6#6	0.88(4)	1.89(4)	2.735(3)	160(5)
O9–H91···O6#7	0.76(3)	2.03(3)	2.770(3)	166(4)

#2 –x, 2–y, 2–z; #3 x, y, –1+z; #4 1–x, 2–y, 1–z; #5 1–x, 1–y, 1–z; #6 1–x, 1–y, 2–z; #7 –1+x, 1+y, z; #8 –x, 2–y, 1–z

A.4.2.2. Interactions of a {Cu_4} complex with its surrounding water chains

The water chains are supported/anchored by the tetranuclear copper complex [$Cu_4(C_{54}H_{46}N_4O_{14})(OH)_2$] in the crystal structure of complex **25** via O–H···O type hydrogen bonding interactions. The hydrogen bonding pattern inside the asymmetric unit is presented in Figure A.5. Each {Cu_4} complex connects four different water chains as shown in Figure A.6. Similarly each water nonamer is anchored by six surrounding {Cu_4} complexes. The lattice water molecules O9 through O13, located in asymmetric unit, interact and result in the formation of two different chain like extended water structures. In the crystal of complex **25**, each copper complex [$Cu_4(C_{54}H_{46}N_4O_{14})(OH)_2$] interacts with four different water chains as shown in Figure A.7. The mode of extension of water chains in the crystal lattice is given in Figure A.8.

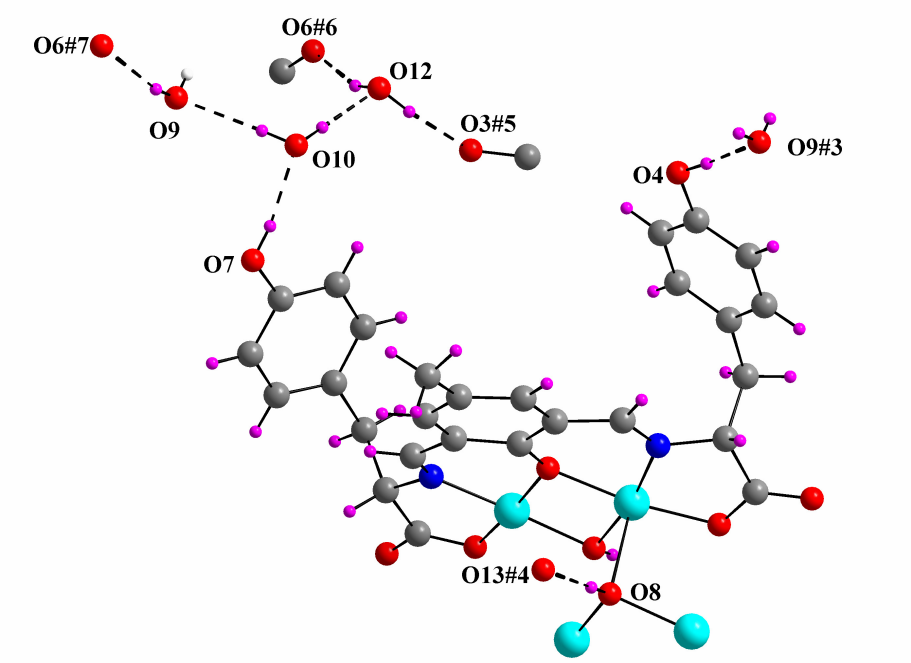

Figure A.5. Hydrogen bonding interactions from the asymmetric unit. O4 and O7 are phenolic oxygen atoms, O3 and O6 are carbonyl oxygen atoms, O8 is μ_3-type oxygen atom coordinated to three copper ions, O9, O10, O12 and O13 are lattice waters (parts of water nonamers). Color code: Cu, cyan; O, red; N, blue; C, gray; H, purple.

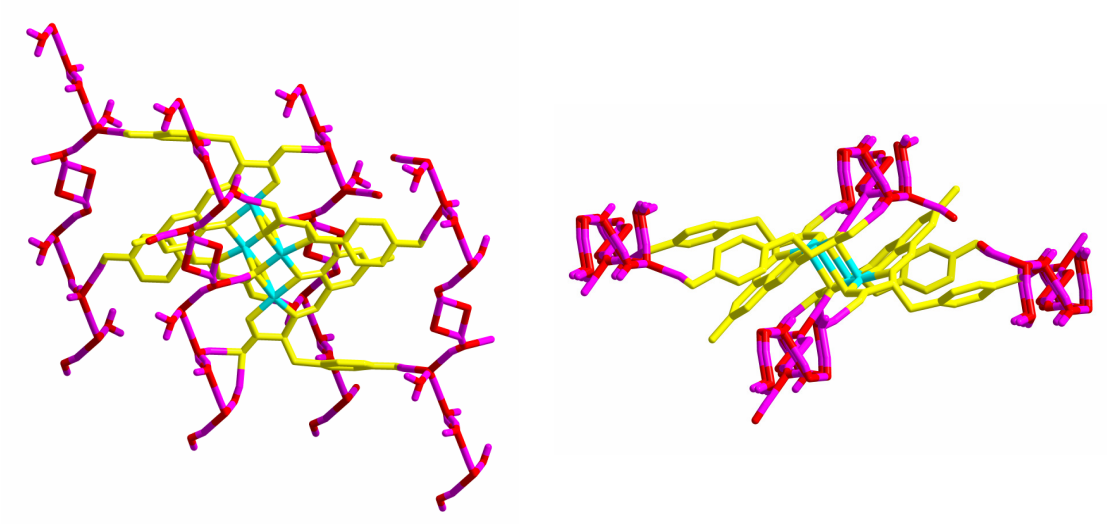

Figure A. 6. Wire-frame representation for interactions of complex $[Cu_4(C_{54}H_{46}N_4O_{14})(OH)_2]$ with its four surrounding water chains in two different views. Copper complex is shown in cyan and yellow colors and water chains are presented in purple and red color.

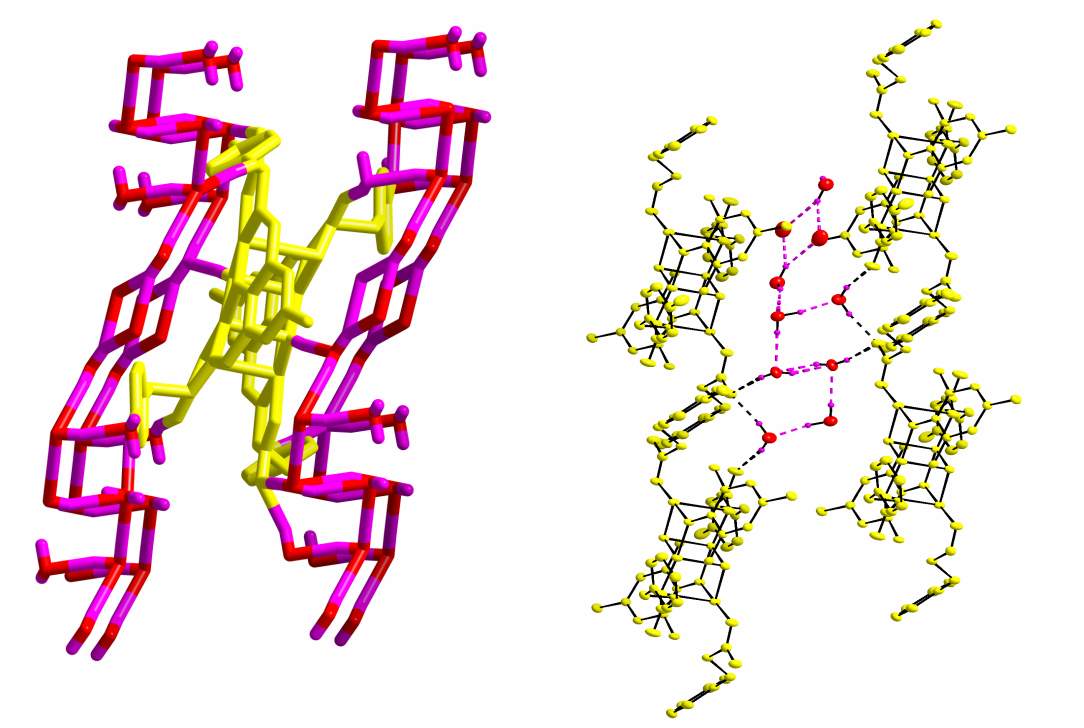

Figure A.7. Left: $[Cu_4(C_{54}H_{46}N_4O_{14})(OH)_2]$ complex exhibiting its hydrogen bonding interactions with four surrounding water chains of $(H_2O)_9$ clusters. Right: A water nonamer is anchored by six surrounding complex molecules. The whole complex is shown in yellow color and the water chain is of red (O) and purple (H) colors.

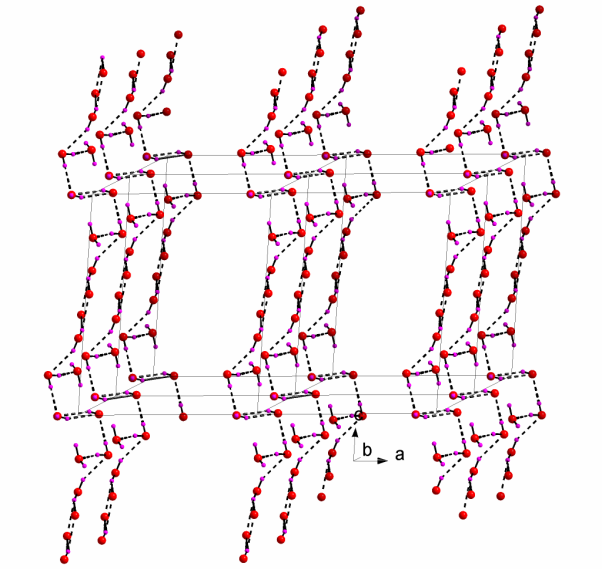

Figure A.8. View of propagation of water chains in (4×4) cells of complex **25.**

Compound $[Cu_4(C_{54}H_{46}N_4O_{14})(OH)_2]\cdot 10H_2O$ (**25**) looses lattice water molecules once the relevant crystals are taken out from mother liquor and kept at room temperature (298 K). This is consistent with elemental analysis data of the crystals dried at room temperature. It is also supported by the TGA analysis which showed almost flat feature up to ~200^oC. The loss of crystal water molecules at ambient conditions (once the crystals are removed from mother liquor) could be due to the fact that all these crystal water molecules are involved in forming a high energy form of water cluster. At ~250^oC, the curve show a sharp loss that corresponds to the loss of two OH^- groups of the complex $[Cu_4(C_{54}H_{46}N_4O_{14})(OH)_2]$.

A.4.3. Variable temperature magnetic data for complex 25

To evaluate the singlet-triplet energy separation (-2*J*), variable temperature magnetic study of the tetranuclear copper complex $[Cu_4(C_{54}H_{46}N_4O_{14})(OH)_2]\cdot 10\ H_2O$ (**25**) was performed in the temperature range of 90-300K. Inspite of the tetranuclear structure, the experimental magnetic susceptibility values were fitted to the Bleaney-Bower's equation with a Curie type of impurity of $S = 0.5$. The complex shows antiferromagnetic interactions between the copper centers. The best fit of the magnetic data to this equation yielded $2J = -217$, g = 2.019 and a TIP value of 60×10^{-6} cm^3mol^{-1}. There is a good agreement between the experimental and calculated values at this temperature region (90-305 K) as shown in Figure A.9.

This result may be interpreted in terms of a predominant magnetic interaction through the endogenous phenolic oxygen atoms O1 and O1#1, the intra- and inter-dimer magnetic interactions through the exogenous hydroxide oxygen atoms O8 and O8#1 contributing little to the magnetic susceptibility. The phenolic oxygen atoms O1 and O1#1 are bound to three atoms and have lone-pair electrons. On the other hand, the exogenous hydroxide oxygen atoms are bound to four atoms and therefore have no lone-pair of electrons. It is likely that each bond involving the bridging oxygen with sp^3-hybridized orbitals is almost perfectly localized so that no spin-exchange interaction is operative.

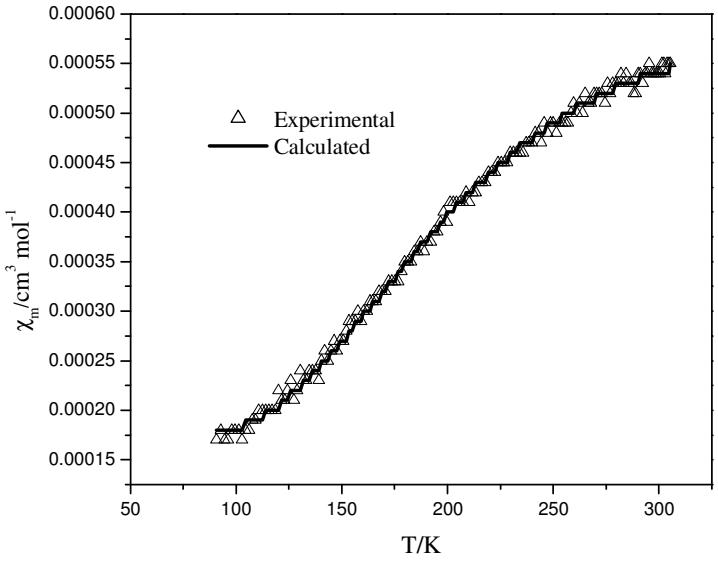

Figure A.9. Temperature dependence of the magnetic susceptibilities for the complex **25.**

A.5. Structure and properties of complex 26

A.5.1. Synthesis and properties

The asymmetric compartmental ligand **B** is prepared by the reduction of the corresponding Schiff base using sodium borohyride in methanol. Reduction of the C=N moiety is expected to give more stability and flexibility to the system. Reaction of the crude reduction product with cupric acetate in ethanol gave the corresponding green complex in moderate yields. Elemental analysis data agree well with the proposed structure. The IR spectrum of the complex shows bands at 3217 cm^{-1} corresponding to the N–H stretch indicating the reduction of the C=N moiety. Bands in the 2920-2876 cm^{-1} range are assigned to aromatic and aliphatic C–H stretches. The strong bands at 1602 and 1458 cm^{-1} are due to the $\upsilon_{(\text{-COO})}$. The electronic spectrum of complex **26** in methanol is presented in Figure A.10. The spectrum consists of a low-intense broad band with a maximum at around 650 nm, which can be assigned to d-d transition for a Cu^{2+} (d^9) system in a tetragonal or square pyramidal arrangement. The

shoulder around 380 nm is due to phenolate to copper charge transfer transition. Another peak observed around 335 nm is assigned to acetate LMCT.[10]

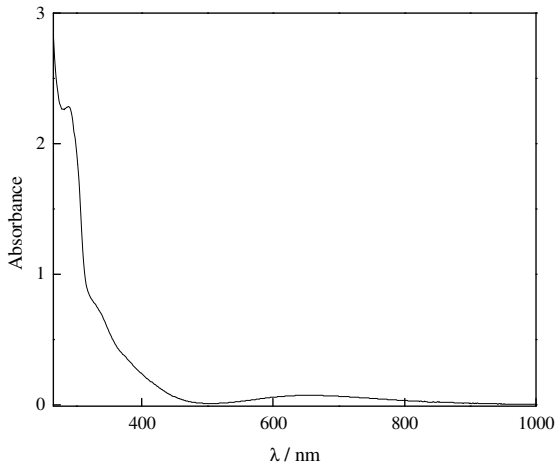

Figure A. 10. Electronic spectrum of complex **26** (10^{-4}M in methanol).

A.5.2. Structural description

The X-ray analysis of the complex revealed a tetranuclear structure which consists of two dinuclear units connected by carboxylate bridging and are related by a center of inversion of the $P2_1/c$ space group. The asymmetric unit consists of half of the tetranuclear complex (dinuclear unit) along with a disordered water molecule and an acetonitrile solvent molecule. Details of the molecular structure and the labeling scheme are shown in Figure A. 11. The relevant crystallographic parameters are presented in Table A.1.

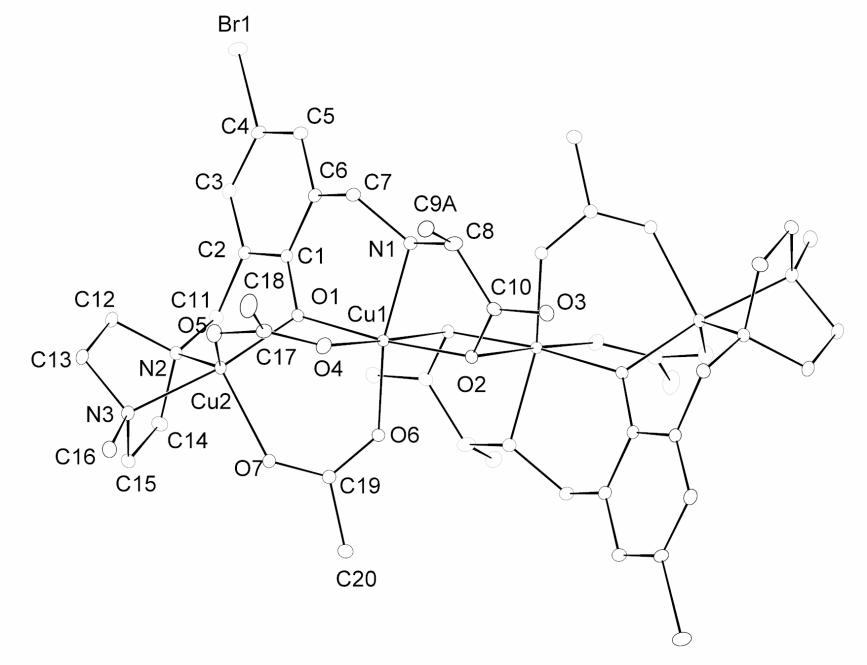

Figure A.11. The thermal ellipsoidal plot (20 % probability) of the structure of complex **26**. Hydrogen atoms and solvent molecules are omitted for clarity.

In each dinuclear unit the asymmetric compartmental ligand acts as a pentadentate donor. The two copper ions Cu1 and Cu2 present in the dinuclear unit are bridged by the phenolate oxygen O1 and have different geometries. The Cu1–O1 and Cu2–O1 distances [1.944(2) and 1.950(2) Å respectively] are almost equal within experimental errors and are in agreement with the similar values reported in the literature.[11(b)] The Cu1-O1-Cu2 angle and the Cu1···Cu2 separation are 114.90(11)^{o} and 3.2824(5) Å respectively. Two acetate groups bridge the two copper centers present in the same dinuclear unit in a *syn-syn* manner. The carboxylate oxygen atoms O2 and O2#1 bridge the two dinuclear units resulting in the tetranuclear structure. A centrosymmetric four membered Cu1-Cu1#1-O2-O2#1 ring is formed as a result of this bridging. The Cu1···Cu1#1 distance is 3.4490(8) Å and the Cu1–O2#1 distance is 2.689(2) Å. The selected bond distances and angles for complex **26** are provided in the Table A.4.

The geometry of Cu1 is distorted octahedral with O_5N coordination sphere. The four basal coordination sites are occupied by O1, O2, O6 and N1. Acetate oxygen O4 and bridging carboxylate oxygen O2#1 from the other dinuclear unit occupy the axial coordination sites. The axial bond lengths are considerably longer than the basal bond lengths (Table A.4).

Table A. 4. Selected bond distances (Å) and angles (°) for complex **26**

Cu(1)-O(1)	1.944(2)	Cu(2)-O(1)	1.950(2)
Cu(1)-O(2)	1.965(2)	Cu(2)-O(5)	1.970(2)
Cu(1)-O(6)	1.968(2)	Cu(2)-N(2)	2.029(3)
Cu(1)-O(4)	2.324(2)	Cu(2)-N(3)	2.034(3)
Cu(1)- N(1)	2.002(3)	Cu(2)-O(7)	2.115(2)
Cu(1)-O(2)#1	2.689(2)	Cu(2)-Cu(1)	3.2824(5)
Cu(1)-Cu(1)#1	3.4490(8)		
O(1)-Cu(1)-O(2)	173.40(9)	N(1)-Cu(1)-O(2)#1	86.34(10)
O(1)-Cu(1)-O(6)	96.42(9)	O(4)-Cu(1)-O(2)#1	178.14(8)
O(2)-Cu(1)-O(6)	87.31(9)	Cu(2)-Cu(1)-Cu(1)#1	143.95(2)
O(1)-Cu(1)-N(1)	93.16(10)	O(1)-Cu(2)-O(5)	96.92(10)
O(2)-Cu(1)-N(1)	82.20(10)	O(1)-Cu(2)-N(2)	91.26(10)
O(6)-Cu(1)-N(1)	165.62(11)	O(5)-Cu(2)-N(2)	141.13(11)
O(1)-Cu(1)-O(4)	88.76(9)	O(1)-Cu(2)-N(3)	164.58(10)
O(2)-Cu(1)-O(4)	96.21(9)	O(5)-Cu(2)-N(3)	93.97(11)
O(6)-Cu(1)-O(4)	97.05(9)	N(2)-Cu(2)-N(3)	73.44(11)
N(1)-Cu(1)-O(4)	93.84(11)	O(1)-Cu(2)-O(7)	97.40(9)
O(1)-Cu(1)-O(2)#1	89.39(8)	O(5)-Cu(2)-O(7)	104.52(10)
O(2)-Cu(1)-O(2)#1	85.64(8)	N(2)-Cu(2)-O(7)	112.02(11)
O(6)-Cu(1)-O(2)#1	83.07(8)	N(3)-Cu(2)-O(7)	90.38(10)

The second copper Cu2 is five coordinated with N_2O_3 coordination sphere. The five donor atoms around the Cu2 are not disposed symmetrically in either square-pyramidal or trigonal bipyramidal arrangement, but adopt a distorted square pyramidal arrangement such that N2 N3 O1 O5 form the basal plane while the acetate oxygen O7 occupies the apical position. The distortion from ideal geometry can be attributed to the ring constraints caused by the piperazine ring which is present in a boat conformation necessary for the coordination of nitrogens N2 and N3. The five membered rings formed as a result of this coordination have envelope conformations. The angle N2-Cu2-N3 is unusually small (73.44^o) and deviate considerably from the ideal value of 90^o.

Considerable twisting can be observed in the molecule which may be due to the flexibility of the reduced Schiff base part of the molecule. The basal planes of the two copper centers are at a dihedral angle of 82.81^o to each other. The two bridging acetate groups are not equally bonded to each Cu center. For example the Cu1–O6 being a basal plane bond (1.968(2) Å) is shorter than Cu2–O7, which is an apical bond (2.115(2) Å).

The amino acid L-alanine gets racemized under the experimental conditions and the chiral centers C8 and C8#1 [also N1 and N#1] present in the complex molecule have opposite chirality. As a result of which the complex crystallizes in the centro-symmetric space group.

A.6. Conclusion

Two new tetranuclear copper(II) complexes are prepared from symmetric Schiff base and asymmetric reduced Schiff base compartmental ligands containing amino acid side arms. The carboxylate oxygen acts as the bridging group in both cases. In complex **25** additional bridging by hydroxide oxygen leads to the formation of an interesting Cu_4O_6 'double open-faced shared dicubane' geometry in the crystal structure. Magnetic studies revealed an antiferromagnetic interaction between the copper centers in this complex. Hydrogen bonding groups present on the ligand

backbone of complex **25** supports an unusual water nonamer which extends throughout the crystal lattice. The asymmetric compartmental ligand **B** is novel in its class since similar reduced Schiff base systems with amino acid side arms are not reported before. The dissymmetry and flexibility of the ligand provides different coordination environments for the two adjacent copper centers. Complexes **25** and **26** present two novel tetranuclear copper complexes having widely different structural motifs.

A.7. References

1. P. A. Vigato and S. Tamburini, *Coord. Chem. Rev.*, 2004, **248**, 1717; V. Alexander, *Coord. Chem. Rev.*, 1995, **95**, 273.
2. M. Lubben, R. Hage, A. Meetsma, K. Bÿma and B. L. Feringa, *Inorg. Chem.*, 1995, **34,** 2217.
3. J. D. Crane, D. E. Fenton, J. M. Latour and A. J. Smith, *J. Chem. Soc., Dalton Trans.,* 1991, 2979.
4. S. K. Dey, B. Bag, K. M. A. Malik, M. S. El Fallah, J. Ribas and S. Mitra, *Inorg. Chem.*, 2003, **42**, 4029; K. –Y. Choi, Y. –M. Jeon, H. Ryu, J. –J. Oh, H. –H. Lim and M. –W. Kim, *Polyhedron*, 2004, **23**, 903; E. Colacio, J. P. Costes, R. Kivekäs, J. P. Laurent and J. Ruiz, *Inorg. Chem.,* 1990, **29**, 4240.
5. R. R. Gagne, C. L. Spiro, T. J. Smith, C. A. Hamann, W. R. Thies and A. K. Shiemke, *J. Am. Chem. Soc.,* 1981, **103**, 4073.
6. Bruker *SADABS, SMART, SAINTPLUS and SHELXTL*, Bruker AXS Inc., Madison, Wisconsin, USA, 2003.
7. G. M. Sheldrick, *Program for Crystal Structure Solution and Analysis,* University of Göttingen, Germany, 1997.
8. R. D. Gillard and P. O'Brien, *J. Chem. Soc.*, *Dalton Trans.,* 1978, 1444.
9. L. Zhang, L. –F. Tang, Z. –H. Wang, M. Du, M. Julve, F. Lloret and J. –T. Wang, *Inorg. Chem.,* 2001, **40**, 3619.
10. (a) A. B. P Lever, *Inorganic Electronic Spectroscopy*, 2nd ed., Elsevier, Amsterdam, 1984; (b) T. M. Rajendiran, R. Kannappan, R. Venkatesan, P. S. Rao and M. Kandaswamy, *Polyhedron*, 1999, **18**, 3085.

List of Publications

1. First structurally characterized optically active mononuclear Mn(IV) complex: synthesis, crystal structure and properties of $[Mn^{IV}L_2]$ {H_2L = S-(−)-2-[(2-hydroxy-1-phenylethylimino)methyl]phenol}.
   C. P. Pradeep, T. Htwe, P. S. Zacharias and S. K. Das, *New. J. Chem.*, 2004, **28**, 735.
2. A chiral copper complex forms supramolecular homochiral helices via O–H···Cl–Cu interactions.
   C. P. Pradeep, P. S. Zacharias and S. K. Das, *Eur. J. Inorg. Chem.,* 2005, 3405.
3. Synthesis, structural characterization and properties of an optically active mononuclear Mn(IV) complex.
   C. P. Pradeep, P. S. Zacharias and S. K. Das, *Polyhedron,* 2005, **24**, 1410.
4. Synthesis and characterization of a chiral dimeric copper(II) complex: Crystal structure of $[Cu_2(\mu\text{-}Cl)_2(HL)_2]\cdot H_2O$ (H_2L = S-(−)-2-[(2-hydroxy-1-phenyl-ethylimino)-methyl]-phenol).
   C. P. Pradeep, P. S. Zacharias and S. K. Das, *J. Chem. Sci*., 2005, **117**, 133.
5. Intramolecular hydrogen transfer in (S)-2-[(1-benzyl-2-hydroxyethylimino)methyl]-4-nitrophenol, a new chiral Schiff base.
   C. P. Pradeep, *Acta Cryst*., 2005, **E61**, o3825.
6. Synthesis, structures and properties of two Ni(II) complexes with anthracene based Schiff bases.
   T. Htwe, V. K. Muppidi, **C. P. Pradeep**, P.S. Zacharias and S. Pal, *J. Coord. Chem*. (in press).

7. A chiral Mn(IV) complex and its supramolecular assembly: synthesis, characterization and properties.

   C. P. Pradeep, P. S. Zacharias, and S. K. Das (communicated).

8. A rare conformation of water nonamer $(H_2O)_9$ that incorporates an unusual cyclic water dimer $(H_2O)_2$ in a crystalline hydrate of a tetra-nuclear copper(II) complex $[Cu_4(C_{54}H_{46}N_4O_{14})(OH)_2]\cdot 10H_2O$.

   C. P. Pradeep, S. Supriya, P. S. Zacharias and S. K. Das (communicated).

9. Synthesis, structure and properties of a series of alkoxo bridged mixed valent trinuclear Co(III)-Co(II)-Co(III) complexes and a trigonal prismatic tetranuclear cobalt complex derived from chiral amino alcohol based Schiff bases.

   C. P. Pradeep, P. S. Zacharias and S. K. Das (to be communicated).

10. Synthesis, magnetic studies and supramolecular chemistry of a series of dinuclear copper(II) complexes derived from chiral amino alcohol based Schiff bases.

    C. P. Pradeep, P. S. Zacharias and S. K. Das (to be communicated).